AD_____

Award Number: DAMD17-01-1-0130

TITLE: New Approaches for Early Detection of Breast Tumor Invasion or Progression

PRINCIPAL INVESTIGATOR: Yan-Gao Man, M.D., Ph.D.

CONTRACTING ORGANIZATION: American Registry of Pathology
Washington, DC 20306

REPORT DATE: May 2003

TYPE OF REPORT: Annual

PREPARED FOR: U.S. Army Medical Research and Materiel Command
Fort Detrick, Maryland 21702-5012

DISTRIBUTION STATEMENT: Approved for Public Release;
Distribution Unlimited

The views, opinions and/or findings contained in this report are those of the author(s) and should not be construed as an official Department of the Army position, policy or decision unless so designated by other documentation.

REPORT DOCUMENTATION PAGE

Form Approved
OMB No. 074-0188

1. AGENCY USE ONLY (Leave blank)	2. REPORT DATE	3. REPORT TYPE AND DATES COVERED
	May 2003	Annual (16 Apr 02 - 15 Apr 03)

4. TITLE AND SUBTITLE
New Approaches for Early Detection of Breast Tumor Invasion or Progression

5. FUNDING NUMBERS
DAMD17-01-1-0130

6. AUTHOR(S)
Yan-Gao Man, M.D., Ph.D.

7. PERFORMING ORGANIZATION NAME(S) AND ADDRESS(ES)
American Registry of Pathology
Washington, DC 20306

E-Mail: man@afip.osd.mil

8. PERFORMING ORGANIZATION REPORT NUMBER

9. SPONSORING / MONITORING AGENCY NAME(S) AND ADDRESS(ES)

10. SPONSORING / MONITORING AGENCY REPORT NUMBER

11. SUPPLEMENTARY NOTES
Original contains color plates: All DTIC reproductions will be in black and white.

12a. DISTRIBUTION / AVAILABILITY STATEMENT
Approved for Public Release; Distribution Unlimited

12b. DISTRIBUTION CODE

13. ABSTRACT (Maximum 200 Words)

None provided

14. SUBJECT TERMS
No subject terms provided

15. NUMBER OF PAGES
132

16. PRICE CODE

17. SECURITY CLASSIFICATION OF REPORT	18. SECURITY CLASSIFICATION OF THIS PAGE	19. SECURITY CLASSIFICATION OF ABSTRACT	20. LIMITATION OF ABSTRACT
Unclassified	Unclassified	Unclassified	Unlimited

Table of Contents

Introduction

To assess interactions between epithelial (EP) and myoepithelial (ME) cells in association with breast tumor progression and invasion, a double immunostaining technique with antibodies to smooth muscle actin (SMA) and estrogen receptor (ER) was used to elucidate both the ME and EP cells in mammary tissues harboring ductal carcinoma in situ. Single or clusters of EP cells with a marked diminution or a total loss of ER expression were found immediately overlying focally disrupted ME cell layers, in contrast to the dominant population of ER (+) cells within the same duct that showed no associated ME cell layer disruptions. This study attempted to confirm our previous findings on a larger number of cases, and to compare the immunohistochemical and molecular biological profiles of the ER (-) cells overlying disrupted ME cell layers with those of adjacent ER (+) cells and surrounding stromal (ST) cells. Since ME cell layers are physical barriers protecting the microenvironment and integrity of EP cells, and the disruption of ME cell layers is an absolute pre-requisite for breast tumor invasion, the outcomes of this project could have significant values in early detection of breast tumor progression and/or invasion.

Body

Statement of work

A total of 7 tasks were listed in the Statement of Work of the original proposal:

Task 1. To repeat our previous studies and to identify epithelial (EP) cells overlying disrupted myoepithelial (ME) cell layers (months 1-6).

a. Select 500 female cases of ductal carcinoma in situ (DCIS) from our file with detailed information regarding age, race, and follow-up data
b. Retrieve paraffin and frozen tissue blocks, and make 6-8 serial sections for each case
c. Stain the first and the last sections of each case with H & E for morphological assessment
d. Immunostain 3-4 sections from each case with antibodies to estrogen receptor (ER) and smooth muscle actin (SMA)
e. Observe stained sections to identify cells overlying disrupted ME cell layers
f. Select the cases with cells overlying disrupted ME cell layers

Task 2. To compare the biological behavior of cells overlying a disrupted ME cell layer with that of adjacent cells within the same duct (months 6-9)

a. Make 40-50 serial sections for each of the selected cases
b. Immunostain sections with different bio-markers that have been found associated with more aggressive biological behavior

Task 3. To microdissect phenotypically different EP cells and the surrounding ME and stromal (ST) cells for molecular biological analyses (months 9-12)

Task 4. To compare the frequency and pattern of loss of heterozygosity (LOH), and clonality among EP, ME, and ST cells (months 12-20)

Task 5. To assess the gene expression pattern in cells from frozen section sections with cDNA expression array technique, and to generate probes based on sequences exclusively or mainly expressed in cells overlying disrupted ME cell layers (months 20-24)

Task 6. To apply the probes to both paraffin and frozen sections, to identify the gene expressing cells and their morphologic features (months 24-32)

Task 7. To correlate the laboratory findings with that of clinical following-up data (months 32-36).

Experimental procedures:

Consecutive sections were made from formalin-fixed, paraffin-embedded breast tissues from over 400 patients with various grades of ductal carcinoma in situ (DCIS), and double imunostained for ER and SMA. Cross sections of all ducts lined by ≥ 40 EP cells were examined for a focal ME cell layer disruption, defined as an absence of ME cells, resulting in a gap equal to or greater than the combined size of 3 EP or ME cells. A focal loss of ER expression was defined as marked diminution or a total loss of ER staining in cells immediately overlying a disrupted ME cell layer, in contrast to strong ER expression in adjacent cells within the same duct.

After immunostaining for ER and SMA, cells overlying disrupted ME cell layers, adjacent ER (+) cells within the same duct, adjacent stromal (ST) cells, and other controls were microdissected for DNA extraction and assessment for loss of heterozygosity (LOH) and microsatelite instability (MI), using PCR amplification with a panel of DNA markers at 6 chromosomes. The frequency and pattern of LOH and MI among samples were compared.

Consecutive sections were also prepared from frozen breast tissues of patients with DCIS and invasive ductal carcinomas (IDC), and were double immunostained for ER and SMA. Immunostained sections were examined for ER expression and focal ME cell layer disruptions. ER (-) cells overlying disrupted ME cell layers and adjacent (+) cells within the same duct in DCIS, along with cytologically and immunohistochemically similar cells in IDC, were microdissected for RNA extraction, using the RNA extraction kits from Arcturus Engineering, Inc (Mountain View, CA). The RNA extracts were subjected to RT PCR amplification. The gene expression profiles among samples were compared, using the software and reagents from Affymetrix, Inc (Santa Clara, CA) and SuperArray Bioscience Corporation (Frederick, MD).

A total of 7 biotin-labeled probes and detection kits from our collaborators, DAKO Corporation (Carpinteria, CA), and Sigma (St. Louis, MO) have been using in both paraffin-embedded and frozen sections from selected cases, to establish and optimize the in situ hybridization method that will be used with the new probes generated by our own study.

All above experimental procedures were carried out according to the methods described in the proposal without any major modifications. Also, all the laboratory efforts have been strictly adhered to address the issues listed in "Statement of Work".

Key research accomplishments

All the laboratory procedures for Tasks 1 to 4 had been completed, and the outcomes have been reported and published (see below).

The laboratory protocols for Tasks 5 and 6 have been established and optimized. Preliminary studies in selected cases had been carried out before April 15, 2003, and main experiments have been undertaken since then. The preliminary results from these studies are in a total agreement with our hypotheses. These results will be summarized and presented to the related international and national conferences, and submitted to journals for publications this year (2003).

The clinical follow-up data for Task 7 for a portion of the selected cases have been collected

Reportable outcomes

During year 2002 to 2003, the following reportable outcomes were generated:

1. A total of 12 abstracts that exclusively address the issues listed in the proposal were accepted for presentation at international or national conferences, and published in indexed journals or references (1-12).
2. Four manuscripts that exclusively address the issues listed in the proposal had been submitted for publication (13-16).
3. Five additional manuscripts that exclusively address the issues listed in the proposal are near completion, and will be sent out for publication in 2003.
4. Four related papers were published (17-20).

Conclusions

1. Of 220 ER (+) cases with a total of 5,698 duct cross sections examined so far, 94 (42.7%) contained disrupted ME cell layers with a total of 405 focal disruptions. Of these disruptions, 350 (86.4%) were subjacent to cells with focal losses of ER expression, while only 55 (13.6%) were associated with cells showing a strong ER expression. These findings are consistent with those of our previous studies (1), suggesting that focal losses of ER expression in EP cells and disruptions of subjacent ME cell layers are correlated events in ER (+) tumors.

2. Of 100 cases with various grades of ER (-) tumors evaluated so far, focal disruptions of ME cell layers were found in about a half of the cases. These focal ME cell layer disruptions, however, appeared to correlate with either a focal loss or elevation of p27 expression, suggesting that the progression and/or invasion of ER (-) tumors might differ from those of ER (+) tumors.

3. Several tumor suppressor gene products have been found co-expressed in ME cell layers, and a diminution or absence of these proteins correlated with an increased frequency of ME cell layer disruptions. A substantially higher cell proliferation rate was seen in ducts with disrupted ME call layers than ducts with intact ME cell layers, suggesting that EP cells overlying disrupted ME cell layers may have a more aggressive biologic behavior.

4. As previous studies have shown that it is difficult or impossible to utilize immunostained tissues pre-treated with antigen unmasking methods for molecular analyses, an innovative antigen retrieval protocol that satisfies both immunohistochemical and subsequent molecular assessments has been developed in our laboratory. This protocol allows us to microdissect double immunostained cells for LOH and MI assessments, to assess the possible correlation between immunohistochemical and genetic alterations.

5. A vast majority of the ER (-) cells overlying disrupted ME cell layers showed a substantially higher frequency and different pattern of LOH and MI, compared to adjacent ER (+) counterparts within the same duct. In a small proportion of cases, however, ER (-) cells showed a substantially lower frequency of LOH and MI than adjacent ER (+) cells, or even displayed no distinct genetic changes. These findings are largely in support of our hypothesis that ER (-) cells overlying disrupted ME cell layers represent a more aggressive clone, while also suggest that a few of these cells might belong to a population involving in a normal replenishment or expansion of ducts.

6. Protocols for Tasks 5 and 6 have been established and optimized, and the preliminary results from recent studies on Tasks 5 and 6 are in a total agreement with the hypotheses in our proposal.

References (Published and submitted papers and abstracts during 2002 to 2003)

1. Man YG, Saenger JS, Strauss B, Vang RS, Bratthauer GL, Chen PY, Tavassoli FA. Focal alterations of p27 expression and subjacent myoepithelial cell layer disruptions are correlated events in ER (-) ductal intraepithelial neoplasia. Proceedings of Department of Defense Breast Cancer Research Program Meeting, Volume 1: P9:14. Orlando, Florida, September 25-28, 2002
2. Man YG, Strauss B, Saenger JS, Tai L, Bratthauer GL, Chen PY, Tavassoli FA. Genetic alterations in ER (-) mammary epithelial cells overlying focally disrupted myoepithelial cell layers. Proceedings of Department of Defense Breast Cancer Research Program Meeting, Volume 1: P9:15. Orlando, Florida, September 25-28, 2002
3. Man YG, Vang RS, Saenger JS, Strauss B, Bratthauer GL, Chen PY, Tavassoli FA. Co-expression of maspin and wilms' tumor 1 proteins in mammary myoepithelial cells--- Implication for tumor progression and invasion. Proceedings of Department of Defense Breast Cancer Research Program Meeting, Volume 1: P9:16. Orlando, Florida, September 25-28, 2002
4. Man YG, Tai L, Barner Ross, Liang CY, Vang RS, Saenger JS, Shekitka KM, Bratthauer GL, Chen PY, Tavassoli FA. Focal losses of ER expression in epithelial cells and disruptions of subjacent myoepithelial cell layers are correlated events in ER (+) ductal intraepithelial neoplasia. Proceedings of Department of Defense Breast Cancer Research Program Meeting, Volume 1: P9:17. Orlando, Florida, September 25-28, 2002
5. Man YG, Burga A. An antigen retrieval protocol that satisfies both immunohistochemical and subsequent molecular assessments. . Proceedings of Department of Defense Breast Cancer Research Program Meeting, Volume 1: P9:18. Orlando, Florida, September 25-28, 2002
6. Tavassoli FA, Man YG, Strauss B, Vang RS, Bratthauer GL, Chen PY. Morphologically similar stromal cells associated with benign and malignant mammary epithelial tumors display different immunohistochemical and molecular profiles. Proceedings of Department of Defense Breast Cancer Research Program Meeting, Volume 2: P25:18. Orlando, Florida, September 25-28, 2002.
7. Man YG, Shekitka KM. Saenger JS, Tai L, Bratthauer GL, Chen PY, Tavassoli FA. Focal loss of estrogen receptor (ER) expression in ER positive ductal intraepithelial neoplasia is associated with disruption of the immediate subjacent myoepithelial cell layer. Mod Pathol 15(1):42A, 162, 2002
8. Man YG, Shekitka KM, Bratthauer GL, Tavassoli FA. Immunohistochemical and genetic alterations in mammary epithelial cells overlying focally disrupted myoepithelial cell layers. Breast Cancer Res Treat, 76 (Supplement 1): 143: 569, 2002
9. Man YG, Vang RS, Saenger JS, Strauss BL, Barner R, Wheeler D, Liang CY, Bratthauer GL, Mannion C. Development and progression of mammary ductal tumors appear to be mediated by surrounding myoepithelial cells. Accepted by the 2003 USCAP Meeting, and published in mod pathol 15: 39a, 165, 2003
10. RR Zhang, YG Man, BL Strauss, RS Vang, JS Saenger, R Barner, DT Wheeler, CY Liang. A subset of morphologically identifiable mammary myoepithelial (me) cells lacks expression of corresponding phenotypic markers. Accepted by the 2003 USCAP meeting, and published

in Mod Pathol 15: 39A, 165, 2003
11. Man YG, Strauss BL, Saenger JS, Vang RS, Barner R, Wheeler D, Martinez A, Mulshine JL. Identification of invasive precursor cells in normal and hyperplastic appearing breast Tissues. Accepted by the 2003 American association for Cancer Research Meeting and will be published in Cancer Research (Abstract), 2003
12. Man YG, Zhang R. Mattu R. Immunohistochemical assessment of primary lesions of breast epithelial invasion into blood vessels. Breast J, In press (Abstract, 2003).
13. Roy R. Zhang, Yan-Gao Man, Russell Vang, Jeffrey S. Saenger, Ross Barner, Darren T. Wheeler, Chang Y. Liang, Tuyethoa N. Vinh, Gary L. Bratthauer. .A subset of morphologically distinct mammary myoepithelial cells lacks corresponding immunophenotypic markers. Manuscript submitted for publication
14. Yan-gao Man, Lisa Tai, Ross Barner, Russell Vang, Jeffrey S. Saenger, Kris M.Shekitka, Gary L. Bratthauer, Darren T. Wheeler, Chang Y. Liang, Tuyethoa N, Vinh, and Brian L. Strauss. Focal disruptions in mammary myoepithelial cell layers and loss of estrogen receptor expression in overlying epithelial cells are correlated events: Implications for tumor progression. Manuscript submitted for publication
15. Man YG and Burgar A. An antigen unmasking protocol that satisfies both immunohistochemical and subsequent molecular biological assessments. Manuscript submitted for publication
16. Man YG, Magrine GG, Lininger RA, Shen T, Kuhls E, Bratthauer GL, Waldman FM. Morphologically similar epithelial cells and stromal tissues in primary bilateral breast tumors display different genetic profiles: implications for treatment. Manuscript submitted for publication.
17. Garayoa M, Man YG, Marinez A, Cuttitta F, Venzon DJ, Mulshine JL Down regulation of hRNP A2/B1 expression in tumor cells under prolonged hypoxia. Am J respir Cell Mol Biol, 28(1): 80-85, 2003
18. Bratthauer GL, Moinfar F, Stamatakos M, Mezzetti TP, Shekitka KM, Man YG, Tavassoli FA. Combined E-Cadherin and high molecular weight cytokeratin immunoprofile differentiates lobular ductal, and hybrid mammary intraepithelial neoplasias. Human Pathol 33: 620-627, 2002
19. Bratthauer GL, Lininger RA, Man YG, Tavassoli FA. Androgen and estrogen receptor mRNA status in apocrine carcinomas. Dign Mol Pathol 11: 113-118, 2002
33: 620-627, 2002
20. Man YG. Man kicking soccer ball. Intern J surg Pathol. 10(3): 207, 2002

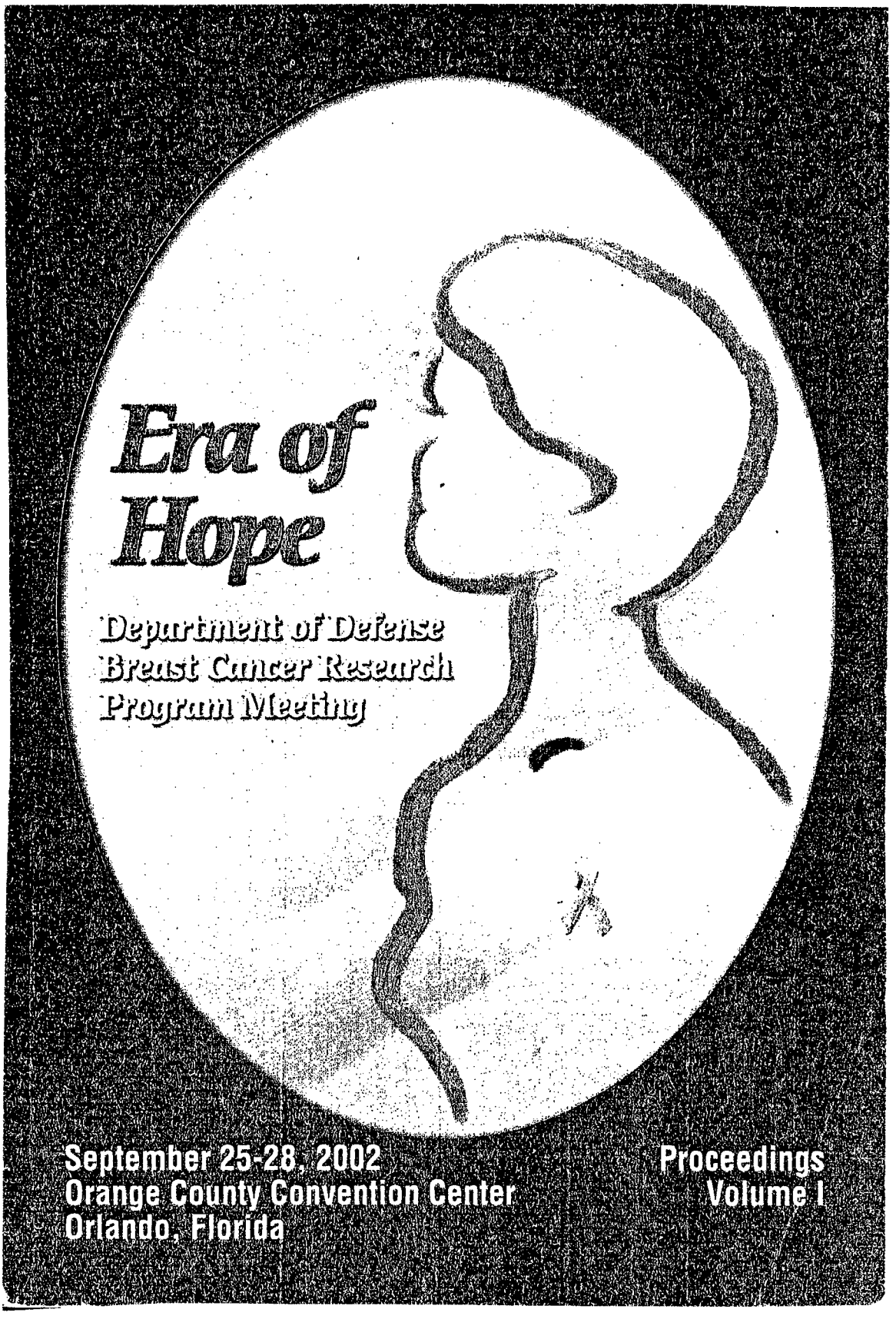

FOCAL ALTERATIONS OF P27 EXPRESSION AND SUBJACENT MYOEPITHELIAL CELL LAYER DISRUPTIONS ARE CORRELATED EVENTS IN ER (-) DUCTAL INTRAEPITHELIAL NEOPLASIA

Yan-gao Man, M.D., Ph.D., Jeffery S. Saenger, M.D., Brian Strauss, M.D., Ph.D., Russell S. Vang, M.D., Gary L. Bratthauer, M.S., M.T., Ping-yu Chen, and Fattaneh A. Tavassoli, M.D.

Department of Gynecologic and Breast Pathology, American Registry of Pathology and Armed Forces Institute of Pathology, 6825 16th Street, NW, Washington, DC 20306

man@afip.osd.mil

Our previous studies, using a double immunostaining technique with antibodies to smooth muscle actin (SMA) and estrogen receptor (ER), revealed that a focal loss of ER expression and disruption of a subjacent myoepithelial (ME) cell layer were correlated events in ER (+) ductal intraepithelial neoplasia (DIN). Focal disruptions of ME cell layers were also found in various grades of ER (-) DIN. This study intended to assess whether ME cell layer disruptions in ER (-) DIN may correlate with a deregulated expression of p27, a cyclin dependent kinase inhibitor that arrests cell division.

Consecutive sections were made from formalin-fixed, paraffin-embedded breast tissues from 100 patients with ER (-) DIN. Two adjacent sections were double immunostained with [1] p27 plus SMA, and [2] SMA plus a mixture of antibodies to Ki-67, Cyclin A and D3. Cross sections of all ducts lined by $\geq$ 40 EP cells were examined for focal ME cell layer disruptions and focal alterations of p27 expression, defined as a marked reduction or elevation of p27 staining in cells immediately overlying disrupted ME cell layers. The cell proliferation rates in ducts with an intact and with a disrupted ME cell layer were statistically compared.

Distinct p27 immunoreactivities were seen in a vast majority of the normal ductal and lobular cells. Although the overall level of p27 expression was generally reduced with the progression of lesions and increase of tumor histological grades, a marked reduction or total loss of p27 expression was occasionally seen in normal appearing ducts, and intense p27 immunostaining was seen in some malignant tumors. In contrast, the rate of focal alterations of p27 expression seemed to be linearly correlated with the frequency of ME cell layer disruptions in both normal appearing and neoplastic ducts. Ducts with a disrupted or no distinct ME cell layer displayed a significantly higher cell proliferation rate than ducts with an intact ME cell layer.

These findings suggest that focal alterations of p27 expression and elevated rates of ME cell layer disruptions and cell proliferation might be correlated events. Since the disruption of ME cell layer is an absolute pre-requisite for tumor invasion, elucidation of the dynamic relationship of these events and the underlying mechanism may have significant diagnostic and prognostic values.

The U.S. Army Medical Research and Materiel Command under DAMD17-01-1-0129 and DAMD17-01-1-0130 supported this work.

GENETIC ALTERATIONS IN ER (-) MAMMARY EPITHELIAL CELLS OVERLYING FOCALLY DISRUPTED MYOEPITHELIAL CELL LAYERS

Yan-gao Man, M.D., Ph.D., Brian Strauss, M.D., Ph.D., Jeffery S. Saenger, M.D., Lisa Tai, M.D., Gary L. Bratthauer, M.S., M.T, Ping-yu Chen, and Fattaneh A. Tavassoli, M.D.

Department of Gynecologic and Breast Pathology, American Registry of Pathology and Armed Forces Institute of Pathology, 6825 16th Street, NW, Washington, DC 20306

man@afip.osd.mil

To observe the dynamic alterations of myoepithelial (ME) cells in association with mammary tumor progression, a double immunostaining technique with antibodies to smooth muscle actin (SMA) and estrogen receptor (ER) was used to elucidate the ME and epithelial (EP) cells in mammary biopsies harboring ductal carcinoma in situ. Single or clusters of EP cells with a marked diminution or a total loss of ER expression were found immediately overlying focally disrupted ME cell layers, in contrast to the dominant population of ER (+) cells within the same duct that had no associated ME cell layer disruptions. This study intended to test a hypothesis that these ER (-) cells may represent a more aggressive clone that genetically differs from adjacent ER (+) cells within the same duct.

Consecutive sections were made from formalin-fixed, paraffin-embedded mammary tissues from 220 patients with various grades of ductal intraepithelial neoplasia, and double immunostained for ER and SMA. The cross sections of ducts lined by ≥ 40 EP cells were examined to identify ducts with focal ME cell layer disruptions. The cells overlying disrupted ME cell layers, adjacent ER (+) cells within the same duct, adjacent stromal (ST) cells, and other controls were microdissected for DNA extraction and assessment for loss of heterozygosity (LOH) and microsatellite instability (MI), using PCR amplification with 18 DNA markers at 6 chromosomes. The frequency and pattern of LOH and MI among samples were compared.

The ER (-) cells overlying disrupted ME cell layers and the adjacent ER (+) cells displayed distinct LOH and MI in each of the 18 DNA markers, with highest frequencies at chromosomes 11p and 16q. A vast majority of the cells overlying disrupted ME cell layers showed a substantially higher frequency and different pattern of LOH and MI, compared to adjacent ER (+) counterparts within the same duct. In a small proportion of cases, however, ER (-) cells showed a substantially lower frequency of LOH and MI than adjacent ER (+) cells, or even displayed no distinct genetic changes.

Overall, ER (-) cells overlying disrupted ME cell layers among different foci and cases displayed a more homogeneous genetic profile than their ER (+) counterparts within the same duct.

These findings are largely in support of our hypothesis that ER (-) cells overlying disrupted ME cell layers represent a more aggressive clone, while also suggest that a few of these cells might belong to a population involving in a normal replenishment or expansion of the duct.

The U.S. Army Medical Research and Materiel Command under DAMD17-01-1-0129 and DAMD17-01-1-0130 supported this work.

CO-EXPRESSION OF MASPIN AND WILMS' TUMOR 1 PROTEINS IN MAMMARY MYOEPITHELIAL CELLS---IMPLICATION FOR TUMOR PROGRESSION AND INVASION

Yan-gao Man, M.D., Ph.D., Russell S. Vang, M.D., Jeffery S. Saenger, M.D., Brian Strauss, M.D., Ph.D., Gary L. Bratthauer, M.S., M.T., Ping-yu Chen, and Fattaneh A. Tavassoli, M.D.

Department of Gynecologic and Breast Pathology, American Registry of Pathology and Armed Forces Institute of Pathology, 6825 16th Street, NW, Washington, DC 20306

man@afip.osd.mil

Maspin and Wilms's tumor 1 (WT-1) proteins have been suggested as products of tumor suppressor genes, as they display inhibitory functions on tumor progression in both tissue cultures and animal models. The expression pattern and functions of these two proteins in human mammary tissues, however, have not been established. This study attempted to address these issues with an emphasis on the correlation of the proliferation rate in mammary ductal cells with the expression of these two proteins in surrounding myoepithelial (ME) cells, and with the physical integrity of ME cell layers.

Consecutive sections were made from formalin-fixed, paraffin-embedded mammary tissues from 100 patients with various grades of ductal intraepithelial neoplasia. Three adjacent sections were double immunostained with [1] smooth muscle actin plus Ki-67, [2] maspin plus Ki-67, and [3] WT-1 plus Ki-67 antibodies. The expression status of maspin and WT-1 in the same cells of each case was compared to determine the extent of co-expression of these proteins. The proliferation rates of epithelial (EP) cells in ducts with and without maspin or WT-1 expression, as well as with and without an intact ME cell layer were statistically compared.

Distinct immunostaining and the co-localization of maspin and WT-1 proteins were seen in most morphologically definable ME cells in sections from each of the 100 patients, while they were barely seen in EP or stromal cells. The expression of these proteins were closely correlated with the morphology of ME cells, but were generally independent of the size, length, or architecture of the ducts. Both morphologically normal appearing and neoplastic ducts with a reduced maspin or WT-1expression in surrounding ME cells, or ducts with focally disrupted or no ME cell layers displayed a significantly higher cell proliferation rate than ducts with a normal maspin or WT-1 expression and with an intact ME cell layer.

These findings suggest that maspin and WT-1 proteins may possess inhibitory functions on EP cell growth and consequently suppress progression or invasion of mammary tumors, and that maspin and WT-1 proteins might also impact the functions of ME cells. Since ME cell layers are physical barriers protecting the microenvironment and integrity of EP cells, and preventing an in situ lesion from invasion, quantitative assessments of the expression of maspin and WT-1 proteins in ME cells might have significant diagnostic and prognostic values.

The U.S. Army Medical Research and Materiel Command under DAMD17-01-1-0129 and DAMD17-01-1-0130 supported this work.

FOCAL LOSSES OF ER EXPRESSION IN EPITHELIAL CELLS AND DISRUPTIONS OF SUBJACENT MYOEPITHELIAL CELL LAYERS ARE CORRELATED EVENTS IN ER (+) DUCTAL INTRAEPITHELIAL NEOPLASIA

Yan-gao Man, M.D., Ph.D., Lisa Tai, M.D., Ross Barner, M.D, Chang Y. Liang, M.D, Russell S. Vang, M.D., Jeffery S. Saenger, M.D., Kris M. Shekitka, M.D., Gary L. Bratthauer, M.S., M.T., Ping-yu Chen, and Fattaneh A. Tavassoli, M.D.

Department of Gynecologic and Breast Pathology, American Registry of Pathology and Armed Forces Institute of Pathology, 6825 16th Street, NW, Washington, DC 20306

man@afip.osd.mil

The purpose of this study was to assess the possible correlation between focal losses of estrogen receptor (ER) expression in epithelial (EP) cells and disruptions of subjacent myoepithelial (ME) cell layers. Consecutive sections were made from formalin-fixed, paraffin-embedded breast tissues from 220 patients with various grades of ductal intraepithelial neoplasia, and double immunostained for ER and smooth muscle actin. Cross sections of all ducts lined by ≥ 40 EP cells were examined for a focal ME cell layer disruption, defined as an absence of ME cells, resulting in a gap equal to or greater than the combined size of 3 EP or ME cells. A focal loss of ER expression was defined as a marked diminution or a total loss of ER staining in cells immediately overlying a disrupted ME cell layer, in contrast to strong ER expression in adjacent cells within the same duct.

Of the 220 ER (+) cases with a total of 5,698 duct cross sections examined, 94 (42.7%) contained disrupted ME cell layers with a total of 405 focal disruptions (7.1%). Of these disruptions, 350 (86.4%) were associated with a focal loss of ER expression, whereas 55 (13.6%) were subjacent to cells with a strong ER expression. The frequency of ME cell layer disruptions associated with ER (-) cells was significantly higher ($p < 0.01$) than that associated with ER (+) cells. The frequency and pattern of ME cell layer disruptions were generally independent of the size, length, and architecture of the ducts. The cells overlying disrupted ME cell layers were often architecturally and morphologically indistinguishable from adjacent cells within the same duct on routine H & E stained sections.

This study suggests that a focal loss of ER expression among a group of ER (+) cells and disruption of the subjacent ME cell layer might be correlated events. As the disruption of ME cell layers are an absolute pre-requisite for tumor invasion, these events are possibly associated with progression and/or early invasion of the mammary tumors.

The U.S. Army Medical Research and Materiel Command under DAMD17-01-1-0129 and DAMD17-01-1-0130 supported this work.

AN ANTIGEN RETRIEVAL PROTOCOL THAT SATISFIES BOTH IMMUNOHISTOCHEMICAL AND SUBSEQUENT MOLECULAR ASSESSMENTS

Yan-gao Man, M.D., Ph.D., Ana Burga, M.D., and Ping-yu Chen

Department of Gynecologic and Breast Pathology, American Registry of Pathology and Armed Forces Institute of Pathology, 6825 16th Street, NW, Washington, DC 20306

man@afip.osd.mil

Molecular analysis on DNA extracts from selected areas of immunohistochemically stained sections is a useful approach for studying the direct correlation between genetic and biochemical alterations. Immunohistochemical analyses of a variety of gene products in formalin-fixed, paraffin-embedded tissues, however, require a prior antigen unmasking treatment with enzymes or a high temperature using a microwave oven or a pressure cooker, which are found to substantially damage DNA and RNA structures, making subsequent genetic analyses difficult or impossible. This study attempted to develop a protocol that satisfies both immunohistochemical and genetic assessments.

Consecutive sections were made from formalin-fixed, paraffin-embedded breast tissues, and four adjacent sections were treated for antigen unmasking with [1] microwave irradiation; [2] pressure cooker incubation; [3] our modified protocol; [4] untreated. After immunostaining for a variety of cytoplasmic and nuclear antigens, comparable amounts of cells were microdissected from the same area in each of the four sections pretreated with the above four methods. Microdissected cells were subjected to DNA extraction and PCR amplification with a variety of DNA markers. Amplified PCR products among samples were semi-quantitatively compared.

Compared to other antigen unmasking methods, our protocol appeared to possess the following advantages: [1] better preservation of the morphological details; [2] a substantial reduction of the detachment of tissues from slides; [3] effectiveness on all antibodies tested; [4] consistently higher PCR yield; [5] ability to yield PCR products with higher molecular weights. The PCR efficiency in tissues treated with our protocol was comparable to those of both untreated and non-immunostained tissues. This protocol has been successfully used for the detection of over 30 different proteins that are known to require a prior antigen-unmasking treatment for their elucidation, the in situ detection of estrogen receptor mRNA, as well as both double immunohistochemical staining and subsequent molecular analyses.

The U.S. Army Medical Research and Materiel Command under DAMD17-01-1-0129 and DAMD17-01-1-0130 supported this work.

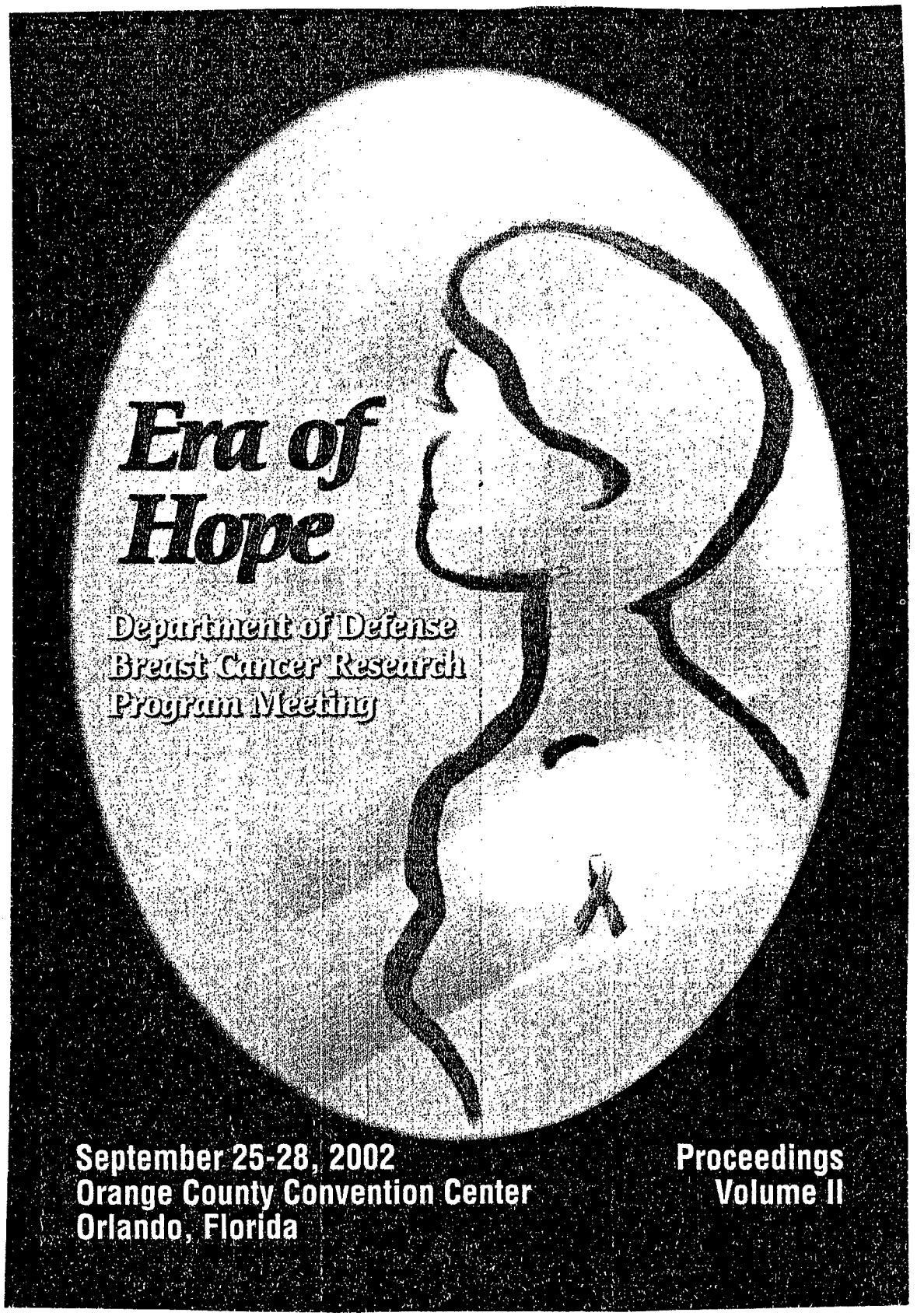
Era of Hope
Department of Defense
Breast Cancer Research
Program Meeting
September 25-28, 2002
Orange County Convention Center
Orlando, Florida
Proceedings
Volume II

MORPHOLOGICALLY SIMILAR STROMAL CELLS ASSOCIATED WITH BENIGN AND MALIGNANT MAMMARY EPITHELIAL TUMORS DISPLAY DIFFERENT IMMUNOHISTOCHEMICAL AND MOLECULAR PROFILES

Fattaneh A. Tavassoli, M.D., Yan-gao Man, M.D., Ph.D., Brian Strauss, M.D., Ph.D., Russell S. Vang, M.D., Gary L. Bratthauer, M.S., M.T., and Ping-yu Chen

Department of Gynecologic and Breast Pathology, American Registry of Pathology and Armed Forces Institute of Pathology, 6825 16th Street, NW, Washington, DC 20306

tavassol@afip.osd.mil

Our previous studies on paraffin embedded tissues from patients with mammary and cervical carcinomas revealed high frequencies of independent and concurrent loss of heterozygosity (LOH) in microdissected epithelial (EP) tumor cells and adjacent or distant stromal (ST) cells. To confirm previous findings on a larger scale and wider spectrum, the current study attempted to compare the immunostaining pattern and the genetic profile in EP and ST cells microdissected from infiltrating syringomatous adenomas and tubular carcinomas, which are two different pathological entities, but with similar reactive background stroma.

Serial sections were made from formalin-fixed, paraffin-embedded mammary tissues from patients with above lesions, and immunostained with a panel of different antibodies. The immunostaining patterns in both the EP and ST components between two lesions were compared. Morphologically similar EP and ST cells in these lesions were microdissected for DNA extraction and assessments for LOH and microsatellite instability (MI), using PCR amplification with a panel of DNA markers at 6 different chromosomes. The frequency and pattern of LOH and MI in samples of two lesions were compared.

The cells from these two lesions displayed a substantially different immunostaining pattern to a majority of the antibodies tested, including those to tumor suppressor gene products, blood vessel components, extracellular matrix molecules, and proliferation-associated proteins. Also, both the EP and ST cells from these two lesions displayed a substantially different frequency and pattern of LOH and MI at multiple chromosomal loci, including 3p, 11p, 13p, 13q and 16q. There was no distinct LOH or MI with multiple DNA markers at chromosome 17p in the ST cells of either lesion, however.

These findings suggest that morphologically comparable ST cells associated with the benign and malignant EP lesions are bio-functionally and genetically different, but closely related with those in their EP counterparts. These findings also suggest that the functions of ST cells in both lesions are not directly subject to regulation by the p53 gene.

The U.S. Army Medical Research and Materiel Command under DAMD17-00-1-0676 supported this work.

VOL. 76, Supplement 1, December 2002

Breast Cancer Research and Treatment

Marc E. Lippman, MD, editor-in-chief

Special Issue

25th Annual

San Antonio Breast Cancer Symposium

Kluwer Academic Publishers

569

Immunohistochemical and genetic alterations in mammary epithelial cells immediately overlying focally disrupted myoepithelial cell layers.

Man YG, Shekitka KM, Bratthauer GL, Tavassoli FA. Armed Forces Institute of Pathology and American Registry of Pathology, Washington, DC

Background: Our previous studies, using a double immunostaining technique with antibodies to smooth muscle actin and estrogen receptor (ER), revealed that focal losses of ER expression in epithelial (EP) cells and disruptions of the subjacent myoepithelial (ME) cell layers were correlated events in ER (+) non-invasive breast lesions. This study attempted to confirm this finding and to assess the genetic profiles of cells overlying disrupted ME cell layers.

Materials and Methods: Tissue sections were made from 220 patients with various types of breast lesions and were double immunostained with the same protocol. Cross sections of ducts lined by ≥ 40 EP cells were examined for focal ME cell layer disruptions, defined as an absence of ME cells, resulting in a gap equal to or greater than the combined size of 3 EP or ME cells. EP cells immediately overlying disrupted ME cell layers and adjacent EP cells within the same duct were microdissected for loss of heterozygosity (LOH) and microsatellite instability (MI) assessment.

Results: Of 5,698 duct cross sections examined, 405 focal disruptions were detected. Of which, 350 (86.4%) were subjacent to cells with a loss of ER expression, while 55 (13.6%) were subjacent to cells with a high level of ER expression. A vast majority of ER (-) cells immediately overlying disrupted ME cell layers displayed a substantially higher frequency or different pattern of LOH and MI, compared to adjacent ER (+) cells within the same duct, while in a small proportion of cases, ER (-) cells showed a marked lower or even no distinct genetic alterations.

Discussion: These results suggest that a vast majority of ER (-) cells overlying disrupted ME cell layers represent an altered clone that may be in the process of early invasion, while a few of these may be involved in a normal expansion or replenishment of the duct.

Supported by the US Army Medical Research and Materiel Command under DAMD 17-01-1-0129 and DAMD 17-01-1-0130 to Yan-gao Man, MD., Ph.D.

Identification Of Invasive Precursor Cells In Normal And Hyperplastic appearing Breast Tissues

Man YG, Strauss BL, Saenger JS, Vang RS, Barner R, Wheeler D, Martinez A*, Mulshine JL*
Department of Gynecologic & Breast Pathology, The Armed Forces Institute of Pathology and American Registry of Pathology, Washington DC 20306; * Department of Cell and Cancer Biology, Medicine Branch, National Cancer Institute, Bethesda, MD

Abstract

We previously reported discreet genetic changes in pre-malignant and adjacent normal appearing bronchial epithelium that were shared with overt cancerous tissues. We recently defined, in the in situ ductal carcinoma, a similar clonal phenotype that showed lost estrogen receptor (ER) expression and were associated with disrupted myoepithelial (ME) cell layers and the basement membrane. The current investigation evaluated if a similar situation existed in normal and hyperplastic breast cells. To define the cell population, paraffin sections harboring normal, hyperplastic, and neoplastic breast tissues were double immunostained with antibodies specific to ME cells, cell growth related proteins, and hormone receptors. Immunostained sections were examined to identify ER (-) cell clusters, defined as a group of ≥ 5 ER (-) cells immediately overlying a disrupted ME cell layer, in contrast to adjacent cells within the same duct that showed intense ER immunostaining and were subjacent to non-disrupted ME cells. The immunohistochemical and genetic features in these clusters were compared to those in their ER (+) counterparts, and to those in invasive lesions.

ER (-) cell clusters were seen in both the normal and hyperplastic appearing ducts in a small portion (≈10%) of the cases. Compared to its ER (+) counterpart within the same duct, the ER (-) cell cluster generally displayed the following unique features: [1] subjacent to disrupted ME cell layer and basement membrane; [2] more abundant stromal and vascular structures in the surrounding, [3] a lower expressing rate of a growth inhibitor, p27; [4] a higher cell proliferation rate; [5] a higher frequency of loss of heterozygosity (LOH) and micro-satellite instability (MI). These features were comparable to those seen in invasive mammary tumors.

Conclusions: ER (-) cell clusters in both normal and hyperplastic appearing ducts generally displayed a biologic behavior similar to that of invasive mammary tumors, suggesting that a subset of these ER (-) cell clusters might represent the direct precursors of invasive tumors.

This study was supported by grants, DAMD17-01-1-0129 and DAMD17-01-1-0130, from The Congressionally Directed Medical Research Programs to Yan-gao Man, MD., Ph D.

DO NOT FOLD
Type Abstract in Box Below

IMMUNOHISTOCHEMICAL ASSESSMENT OF PRIMARY LESIONS OF BREAST EPITHELIAL INVASION INTO BLOOD VESSELS

Man YG*, Zhang R, Mattu R.
Department of Gynecologic and Breast Pathology, Armed Forces Institute of Pathology and American Registry of Pathology, 6825 16th Street, NW., Washington DC 20306

Introduction: Recent studies have shown that blood vessel invasion of epithelial (EP) cells is a high-risk prognostic factor for patients with breast cancer. This study intended to assess the primary lesions, which may facilitate elucidation of the mechanism of blood vessel invasion.
Materials and Methods: Paraffin sections from over 100 patients with benign and in situ breast cancer were double immunostained with antibodies specific to EP cells, blood vessels, and white blood cells. Immunostained sections were examined to identify the primary lesion, defined as a distinct duct or lobule that associates with the stromal component at one end and extends into a blood vessel at the other end.
Results: Distinct primary lesions with vessel invasion were seen in both benign and in situ breast tissues. Compared to adjacent histologically comparable structures, these lesions often displayed several unique features: [1] increased blood vessels and white blood cell aggregates in the surrounding; [2] infiltration of while blood cells; [3] loss or reduction of ER expression; [4] disruptions of myoepithelial cell layers.
Conclusions: These findings suggest that vessel invasion may be triggered by or associated with white blood cells.
Acknowledgement: Supported by grants DAMD17-0-11-0129 and DAMD17-01-1-0130 from Congressionally Directed Medical Research Programs to Yan-gao Man.

Multidisciplinary Symposium on Breast Disease
February 13-16, 2003
Ritz-Carlton, Amelia Island

ABSTRACTS MUST BE RECEIVED BY December 15, 2002

* At least one of the authors must be registered at the symposium.

Abstract to be presented by:

Yan-gao Man
First Name MI Last Name

Complete Mailing Address

Dept. of Gyn & Breast Pathology
6825 16th Street, NW
Washington DC 20306-6000

Phone 202-782-1612 Fax 202-782-3939
Email man@afip.osd.mil

* All abstracts will be published in The Breast Journal

INQUIRIES concerning preparation, submission or acceptance of abstracts should be directed to Dr. Shahla Masood. (904) 244 -3430.

MAIL A COPY OF THIS SHEET AND A COPY ON DISK IN IBM FORMAT TO:

Shahla Masood, MD
University of Florida HSC/ Jacksonville
655 West 8th Street, Box 268
Jacksonville, Fl 32209

INSTRUCTIONS

1. Title is in all capital letters, flush with left margin of box. Type last name followed by initials. Include names of all authors, their institutional affiliations, cities, states and zip codes. **Mark the presenting author with an asterisk.**
2. Title should include significant words that reflect the content of the abstract. Abstracts should adequately describe the objectives and results of the research. Each abstract should contain (a) introductory sentence indicating the purpose of the study; (b) brief description of pertinent experimental procedures; (c) summary of the data; (d) statement of conclusion.
3. Abbreviations may be used in the abstract text if defined. Spell out the term in full at first mention and follow with the abbreviation in parenthesis.
4. **DO NOT USE A DOT MATRIX PRINTER.**
5. **ABSTRACT SUBMITTERS FROM OUTSIDE OF THE U.S.:** If you cannot assure that the original abstract will arrive by the December 15, 2002 deadline, you may fax it to (904) 244-5565. However, be sure to indicate on the fax that you are sending the original and disk immediately, and use EXPRESS DELIVERY SERVICE.
6. Acceptance letters and guidelines for presenters will be sent to the presenters in December.

MODERN PATHOLOGY

Vol. 15, No. 1
January 2002

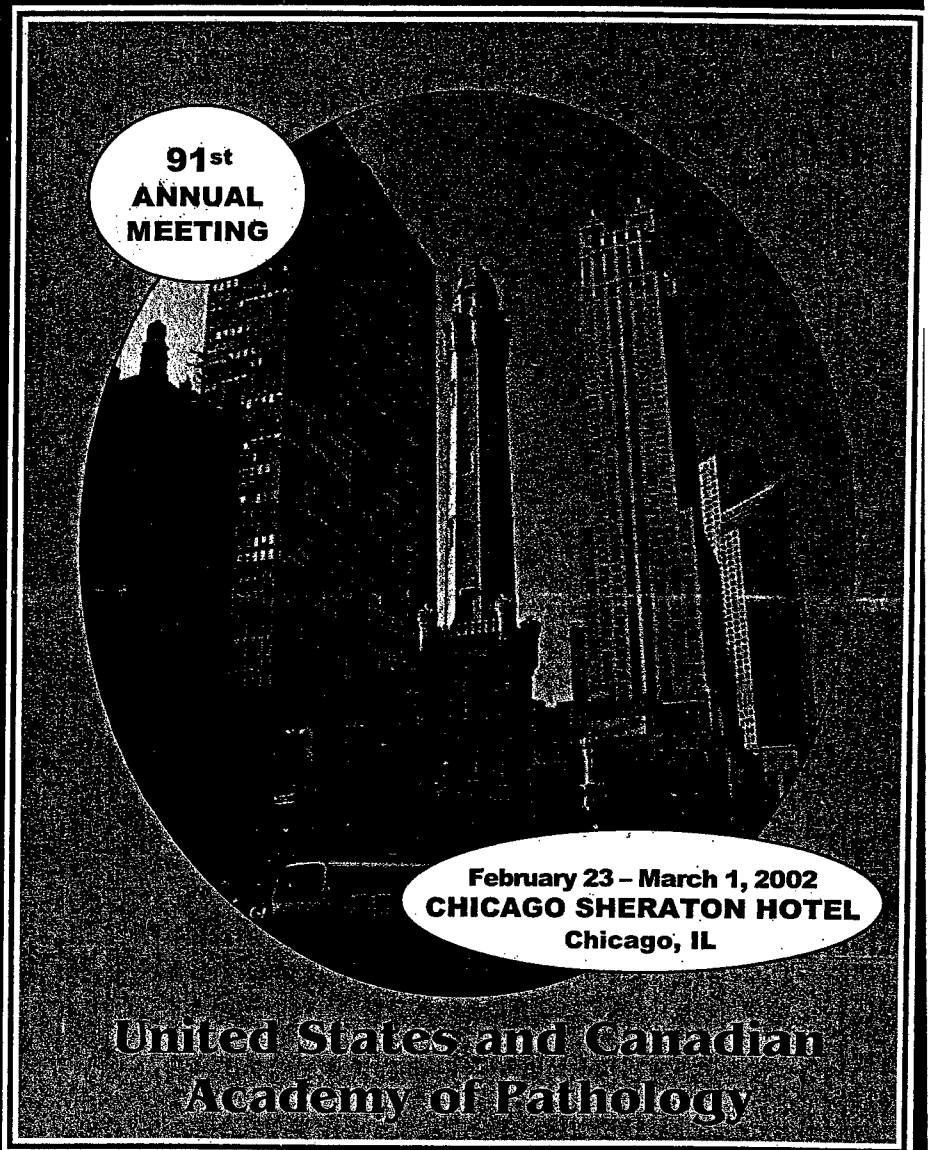

An Official Journal of The
United States and Canadian
Academy of Pathology, Inc.

http://modpath.uscapjournals.org

162 **Focal Loss of Estrogen Receptor (ER) Expression in ER Positive Ductal Intraepithelial Neoplasia Is Associated with Disruptions of the Immediate Subjacent Myoepithelial Cell Layer**

YG Man, KM Shekitka, JS Saenger, L Tai, GL Bratthauer, PY Chen, FA Tavassoli. Department of Gynecological and Breast Pathology, The Armed Forces Institute of Pathology and American Registry of Pathology, Washington, DC.

Background: Our previous study using double immunostaining with antibodies to ER and smooth muscle actin (SMA) revealed patchy disruptions in the myoepithelial (ME) cell layer immediately subjacent to ER negative epithelial (EP) cells in mammary ducts with ostensibly EP proliferation.

Design: To confirm this finding on a larger scale, the same protocol was used to assess the association between ER expression and disruptions of ME cell layers on paraffin tissue sections from 125 patients with various grades of ductal intraepithelial neoplasia. The disruption of ME cell layers is defined as widening of a ME cell layer gap equal to the diameter of at least 3 EP cells in the cross section of a given duct. Focal loss of ER expression is defined as a significant reduction or complete loss of ER expression in a cluster of EP cells immediately overlying the disrupted ME cell layer, compared to strong ER expression in the remaining neoplastic cells within the same duct. The total number of the cross sections of ducts with proliferative changes was counted. All profiles with disrupted ME cell layers were photographed, and prints were made at a magnification of 400-800X for immunohistochemical and morphological assessments.

Results: Of the 125 cases, 62 (49.6%) showed disrupted ME cell layers; 246 (6.6%) disruptions were detected from 3,733 evaluated duct cross sections. Of the 62 cases with disrupted ME cell layers, 40 (64.5%) contained less than 4 and 22 (35.5%) displayed more than 4 disruptions. Of these disruptions, 225 (91.5%) from 59 cases were associated with focal loss of ER expression and 21 (8.5%) from 9 cases were subjacent to ER positive cells. The frequency and pattern of disruptions was generally independent of the size of ducts or the degree of neoplasia. The cells overlying the ME disruptions were generally morphologically indistinguishable from adjacent neoplastic cells within the same duct on routine H&E sections.

Conclusions: These findings suggest that focal loss of ER expression might play an important role in tumor progression and that double immunostaining with SMA and ER could assist in detection of incipient cancer invasion.

Acknowledgement: This study is supported by Congressionally Directed Medical Research Programs, The Idea Award (BC001187) and Career Development Award

MODERN PATHOLOGY

Vol. 16, No. 1
January 2003

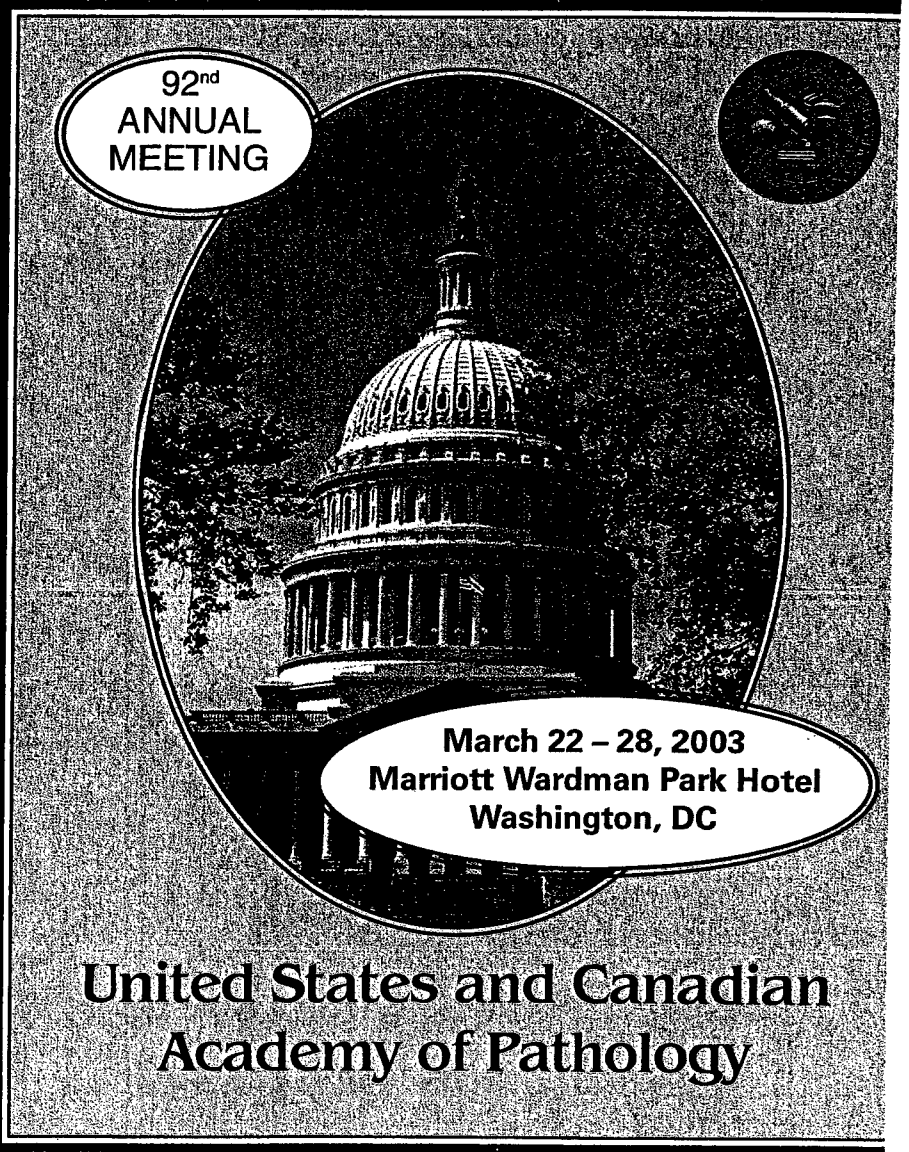

An Official Journal of The
United States and Canadian
Academy of Pathology, Inc.

http://modpath.uscapjournals.org

165 **Development and Progression of Mammary Ductal Tumors Appear To Be Mediated by Surrounding Myoepithelial Cells**

YG Man, RS Vang, JS Saenger, BL Strauss, R Barner, DT Wheeler, CY Liang, GL Bratthauer, C Mannion. Armed Forces Institute of Pathology and American Registry of Pathology, Washington, DC; Hackensack University Medical Center, Hackensack, NJ.

Background: Our previous studies revealed the co-localization of tumor suppressor proteins, maspin and Wilms' tumor 1, in most morphologically identifiable myoepithelial (ME) cells; ducts without these proteins or without intact ME cell layers showed a significantly higher proliferation rate than their counterparts, suggesting that ME cells may impact the biologic behavior of subjacent epithelial cells. The focus of the current study was to assess the possible roles of ME cells in development and progression of mammary ductal tumors.

Design: Sections from normal and non-invasive breast lesions were immunostained with antibodies to ME cells, tumor suppressors and growth related proteins. Cells of interest were microdissected and assessed for micro-satellite instability (MI) or loss of heterozygosity (LOH) with a panel of markers altered in invasive tumors.

Results: ME cell layer disruptions were seen in a subset of normal, hyperplastic, and in situ neoplastic ducts. Compared to cells near an intact ME cell layer, cells subjacent to a disrupted ME cell layer often displayed several unique features: [1] alterations in the duct architecture and cell polarity or density; [2] reduced or lost expression of estrogen receptor; [3] reduced or lost expression of growth inhibitors; [4] elevated

was evaluated by 3 of the above authors without knowledge of response data and results were correlated with response to therapy. Membranous staining of EGFR and nuclear staining of p27, Cyclin D1 and PPARγ were defined as positive. Chi-square test is used for statistical analysis.

Results: Positive staining in >25% of tumor cells for p27 and in >20% of tumor cells for Cyclin D1 was significantly associated with response to trastuzumab based therapy. EGFR and PPARγ staining did not show a significant correlation with response.

Marker (positive staining)	Response (% Patients)	No Response (% Patients)	p value
EGFR	80	55	Not Significant
p27	75	40	<0.05
Cyclin D1	55	0	<0.05
PPARγ	25	14	Not Significant

Conclusions: Cyclin D1 and p27 may be important markers for predicting response to trastuzumab based therapy in patients with metastatic breast cancer and the usage of these markers for selection of therapy in this clinical setting merits further study.

A Subset Of Morphologically Distinct Mammary Myoepithelial Cells Lacks Corresponding Immunophenotypic Markers

Roy R. Zhang, MD, Yan-Gao Man, MD, PhD., Russell Vang, MD, Jeffrey S. Saenger, MD, Ross Barner, MD, Darren T. Wheeler, MD, Chang Y. Liang, MD, Tuyethoa N. Vinh, MD, Gary L. Bratthauer, MS, MT.

Address of corresponding author:

Yan-Gao Man, MD, PhD.

Department of Gyn & Breast Pathology

Armed Forces Institute of Pathology,

6825 16th Street, NW

Washington, DC 20306

USA

Tel: (202) 782-1612, Fax: (202) 782-3939, E-mail: man@afip.osd.mil.

Key Words: Myoepithelial cells, Phenotypic markers; Double immunostaining; Smooth muscle actin; Cytokeratins

Running title: Myoepithelial cell immunophenotypic markers

The opinions and assertions contained herein are the private viewpoints of the authors and do not reflect the official views of The Department of Defense or The Army.

Abstract

Immunohistochemical staining for smooth muscle actin (SMA) is commonly used for identifying mammary myoepithelial (ME) cells, whose presence or absence is usually a reliable criterion for differentiation between in situ and invasive carcinomas. However, some ME cells that are morphologically identifiable on H&E sections fail to stain for SMA. This study intended to assess whether these SMA(-) cells also lack the expression of other ME cell immunophenotypic markers. H&E and SMA immunostained sections from 175 breast cancer patients were examined. Three cases were found to harbor ducts that displayed morphologically distinct ME cell layers by H&E examination, but showed no SMA immunostaining in ≥ 1/3 or the entire of the ME cell layer. Eight additional consecutive sections from each of these three cases were stained for SMA, using a black chromogen. Each section was then re-stained using one of 8 additional myoepithelial markers that are supposed to exclusively or preferentially stain normal ME, using a red chromogen. These same ducts with SMA (-) ME cells were re-examined for the expression of other 8 ME markers. A subset of SMA(-) ME cells also failed to display immunoreactivity for other markers, including Calponin, Maspin, Wilms' tumor-1, CD10, smooth muscle myosin-heavy chain, and cytokeratins 5, 14 , and 17 (CK5, CK14, and CK17, respectively). Some SMA(-) ME cells, however, displayed immunoreactivities for Maspin, CK5, CK14, and CK17. The distribution of these ME cells appeared to be independent of the ductal size, length, and architecture. These findings suggest that these SMA (-) cells may have genetic and biochemical properties that differ from their SMA (+) counterparts, and that the alterations in ME cells may impact the biological behavior of the epithelial cells.

Introduction

The myoepithelial (ME) cell is one of the essential cell populations within the human breast tissue. With few exceptions, the epithelial (EP) component of both normal breast tissue and non-invasive breast lesions are generally surrounded by a distinct layer of ME cells. Although some of the recent studies have suggested that both ME and EP cells are derived from a common progenitor (1), the definite origin and cell kinetics of ME cells remain elusive, as they apparently possess immunohistochemical and ultrastructural features of both EP and smooth muscle cells (2). ME cells have been traditionally regarded as having two roles: a structural barrier, physically separating the mammary EP cells from the surrounding stroma; and a contractile function, assisting with milk secretion (3). Recent studies, however, have suggested that ME cells may be an effective host defense against tumor invasion, since they secrete high levels of Maspin and various proteinase inhibitors, which could prevent tumor cell growth in the tissue culture and animal models (4-6). Our recent studies have further revealed the co-localization of two tumor suppressor gene products, Maspin and Wilms' tumor 1 (WT-1), exclusively in mammary ME cells (7). In a vast majority of the cases, the expression of these two proteins are linearly decreased with tumor progression; and the loss of these proteins, or the focal disruptions of ME cell layers, leads to a significantly higher proliferation rate in subjacent EP cells (7-8).

Although ME cells are readily identified by H&E stain in a majority of breast tissue sections, they are often indistinguishable from subjacent stromal myofibroblastic cells and smooth muscle cells of small vessels. Immunohistochemical staining for smooth muscle actin (SMA) has been commonly used to assist in the identification of ME

cells (9). However, we have repeatedly noted that some ME cells, which are morphologically identifiable on H&E sections, fail to stain for SMA. Our observations are in an agreement with two published reports, which have showed that about 4-6% of morphologically recognizable ME cells in H&E sections fail to display SMA immunoreactivity (10-11). This study attempted to assess whether these SMA(-) cells also lack the expression of 8 additional markers that are exclusively or preferentially present in ME cells.

Materials and Methods

1. Tissue samples and case selection

Paraffin-embedded tissue blocks from female patients were retrieved from the files of Armed Forces Institute of Pathology. Consecutive sections at 4-5 μm thick were cut and placed on positively charged microscope slides for morphological and immunohistochemical assessments. Morphological classifications of the lesions were based on published criteria (2). A total of 175 cases with distinct ME cells, defined as a continuous layer of spindle or cuboidal shaped cells on H&E stained material, that overlie the basement membrane and embrace the EP cells, were selected for this study. Among the 175 cases, all contained non-invasive lesions, including ductal and lobular carcinoma in situ and sclerosing adenosis, and a few cases had invasive components.

2. ME cell markers and other immunohistochemical reagents

Based on our experience and published reports (12-30), a total of 9 antibodies that are specifically or preferentially reactive with ME cells were selected for this study. These included anti-smooth muscle actin (SMA), anti-smooth muscle myosin-heavy chain (SM-MHC), anti-CD10, anti-Calponin, anti-Maspin, anti-Wilms' tumor-1 (WT-1), and anti-cytokeratins 5, 14 , and 17 (CK5, CK14, and CK17). The main features of these antibodies and the manufacturers' recommended immunostaining protocols are listed in Table 1. Other immunohistochemical reagents, including biotinylated anti-mouse and rabbit IgG, ABC detection kit, and chromogen kits, including 3,3'-diaminobenzidine (DAB), Fast Red, and 3-amino-9-ethylcarbazole (AEC), were purchased from Novocastra (Vector Laboratories Inc., Burlingame, CA). Trypsin and protease K recommended by the manufacturer for antigen retrieval were purchased from Sigma (St. Louis, MO). A

microwave oven was commercially purchased and inspected by a certified technician of our institute. A pressure cooker designated for antigen unmasking along with antigen retrieval solution was bought from Biocare Medical (Walnut Creek, CA). Other related reagents were purchased from Fisher Scientific (Pittsburgh, PA).

3. Immunohistochemical staining

A preliminary study was carried out to optimize the immunostaining condition for all antibodies selected for this study. First, each of the 9 antibodies was tested strictly following the manufacturers' recommended protocols, including the methods of antigen retrieval and the length of primary antibody incubation time. Then, each antibody was tested, using our published protocol, which involves an overnight incubation of deparaffinized sections at 70 ^{0}C in antigen retrieval solution and a 3-4 hour or overnight incubation of the primary antibody (31). Two adjacent sections stained using our protocol and the manufacturers' recommended protocols were compared for specificity and sensitivity. As our protocol consistently yielded stronger or comparable immunostaining than that obtained by manufacturers' recommended protocol for each of the antibodies, the final staining for all the 175 cases with SMA and double immunostaining with additional markers in selected cases (see below) was carried out using our published protocol (31).

4. Identification of SMA (-) cases and double immunostaining for other markers

All immunostained sections with SMA and the consecutive H&E stained sections from the 175 patients were independently reviewed by two investigators. Ducts lined by $\geq$ 50 EP cells with distinct ME cell layers on H&E stained sections were examined for SMA immunoreactivity. Three cases were found to contain ducts that displayed

morphologically distinct ME cell layers in H&E sections, while ME cells at $\geq$ 1/3 or the entire layer were devoid of SMA immunostaining. A total of 8 consecutive sections from each of the three selected case were used for a double immunostaining with black and red chromogens to simultaneously highlight two different antigens, using our published protocols (31-32). Briefly, all 8 sections were first immunostained for SMA with a black chromogen. Then, each section was re-stained for one of the 8 additional ME markers with a red chromogen. The same ducts with SMA (-) ME cells were examined for expression of the other markers. In addition, sections from each of the three cases were immunostained for estrogen receptor (ER) and cytokeratin 8, to exclude the possibility that these SMA(-) cells may be epithelial in nature.

Results

All 3 of the selected cases spanned a morphologic spectrum ranging from columnar cell hyperplasia to ductal carcinoma in situ. Case 1 (columnar cell hyperplasia) contained two ducts of interest lined by about 500 EP cells and surrounded by morphologically distinct ME cell layers on the H&E stained section (Figure-1a). The ME cells were cuboidal shaped, morphologically similar to their EP counterparts. The density of the ME cells in this case appeared to be markedly higher than that seen in any other case (Figure 1a). The ME cells in about 2/3 of the layer showed distinct and strong SMA immunostaining, whereas the cells in approximately 1/3 of the layer were devoid of SMA immunostaining (Figure 1b). The SMA (+) and (-) cells were morphologically indistinguishable on both H&E and immunostained sections. These SMA (-) ME cells were present on all 8 sections, but with decreasing numbers. In the double immunostained sections, these SMA (-) ME cells were also non-reactive for SM-MHC (Figure 1c), WT-1 (Figure 1d), CD10 (Figure 1e), and Calponin (Figure 1f). These SMA (-) cells, however, were positive for CK14 (Figure 1i) and CK17 (Figure 1j), and inconsistent weakly positive for CK5 (Figure 1h) and Maspin (Figure 1g).

Cases 2 and 3 contained ductal carcinoma in situ, intermediate grade and low grade, respectively. The ducts were surrounded by morphologically distinct ME cell layer in H&E stained sections (Figure 2a). These ME cell layers were attenuated, consisting of elongated spindle cells with dark and compressed nuclei. The EP cells in these ducts were grade 2-3 nuclear atypia. The entire ME cell layer was devoid of SMA immunostaining (figure 2b), and these cells were present in all 8 sections with similar

numbers. In double immunostained sections, these SMA (-) cells were also devoid of distinct immunostaining for any of the additional 8 markers (Figure 2c-2f).

In addition, the SMA(-) cells in all three cases showed distinct negativity to ER and cytokeratin 8, in sharp contrast to the overlying epithelial cells, which displayed distinct immunopositivity to cytokeratin 8 and or ER (data not shown). The distribution of these SMA (-) ME cells appeared to be independent of the ductal size, length, and architecture.

Since neoplastic epithelial cells compressed at the periphery of nests of invasive carcinoma may mimic a myoepithelial layer (22) and appear SMA (-), it should be emphasized that in all cases the DCIS lesions were classic without confusion with invasive carcinoma.

Discussion

The 9 markers used in the current study have been reported to be exclusively or preferentially present in ME. SMA is one of the microfilamentous contractile polypeptides and is present in cells with myogenous features. In human breast tissues, SMA immunostaining has been reported in about 95% of the ME cells of the normal ducts and lobules, as well as in non-invasive breast lesions (10-11). SMA fails to elucidate about 6% of morphologically identifiable ME cells (10-11), and the reason for this is unknown. The invasive lesions and the rare benign lesion, microglandular adenosis, are devoid of SMA immunoreactivity, because of the lack of surrounding ME cells. False positive SMA staining, however, is not uncommon, due to the cross immuno-reactivity in myofibroblastic cells of the stroma or the smooth muscle cells of small vessels that are commonly located adjacent to the invasive components.

Maspin is a member from the family of the serine proteinase inhibitors (12). It is related to the tumor suppressing activity in breast and prostate cancers (13-14). Reis-Filho et al. described consistent Maspin expression within the cytoplasm and nucleus of the ME cells and ME-derived tumors thereafter(15).

Wilms' tumor 1 (WT-1) functions as a transcription factor regulating gene expression in a similar fashion to p53 (16). The expression of WT-1 in breast carcinoma appears to correlate with the behavior of breast carcinoma (17-18). Our previous study showed that myoepithelial cells also express WT-1, with the reversed relationship of the proliferation index of epithelial cells (7).

Common acute lymphoblastic leukemia antigen (CALLA-CD10) is cell surface metalloendopeptidase. It is also present in human breast ME cells as well as many

nonhematopoietic tissues (19-20). Moritani et al. reported that CD10 is consistently positive in ME cells of normal breast tissue with reduced positivity in ME cells of distended ducts (21), and concluded that CD10 is superior to SMA in differentiating invasive breast cancers from benign entities.

Calponin is restricted to smooth muscle cells, especially cells with contractile capability. Calponin binds tropomyosin and F-actin, and can specifically label the ME cells, but not spindle cells of the stroma. Previous studies have shown that Calponin can be helpful in distinguishing invasive from non-invasion breast lesions, while Calponin staining in ME cells may be occasionally discontinuous or entirely absent in in-situ ductal lesions (22-24).

Smooth Muscle Myosin Heavy Chain (SMMHC) is a cytoplasmic structural protein and is specific for early development of smooth muscle. Working together with other ME cell markers, SMMHC labels the ME cells and helps to distinguish the noninvasive from invasive breast lesions (23, 25).

Cytokeratins are a group of cellular structural proteins in epithelial cells and cells with epithelioid features (26). Cytokeratin 5 (CK5) is found in many non-keratinized epithelia such as luminal cells of the mammary gland and basal cells of the prostate. Bocker et al. suggested that cells with CK5 positivity may represent the stem cells in the adult human breast (1, 27). Cytokeratin 14 and 17 (CK14 and CK17) are reactive predominantly with the basal and ME cell layer (28-29). CK17 is also related to early skin development and wound repairing (30).

In order to assess the phenomenon of the lack of myoepithelial marker expression in histologically evident myoepithelial cells, we undertook a detailed

immunohistochemical analysis of three cases with an expanded panel of myoepithelial markers. In case 1, although all the ME cells surrounding the ducts are morphologically identical or very similar in both H&E and immunostained sections, about 1/3 of the cells were devoid of immunoreactivity for SMA, Calponin, SMMHC, CD10, and WT-1. The other two selected cases also displayed morphologically identifiable ME cells in H&E stained sections. A vast majority of these ME cells were devoid of SMA immunoreactivity. All of these SMA (-) ME cells were also devoid of immunoreactivity to the 8 additional ME markers. Our findings are consistent with those of a recent study, which reveals,in a subset of benign breast lesions and DCIS, a single or few ME cells that fail to show immunoreactivity to three ME cell markers (p63, SMMHC and Calponin), in contrast to the immediate adjacent ME cells, which display distinct positivity to these markers (33). Our study, however, differs from the previous studies (10-11, 33) at four aspects: [1] the SMA(-) cells assessed in our study are morphologically indistinguishable from the adjacent normal ME cells on H&E stained sections; [2] the SMA(-) cells are segmented, accounting for ≥1/3 or the entire population of ME cells in the involved duct; [3] more ME cell markers are tested; [4] our focus is more directed to thoroughly elucidate the detailed immunohistochemical profile than to assess the frequency or morphological correlation of these SMA(-) ME cells.

The mechanism of the loss of myoepithelial markers in ME cells is unknown but could result from the dynamic and the reciprocal interactions between EP and ME cells. It has been well documented that a variety of proteolytic enzymes produced by malignant EP cells could substantially impact the physical integrity or functions of the subjacent ME cells and the basement membrane (34-36). On the other hand, ME cells could

similarly influence the biological behavior of subjacent EP cells. Our recent immunohistochemical studies have revealed the co-localization of Maspin and WT-1, two tumor suppressor gene products, exclusively in mammary ME cells (7). In a vast majority of the cases, the expression of these two proteins are linearly decreased with tumor progression, and the loss of these proteins, or focal disruption of ME cell layers lead to a significantly higher cell proliferation in the subjacent EP cells (7-8). Also, these changes could result from the specific impact of certain chemical compounds. It has been reported that the exposure to lambda-carrageenan could specifically result in filament disassembly and loss of mammary ME cells (37). In contrast, it has been reported that oxytocin could substantially enhance ME cell differentiation and proliferation in the mouse mammary gland (38).

The total loss of all 9 ME cell immunophenotypic markers suggest that these ME cells might have genetic and biochemical properties differing from their SMA (+) counterparts. The significance and consequence of the immunohistochemical changes in ME cells observed in this study are unknown. However, given the fact that the degradation or disruption of the ME cell layer and basement membrane is an absolute pre-requisite for tumor invasion and metastasis, these altered ME cells might impact the biological behavior of the EP cells, making them prone to progression. Our assumption is in an agreement with our previous findings, which have revealed that focal disruptions of ME cell layers could lead to a significantly higher proliferation rate in subjacent EP cells (7-8). Our assumption is also supported by a recent study, which shows that normal and tumor-derived ME cells differ substantially in their ability to interact with luminal breast EP cells for polarity and basement membrane deposition (39). Further studies are

currently in progress to elucidate the biologic behavior and genetic profile of EP cells immediately subjacent to these SMA (-) ME cells.

Acknowledgment

This study was supported in part by grants DAMD17-01-1-0129 and DAMD17-01-1-0130 from The Congressionally Directed Medical Research Programs to Yan-gao Man, MD, PhD.

References

1. Bocker W, Moll R, Poremba C, Holland R, van Diest PJ, Dervan P, Burger H, Wai D, Diallo RI, Brandt B, Herbst H, Schmidt A, Lerch MM and Buchwallow IB. Common adult stem cells in the human breast give rise to glandular and myoepithelial cell lineages: A new cell biological concept. *Lab Invest* 2002;82(6):737-46.
2. Tavassoli FA. *Pathology of the Breast*, 2nd edn. Hong Kong: McGraw-Hill, 1999.
3. Ganong WF. *Review of Medical Physiology*, 15th edn. California: Appleton&Lange, 1992.
4. Sternlight MD, Barsky SH. The Myoepithelial defense: a host defense against cancer. *Med Hypotheses* 1997;48(1):37-46.
5. Sternlight MD, Safarians S, Rivera SP, Barsky SH. Characterization of the extracellular matrix and proteinase inhibitor content of human myoepithelial tumors. *Lab Invest* 1996;74:781-796.
6. Shao ZM, Nguyen M, Alpaugh ML, O'Connell JT, Barsky SH. The human myoepithelial cells exerts antiproliferative effects on breast carcinoma cells characterized by p21WAF1/CIPI induction, G2M arrest, and apoptosis. *Exp Cell Res* 1998;241:394-403.
7. Man YG, Vang RS, Saenger JS, Strauss B, Bratthauer GL, Chen PY, Tavassoli FA. Co-expression of maspin and wilms' tumor 1 proteins in mammary myoepithelial cells---implication for tumor progression and invasion. Proceedings of Department of Defense Breast Cancer Research Program Meeting, Orlando, Florida, September 25-28, 2002, Volume 1: P9:16.
8. Man YG, Saenger JS, Strauss B, Vang RS, Bratthauer GL, Chen PY, Tavassoli FA. Focal alterations of p27 expression and subjacent myoepithelial cell layer disruptions are correlated events in ER (-) ductal intraepithelial neoplasia. Proceedings of

Department of Defense Breast Cancer Research Program Meeting, Orlando, Florida, September 25-28, 2002 Volume 1: P9:14.

9. Masood S, Sim SJ, Lu L. Immunohistochemical differentiation of atypical hyperplasia vs. carcinoma in situ of the breast. *Cancer Detect Prev* 1992;16(4)225-35.
10. Bose S, Derosa CM, Ozzello L. Immunostaining of type IV collage and smooth muscle actin as an aid in the diagnosis of breast lesions. *Breast J* 1999;5(3):194-201.
11. Joshi MG, Lee AK, Pedersen CA, Schnitt S, Camus MG, Hughes KS. The role of immunocytochemical markers in the differential diagnosis of proliferative and neoplastic lesions of the breast. Mod Pathol 1996;9(1):57-62.
12. Blacque OE, Worrall DM. Evidence of a direct interaction between the tumor suppressor serpin, maspin, and types I and III collagen. *J Biol Chem* 2002;277(13):10783-8.
13. Maass N, Hojo T, Zhang M, Sager R, Jonat W, Nagasaki K. Maspin-a novel protease inhibitor with tumor suppressing activity in breast cancer. *Acta oncol* 2000;39:931-4.
14. Zou Z, Zhang W, Young D, Gleave MG, Rennie P, Connell T, Connelly R, Moul J, Srivastava S, Sesterhenn I. Maspin expression profile in human prostate cancer (CaP) and in vitro induction of Maspin expression by androgen ablation. *Clin Cancer Res* 2002;8(5):1172-7.
15. Reis-Filho JS, Milanezi F, Silva P, Schmitt FC. Maspin expression in myoepithelial tumors of the breast. *Pathol Res Pract* 2001;197:817-21.
16. Scharnhorst V, van der Eb AJ, Jochemsen AG. WT1proteins: functions in growth and differentiation. *Gene* 2001;273(2):141-61.
17. Fabre A, McCabb AH, O'Shea D, Broderick D, Keating G, Tobin B, Gorey T, Dervan PA. Loss of heterozygosity of the Wilms' tumor suppressor gene (WT-1) in in-situ and invasive breast carcinoma. *Hum Pathol* 1999;30(6):661-5.
18. Zapata-Benavides P, Tuna M, Lopez-Berestein G, Tari AM. Downregulation of Wilms' tumor 1 protein inhibits breast cancer proliferation. *Biochem Biophys Res* Commun 2002;295(4):784-90.
19. Mahendran R, McIlhinney R, O'Hare M, Monaghan P, Gusterson B. Expression of the common acute lymphoblastic leukaemia antigen (CALLA) in the human breast.

Mol Cell Probes 1989;3(1):39-44.

20. Iwaya K, Ogawa H, Izumi M, Kuroda M, Mukai K. Stromal expression of CD10 in invasive breast carcinoma: a new predictor of clinical outcome. *Virchows Arch* 2002;440(6):589-93.
21. Moritani S, Kushima R, Sugihara H, Bamba M, kobayashi T, Hattori T. Availability of CD10 immunohistochemistry as a marker of breast myoepithelial cells on paraffin sections. *Mod Pathol* 2002;15(4):397-405.
22. Yaziji H, Gown AM, Sneige N. Detection of stromal invasion in breast cancer: the myoepithelial markers. *Adv Anat Pathol* 2000;7:100-9.
23. Damiani S, Ludvikova M, Tomasic G, Bianchi S, Gown AM, Eusebi V. Myoepithelial cells and basal lamina in poorly differentiated in sity duct carcinoma of the breast. An immunocytochemical study. *Virchows Arch* 1999;434(3):227-34.
24. Dabbs DJ, Gown AM. Distribution of calponin and smooth muscle myosin heavy chain in fine-needle aspiration biopsies of the breast. *Diagn Cytopathol* 1999;20(4):203-7.
25. Ohyabu I, Takasaki T, Akiba S, Nomura S, Enokizono N, Sagara Y, Hiroi J, Nagai R, Yoshida H. immunohistochemical studies on expression of human vascular smooth muscle myosin heavy chain isoforms in normal mammary glands, benign mammary disorders and mammary carcinomas. *Pathol Int* 1998;48(6):433-9.
26. Moll R, Franke WW, Schiller DL, Geiger B, Krepler R. The catalog of human cytokeratins: Patterns of expression in normal epithelia, tumors and cultured cells. *Cell* 1982;31:11-24.
27. Bocker W, Moll R, Dervan P, Buerger H, Poremba C, Diallo R, Herbst H, Schmidt A, Lerch MM, Buchwallow IB. Usual ductal hyperplasia of the breast is a committed stem (progenitor) cell lesion distinct from atypical ductal hyperplasia and ductal carcinoma in situ. *J Pathol* 2002;198(4):458-67.
28. Wetzels RH, Kuijpers HJ, Lane EB, Leigh IM, Troyanovsky SM, Holland R, Van Haelst UJ, Ramaekers FC. Basal cell-specific and hyperproliferation-related keratins in human breast cancer. *Am J Pathol* 1991;138(3):751-63.
29. Wetzels RH, Holland R, Van Haelst UJ, Lane EB, Leigh IM, Ramaekers FC. Detection of basement membrane components and basal cell keratin 14 in

noninvasive and invasive carcinomas of the breast. *Am J Pathol* 1989;134(3):571-9.

30. McGowan KM, Coulumbe PA. Onset of keratin 17 expression doindies with the definition of major epithelial lineages during skin development. *J Cell Biol* 1998;143(2):469-86.
31. Man YG, Tavassoli FA. A simple epitope retrieval method without the use of microwave oven or enzyme digestion. *Appl Immunohistochem* 1996;4:139-41.
32. Man YG, Ball WD, Culp AJ, Hand AR, Moreira JE. Persistence of a perinatal cellular phenotype in the ducts of adult glands. *J Histochem Cytochem* 1995;43(12):1203-1215.
33. Werling RW, Hwang H, Yaziji H, Gown AM. Immunohistochemical distinction of Invasive From Noninvasive Breast Lesions. *Am J Surg Path* 2003;27(1):82-90.
34. Goldfarb RH, Liotta LA. Proteolytic enzymes in cancer invasion and metastasis. *Semin Thromb Hemost* 1986;12: 294-307.
35. Mignatti P, Robbins E, Rifkin DB. Tumor invasion through the human amniotic membrane: Requirement for a proteinase cascade. *Cell* 1986;47:487-498.
36. Wang F, Weaver VM, Petersen OW, Larabell CA, Dedhar S, Briand P, Lupu R, Bissell MJ. Reciprocal interactions between betal-integrin and epidermal growth factor receptor in three-dimensional basement membrane breast cultures: a different perspective in epithelial biology. *Proc Natl Acad Sci* 1998;95:14821-14826.
37. Tobacman JK. Filament disassembly and loss of mammary myoepithelial cells after exposure to lambda-carrageenan. *Cancer Res* 1997;57:2823-2826.
38. Sapino A, Macri L, Tonda L, Bussolati G. Oxytocin enhances myoepithelial cell differention and proliferation in the mouse mammary gland. *Endocrinology* ~~133:8~~38.
39. Gudjonsson T, Ronnov-Jessen L, Villadsen R, Rank F, Bissell MJ, Petersen OW. Normal and tumor-derived myoepithelial cells differ in their ability to interact with luminal breast epithelial cells for polarity and basement membrane deposition. *J Cell Sci* 2002;115(Pt1):39-50.

Table-1: Antibodies used in this study

Antibody	Company	Clone	Titer	Staining Pattern
Alpha Smooth Muscle Actin (SMA)	Novocastra	αsm-1	1:50	Cytoplasmic
Maspin	Novocastra	EAW24	1:25	Cytoplasmic and nuclear
Calponin	Novacastra	CLAP	1:25	Cytoplasmic
Smooth Muscle Myosin Heavy Chain (SMMHC)	Dako	SMMS-1	1:100	Cytoplasmic
Wilms Tumor Protein (WT-1)	Cell Marque	6F-H2	1:10	Cytoplasmic
CD10	Novocastra	56C6	1:80	Cytoplasmic
Cytokeratin 5 (CK-5)	Novocastra	XM26	1:100	Cytoplasmic
Cytokeratin 14 (CK-14)	Novocastra	LL002	1:20	Cytoplasmic
Cytokeratin 17 (CK-17)	Novocastra	E3	1:20	Cytoplasmic

Figure Legend

Figure 1: Immunostaining pattern of ME cells in a hyperplastic duct with columnar hyperplasia (case 1). a, H&E. b, the negativity of SMA is displayed on portion of the myoepithelial cell layer. c, d, e and f, the double immunostains of SMA with SMMHC, WT-1, CD10 and Calponin, respectively, are negative on the segment of myoepithelial cell layer. g and h, the double immunostains of SMA plus Maspin or CK5 show the weakly inconsistent positivity of Maspin and CK5 on the segment of myoepithelial cell layer. i and j, the double immunostains of SMA plus CK14 or CK17 are positive of CK14 or CK17 on the segment of myoepithelial cell layer.

Figure 2: Immunostaining pattern of ME cells in the case of ductal carcinoma in situ (Case 2). a, H&E. b, the ME cells are negative to SMA. c to f, the double immunostains of SMA plus Maspin, CK5, CK14 and CK17, respectively, are all negative for the myoepithelial cells. The results of the double immunostain of SMA and SMMHC, WT-1 CD10, Calponin are not shown, which are also negative.

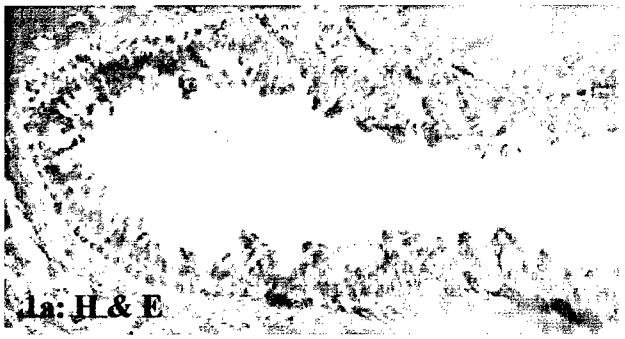

1a: H & E

1f: SMA+Calponin

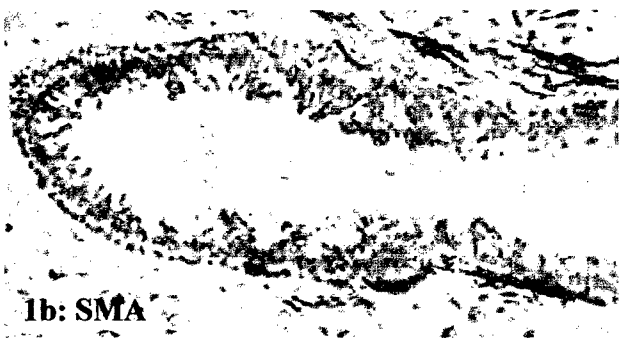

1b: SMA

1g: SMA+Maspin

1c: SMA+SMMHC

1h: SMA+CK5

1d: SMA+WT-1

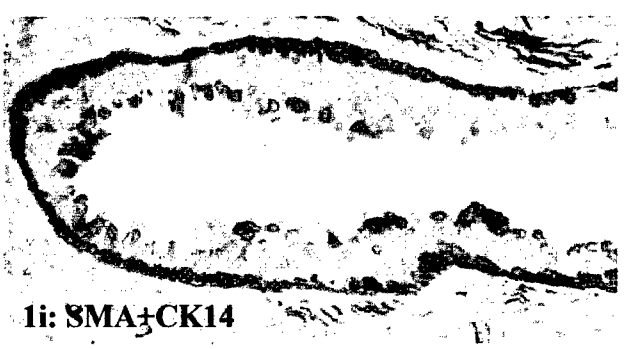

1i: SMA+CK14

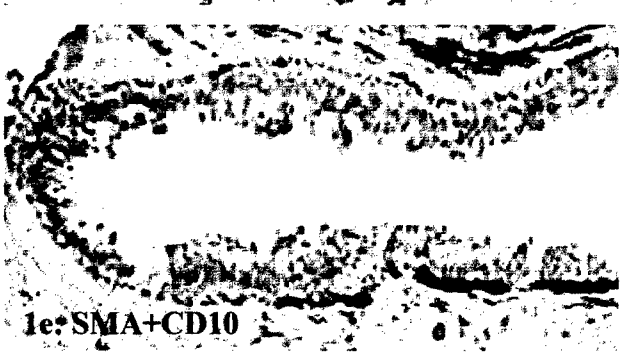

1e: SMA+CD10

1j: SMA+CK17

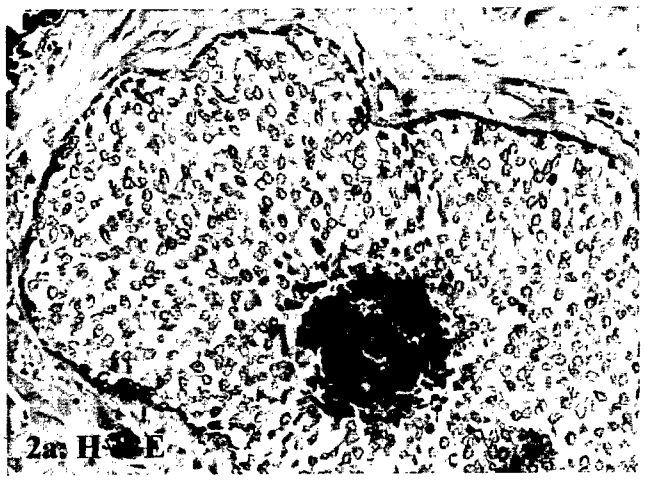

2a: H & E

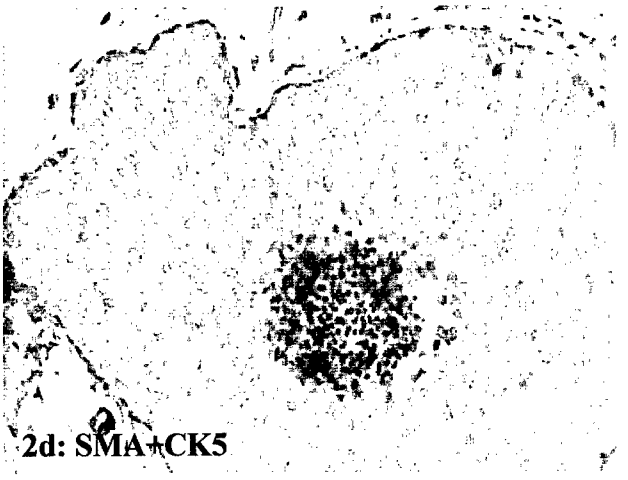

2d: SMA+CK5

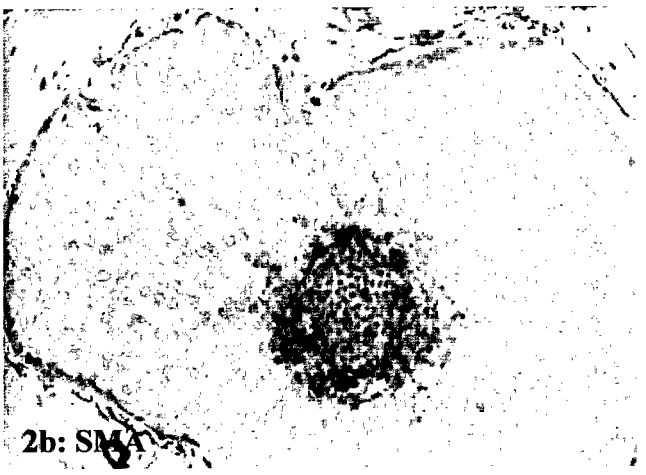

2b: SMA

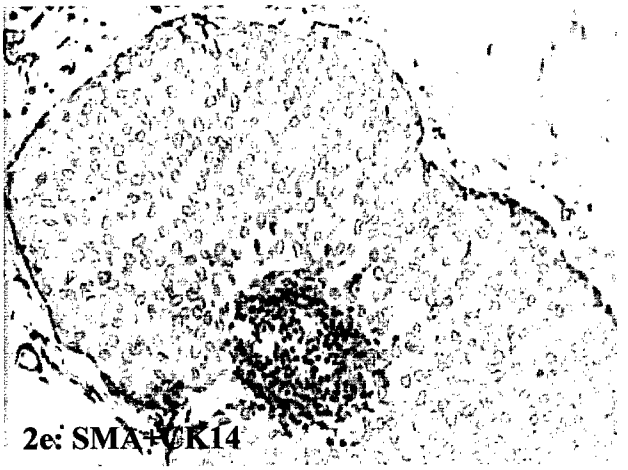

2e: SMA+CK14

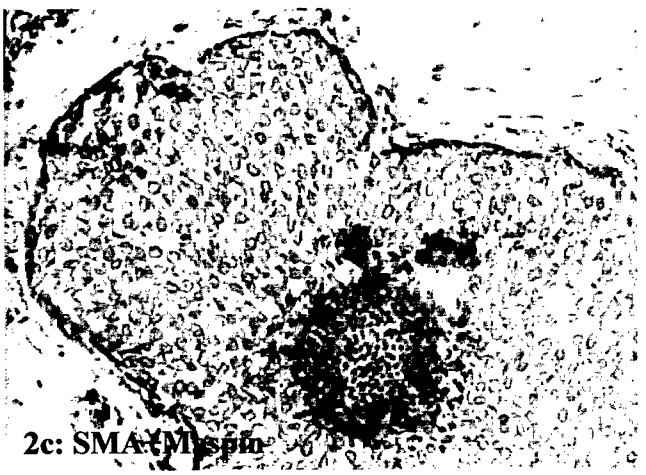

2c: SMA+Myosin

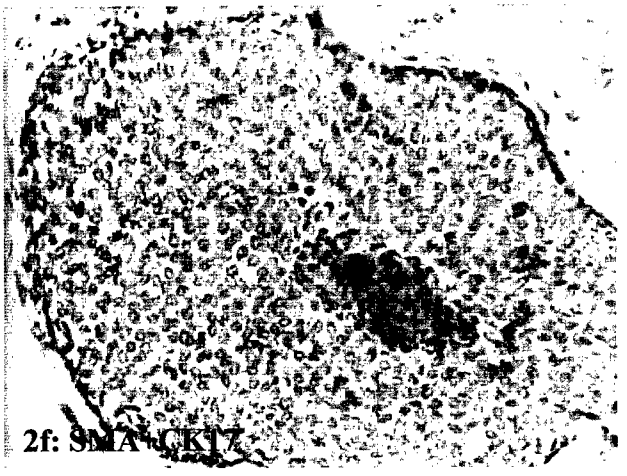

2f: SMA+CK17

Focal Disruptions In Mammary Myoepithelial Cell Layers and Loss Of Estrogen Receptor Expression In Overlying Epithelial Cells Are Correlated Events: Implications For Tumor Progression

Yan-gao Man, Lisa Tai, Ross Barner, Russell Vang, Jeffrey S. Saenger, Kris M.Shekitka, Gary L. Bratthauer, Darren T. Wheeler, Chang Y. Liang, Tuyethoa N, Vinh, and Brian L. Strauss

Department of Gynecologic and Breast Pathology, Armed Forces Institute of Pathology and American Registry of Pathology, 6825 16th Street, NW, Washington, DC 20306

Running title: Disruptions of myoepithelial cell layer and loss of ER expression in pre-invasive breast cancer

Key words: Estrogen receptor expression, myoepithelial cell layer, ductal carcinoma in situ, tumor progression, tumor invasion

Corresponding author:

Yan-gao Man, M.D., Ph.D.
Director of Gynecologic and Breast Research Laboratory
Department of Gynecologic and Breast Pathology
Armed Forces Institute of Pathology and American Registry of Pathology
6825 16th Street, NW
Washington DC 20306-6000

Phone: 202-782-1612; Fax: 202-782-3939; E-mail: man@afip.osd.mil

Abstract

Our previous immunohistochemical study with antibodies to smooth muscle actin and estrogen receptor (ER) revealed several focal disruptions in the myoepithelial (ME) cell layer (defined as the absence of ME cells resulting in a gap equal to or greater than the combined size of 3 ME cells) in several ducts with ductal carcinoma in situ (DCIS). Each of the disruptions was overlain by a cluster of cells with a marked reduction or total loss of ER expression, in contrast to the adjacent non-disrupted ME cell layer within the same duct, which was overlain by ER positive cells. To confirm previous findings, paraffin sections from 220 patients with ER positive intraductal breast tumors were double immunostained using the same protocol. Cross sections of ducts lined by ≥ 40 epithelial cells were examined for ME cell layer disruptions and ER expression. In 5 selected cases, ER negative cells overlying the disrupted ME cell layer and adjacent ER positive cells within the same duct were separately microdissected and assessed for loss of heterozygosity (LOH) and microsatellite instability (MI). Of the 220 cases with 5,698 duct cross sections, 94 contained disrupted ME cell layers with 405 focal disruptions. Of the 94 cases, 9 (9.6%) were associated with both ER positive and negative cells, 79 (84%) were exclusively associated with ER negative cells, and 6 (6.4%) were exclusively associated with ER positive cells. Of the 405 disruptions, 350 (86.4%) were overlain by ER negative and 55 (13.6%) by ER positive cell clusters ($p < 0.01$). Over 90% of the ER negative cell clusters were small (<15 cells) and morphologically indistinguishable from adjacent ER positive cells within the same duct on H & E sections, whereas a few larger clusters displayed noticeable alterations in shape, density, and polarity. The frequency of ME cell layer disruptions appeared to be independent of the size, length, architecture,

and overall ER negativity of the ducts, or histologic grade of the lesions. Microdissected ER negative and positive cells from 5 selected cases showed a different frequency or pattern of LOH and/or MI at 10 of the 15 DNA markers. Together, these findings suggest that focal disruptions in ME cell layers and loss of ER expression in overlying EP cells are correlated events, potentially representing an early sign of the ME cell layer breakdown, and the formation of a biologically more aggressive cell clone.

Introduction

The epithelial (EP) cell component of the normal and non-invasive human breast tissues is normally embraced by a layer of myoepithelial (ME) cells that are surrounded by a continuous layer of the basement membrane (BM) (1, 2). Because of this structural feature, EP cells have to first pass through the ME cell layer, and, then, the BM layer, in order to reach the stroma for tumor invasion and metastasis. In H & E stained sections, most ME cells are readily identifiable, while are often indistinguishable from subjacent myofibroblastic cells of the stroma and smooth muscle cells of the small blood vessels. Immunohistochemical staining for smooth muscle actin (SMA) has been routinely used in the clinic to assist in the identification of ME cells (3,4). The presence or absence of the BM and ME layers in H & E and/or immunostained sections has been considered a very reliable criterion in distinguishing in situ from invasive breast lesions (3,4). The intrinsic functions and cell kinetics of ME cells, and the potential interactions among EP and ME cells, as well as the BM layer during tumor invasion or progression, however, have not been well documented or remain totally unknown.

To address these issues, our previous study utilized a double immunostaining method with antibodies to SMA and estrogen receptor (ER) to assess both EP and ME cells in breast tissue sections. Several focal ME cell layer disruptions were seen in several ducts that were classified as ductal carcinoma in situ (DCIS) based on H & E slide examination. Each of the disruptions was exclusively overlain by a cluster of cells that showed a marked reduction or total loss of ER expression, in contrast to the adjacent non-disrupted ME cell layer within the same duct, which was overlain by cells with strong ER expression (5). Those ER negative cells were generally morphologically

indistinguishable from the adjacent ER positive cells within the same duct (5). Our subsequent studies in ER negative DCIS detected similar ME cell layer disruptions that were exclusively overlain by cell clusters with altered expression of p27, a cell growth inhibitor (6). Our recent studies further revealed that ducts with a disrupted ME cell layer had a significantly higher proliferation rate than ducts with an intact ME layer (6,7).

As it has been well documented that [1] the disruption of the BM and ME cell layers is an absolute pre-requisite for tumor invasion and metastasis, [2] the development and/or progression of tumors result from correlative alterations in EP and stromal cells (8,9), and [3] the progression of breast tumors is paralleled by a progressive hormonal independence (10, 11, 12, 13), our findings appear to have several potential implications. First, a focal ME cell layer disruption may represent an initial or early sign of the BM and ME cell layer breakdown. Second, those ER negative cells overlying the disrupted ME cell layer may represent a newly formed cell clone that is biologically more aggressive than the adjacent ER positive cells within the same duct. Third, focal disruptions in the ME cell layer and the loss of ER expression in overlying cells might be correlated events, directly triggering or signifying tumor progression or potential invasion in some cases. Based on these assumptions, this study attempted to confirm our previous findings on a larger number of cases and a wider spectrum. In addition, this study attempted to carry out a preliminary molecular study, to compare the frequency and pattern of LOH and MI between ER negative and the adjacent ER positive cells within the same duct, if the results of the current study confirm our previous findings.

Materials and Methods

Formalin-fixed, paraffin-embedded breast tissue blocks harboring various grades and subtypes of ER positive, non-invasive breast lesions from 220 female patients were retrieved from the files of The Armed Forces Institute of Pathology. Serial sections at 5-7 μm thickness were cut and placed on positively charged microscopic slides for morphologic and immunohistochemical assessment. Morphologic classifications were based on published criteria (5). Double immunohistochemical staining with antibodies to ER and SMA (Vector Laboratories, Burlingame, CA) was carried out as previously described (5, 14, 15). A micrometer was inserted into the objective of a microscope to facilitate the reviewing of the whole section and the localization of a specific lesion (16). Cross sections of ducts lined by ≥ 40 EP cells were examined under a microscope for ME cell layer disruptions and ER expression. A focal disruption of the ME cell layer was defined as a total loss of SMA immunoreactivity and absence of ME cells, resulting in a gap that is equal to or greater than the combined size of at least 3 EP or ME cells, or multiple such gaps in a given duct. A focal loss of ER expression was defined as a substantial reduction or total loss of ER immunostaining in cells overlying disrupted ME cell layers, compared to the strong ER immunostaining in the immediate adjacent EP cells within the same duct that overlay the non-disrupted ME cell layer. A focal positive ER expression was defined as a more intense or comparable ER immunostaining in cells overlying disrupted ME cell layers, compared to the ER immunostaining in the adjacent EP cells within the same duct that overlay the non-disrupted ME cell layer. The profiles of ducts containing disrupted ME cell layers were photographed and reprints were made at a magnification of 400-800X for immunohistochemical and morphological evaluation.

The frequencies of ME cell layer disruptions associated with ER negative and positive cell clusters were statistically compared by the Student's t-Test. In addition, the adjacent sections from 20 cases with focal disruptions of the ME cell layer were immunostained with the mixture of antibodies to SMA and collagen IV (Dako Corporation, Carpinteria, CA), to assess the integrity of the basement membrane underneath the disrupted ME cell layer. The sections from these cases were also immunostained with a monoclonal antibody to cytokeratins AE1/AE3, to assess whether the cells overlying disrupted ME cell layers are epithelial in nature.

For molecular analyses, paired ER negative and adjacent ER positive cells within the same duct, along with clear cut normal EP or ST cells were separately microdissected from each of 5 selected cases, including one mild ductal hyperplasia and four DCIS or atypical intraductal hyperplasia (AIDH) (based on quantitative criteria). To obtain a sufficient number of cells for molecular analysis, multiple consecutive sections were immunostained, and ER negative cell clusters in different sections were microdissected and pooled. Microdissected cells were subjected to DNA extraction and assessed for LOH and MI with 15 fluorescent labeled DNA markers (Research Genetics, Huntsville, AL), as previously described (17). DNA markers used and their main features are listed in Table 1. Amplified PCR products were subjected to electrophoresis, detection, and comparison with an automated 377 DNA sequencer (Perkin-Elmer, Foster City, CA), as previously described (18, 19).

Results

Of the 220 cases, 14 (6.4%) contained less than 3 and 206 (93.6%) contained more than 3 profiles of duct cross sections, with a total of 5,698 profiles available for assessment. Of the total cases and cross sections examined, 94 (42.7%) contained a disrupted ME cell layer with a total of 405 (7.1%) focal disruptions. Of the 94 cases, 61 (65%) contained 1 to 4 disruptions, and 33 (35%) contained 5 or more disruptions. Disruptions occurred in two forms: [1] a cell-free gap between the two ends of the ME cell layer; [2] a gap filled with bud-like protrusions of EP cells. The size of disruptions varied substantially among ducts, ranging from the combined size of 3 to over 30 ME cells. The frequency of disruptions also varied substantially among cases. In two cases that contained 129 and 130 profiles of duct cross sections, respectively, no disruption was seen, while in another two cases, 2 of the 2 and 5 of the 7 profiles demonstrated focal ME layer disruptions. The form, size, or frequency of disruptions seemed to be independent of the size, length, architectural, and overall ER negativity of the ducts, and also of the histological grade of the lesions (Fig 1).

The frequency and pattern of ME cell layer disruptions, however, were closely associated with the ER expression status in overlying cells. Of the 94 cases, 79 (84%) were exclusively associated with ER negative cells, 9 (9.6%) were associated with both ER negative and positive cells, and 6 (6.4%) were exclusively associated with ER positive cells. Of the 405 disruptions, 350 (86.4%) were overlain by ER negative cell clusters, and 55 (13.6%) were subjacent to cells with a strong ER expression (Table 2). The frequency of ME cell layer disruptions associated with ER negative cells was significantly higher ($p < 0.01$) than that associated with ER positive cells. The number

of ER negative cells overlying the disrupted ME cell layer varied markedly, ranging from 3 to over 100 cells. These cells were generally distributed as clusters, and cells of the same cluster were morphologically similar, suggesting that they were derived from a common progenitor. The ER negative cells in a majority of small clusters (<15 cells), which account for over 90% of the total ER negative cell clusters, were morphologically indistinguishable from their ER positive counterparts within the same duct on H & E stained sections (Fig 2). The ER negative cells in some of the larger clusters (>15 cells), however, showed noticeable alterations in shape, density, and polarity, morphologically distinct from their adjacent ER positive counterparts within the same duct (Fig 3). Over 95% of the ducts contained only one or two, while a few displayed multiple disruptions in the ME cell layer (Fig 4). The stromal tissues surrounding ducts with ME cell layer disruptions were often more vascular and contained more white blood cell aggregates, compared to ST tissues around ducts with an intact ME cell layer (data not shown).

Although over 86% of the ME cell layer disruptions were overlain by ER negative cell clusters, nearly 14% of the disruptions were subjacent to ER positive cell clusters. These ER positive clusters were generally distinct from their ER negative cell clusters in three aspects: [1] most of them occurred in ducts with markedly attenuated ME cell layers; [2] they usually showed no alterations in cell shape, density, or polarity; [3] the surrounding ST tissues displayed no distinct morphological alterations (Fig 5).

In over 90% of the cases, ME cell layer disruptions and their associated ER negative cell clusters occurred in ducts with DCIS. In approximately 10% of the cases, however, ME cell layer disruptions and their associated ER negative cell clusters were also seen in hyperplastic and even normal appearing ducts (Fig 6).

Immunohistochemical staining with the mixture of antibodies to collagen IV and SMA in all 20 selected cases revealed distinct immunostaining surrounding non-disrupted ME cell layers, whereas no appreciable staining surrounding the disrupted ME cell layer, suggesting that the basement membrane is also disrupted (data not shown). All the ER negative cell clusters overlying the disrupted ME cell layer and their adjacent ER positive counterparts in all 20 cases displayed distinct immunostaining to AE1/AE3, suggesting that they are epithelial in origin.

Molecular analyses on microdissected cells from the five selected cases revealed distinct LOH and MI in both ER negative and adjacent ER positive cells within the same duct at each of the 15 DNA markers. The frequency of LOH and MI among the DNA markers, however, varied from 12% to over 70%. The ER negative and ER positive cells showed a different frequency or pattern of LOH and MI at 10 of the 15 markers, including those at chromosomes 3p, 11p, 13q, and 16q. Figure 7 shows examples of the LOH pattern in ER negative and adjacent ER positive cells from a previously selected case. Subsequently and currently, additional cases with ME cell layer disruptions associated with ER negative cell clusters have been selected for a larger scale comparison at a wider spectrum. The preliminary results were comparable to those seen in the 5 previously selected cases. The detailed findings in all these cases will be pooled and reported separately.

Discussion

The results of our current study have confirmed our previous findings, suggesting that focal disruptions in ME cell layers and loss of ER expression in overlying cells are correlated events, potentially representing the early sign of the ME cell layer breakdown and the formation of a biologically more aggressive cell clone. The ME cell layer has been traditionally regarded as a structural barrier for separating mammary EP cells from the surrounding stroma and for contracting ductal and lobular spaces assisting milk secretion (20, 21,22). Recent studies, however, have revealed several lines of evidence, suggesting that ME cells may play active roles in preventing in-situ tumors from invasion, and in regulating the functions of the EP cells. First, normal ME cells secrete several cell growth inhibitors, including maspin, which inhibits tumor cell growth in both tissue cultures and in animal models (23, 24, 25). Second, normal ME cells could convert precursor hormones into active steroid hormones within the mammary EP tissue (26). Third, the protein of a tumor suppressor gene, Wilms' tumor 1, is co-localized with maspin exclusively in ME cells, and the expression of these two proteins are linearly decreased with tumor progression in a vast majority of the cases assessed (6,7). The loss of maspin and WT-1 expression, or disruption of ME cell layers leads to a significantly higher EP cell proliferation (6,7). On the other hand, recent studies have also suggested that ME cells could be the specific target of external and internal insults and frequently subject to a variety of normal and pathologic changes. Exposure to lambda carrageenan could specifically result in a filament disassembly and loss of mammary ME cells, while exposure to oxytocin could markedly enhance ME cell differentiation and proliferation (27, 28). Our recent study has revealed a subset of ME cells that are morphologically

distinct on H & E stained sections, but are devoid of expression of 9 ME cell phenotypic markers that are supposed to exclusively or preferentially express in ME cells (29).

Despite these recent progresses in ME cell research, the cell kinetics of ME cells has not been elucidated, and the mechanism of ME cell layer disruptions remains elusive. It has been generally accepted that an elevated level of proteolytic enzymes, produced by malignant EP and/or ST cells, is the primary, if not the only, cause for the degradation of the BM and subsequent tumor invasion (30, 31,32). This theory, however, might not reflect the intrinsic mechanism of these events, because of two main reasons: [1] the ME cell is an essential population of the normal breast parenchyma, which should not be the target of the host's own proteolytic enzymes; [2] proteolytic enzyme inhibitor based therapies have been highly successful in tumor models for prevention of tumor invasion, whereas have been very disappointing in human clinical trials (33). As our recent studies have revealed that the physical and functional integrity of ME cells significantly impact the biological behavior of EP cells (6,7), we hypothesize that disruptions of BM and ME cell layers and tumor invasion may be initiated or mediated by ME cells. Our hypothesized mechanism and the involved processes are the following: [1] normal ME cells frequently undergo proliferation and differentiation to replace aged or injured cells; [2] an external or internal insult disrupts the normal replacement process, resulting in a cluster of dying ME cells; [3] the degraded products of dead ME cells attract lymphocyte infiltration, which physically disrupts the BM; [4] a focal disruption in ME cell and BM layers results in an increased permeability for metabolism and growth related molecules; [5] the altered micro-environment changes the gene expression and behavior of adjacent EP cells, facilitating the formation of a biologically more aggressive cell clone; [6] EP

cells overlying disrupted ME cell layers undergo a localized EP cell proliferation, which may occur in two forms: a. A stem cell mediated proliferation that gives rise to those ER negative cell clusters, and b. A differentiated cell mediated proliferation that produces those ER positive cell clusters; [7] Cells overlying disrupted ME cell layers undergo cytodifferentiation, and release stage-restricted and invasion-associated bio-molecules into the stroma; [8] alterations in EP cells trigger angiogenesis, tissue remodeling, and increasing production of growth factors in the stroma, providing a favorable environment for EP cell growth (34, 35, 36). These interactive changes between EP and ST lead to further degradation of the BM and ME cell layers, and a clonal expansion and stromal invasion of the cells overlying disrupted ME cell layers.

It is not known whether or to what extent our hypothesis reflects the intrinsic mechanism of the BM and ME cell layer disruptions, as [1] our hypothesis is based on very limited experimental data, [2] the clinical significance of our findings has not been elucidated, [3] the morphological correlation has not been statistically analyzed, [4] the intrinsic mechanism and detailed pathway for each of our hypothesized processes remain to be identified. However, given the fact that the disruption of the BM and ME cell layers is an absolute pre-requisite for tumor invasion and metastasis, and that the progression of breast tumors is paralleled by a progressive hormonal independence (10, 11,12,13), our hypothesized model might open a new window for exploring these issues. Currently, we are testing our hypothesis by assessing the interactions among EP, ME, and ST cells in breast tumors that simultaneously harbor normal, hyperplastic, in situ, and invasive lesions, using multidisciplinary approaches.

The ER negative cells overlying disrupted ME cell layers seem to be genetically and

biochemically different from their adjacent ER positive counterparts within the same duct, suggested by several lines of evidence. First, our preliminary molecular analysis has revealed that microdissected ER negative and ER positive cells display a different frequency and pattern of LOH and MI at 10 of the 15 markers tested. Second, some of the larger ER negative cell clusters (≥ 15 cells) display noticeable alterations in shape, density, and polarity. Third, our recent studies have shown that cells in ducts with disrupted ME cell layers have a significantly higher EP cell proliferation rate than cells in ducts without ME cell layer disruptions (6,7). Fourth, previous studies have shown that ER positive cells have a higher proliferation rate than ER negative cells in hyperplastic breast lesions, but ER negative cells have a higher proliferation rate and more aggressive clinical behavior than ER positive cells in both in situ and invasive cancer, reinforcing the hypothesis that progression of breast tumors is paralleled by a progressive hormonal independence (10, 11, 12, 13).

The mechanism for the loss or diminution of ER expression in cells overlying a disrupted ME cell layer is unknown, but appears to relate to the age and differentiation status of the cells. Our previous autoradiographic and immunohistochemical studies have shown that at the initial stage of both normal cellular replacement and regeneration, over 95% of the proliferating cells were devoid of expression of two perinatal proteins that were strongly expressed in adjacent non-proliferating cells (37, 38). Two weeks later, however, some of the transitional cells also started to express these two proteins (37, 38). A similar study in the normal human breast has shown that none of the cells with ER and progesterone receptor (PR) expression was proliferating, and none of these proliferating cells showed ER or PR expression (39). On the other hand, a number of

bio-molecules, including stromelysin-3, insulin-like growth factor II, and proteins of the breast cancer susceptibility genes 1 and 2, are preferentially expressed in rapidly proliferating cells (40, 41, 42). Our recent study has further shown that phenotypically different pre-malignant and malignant respiratory epithelial cells with hnRNP expression display a very similar genetic profile that differs substantially from the genetic profile of the morphologically comparable cells without hnRNP expression (43). Together, these findings suggest that alterations in expression of certain proteins man signify substantial changes in DNA and RNA, as well as the biological behavior of involved cells. These findings also suggest that ER negative cells overlying disrupted ME cell layers are newly formed and are not mature enough to express ER, whereas they might express other bio-molecules, including those associated with tumor progression and/or invasion. Therefore, further characterization of those ER negative cells and associated changes would facilitate the elucidation of the mechanism of tumor progression, as well as lead to the identification of a unique marker that can be used for early detection. This is an ongoing project, supported by The Congressionally Directed Medical Research Programs. Currently, several studies are simultaneously in progress, for more detailed comparison of these ER negative and the adjacent ER positive cells at DNA, RNA, and protein levels. Also, a series of studies have been carried out to assess the frequency, pattern, and potential significance of ME cell layer disruptions and overlying ER negative cell clusters in hyperplastic and normal appearing ducts. The results from these studies will be separatly reported. The clinical significance and morphological correlation of our findings will be statistically analyzed at the end of the project.

Acknowledgement

The authors are grateful to Doug Landry of AFIP exhibition section and Kenneth J. Vrtacnik of AFIP photography Lab, for their technical assistance in preparing some of the figures.

This study was supported by The Congressionally Directed Medical Programs, grants DAMD 17-01-0129 and DAMD17-01-0130 to Yan-gao Man, M.D., Ph.D.

Reference

1. Tsubura, A., Shikata, N., Inui, T., Morii, S., Hatano, T., and Oikawa, T. Immunohistochemical localization of myoepithelial cells and basement membrane in normal, benign and malignant human breast lesions. Virchows Arch., 413: 133-139, 1988
2. Pasqualini, J.R. Breast cancer-Prognosis, treatment, and prevention. Marcel Dekker, Inc, New York, 2002
3. Masood. S., Lu, L., Assaf-Munasifi, M., and McCaulley, K. Application of immunostaining for muscle specific actin in detection of myoepithelial cells in breast fine-needle aspirates. Diagn Cytopathol., 13: 71-74, 1995
4. Gottleib, C., Raju, U., and Greenwald, K.A. Myoepithelial cells in the differential diagnosis of comlex benign and malignant breast lesions: an immunohistochemical study. Mod Pathology., 3(2): 135-140, 1990
5. Tavassoli, F.A., and Man, Y.G. Morphofunctional features of intraductal hyperplasia, atypical hyperplasia, and various grades of intraductal carcinoma. The Breast J., (3): 155-162, 1995
6. Man, Y.G., Saenger, J.S., Strauss, B., Vang, R.S., Bratthauer, G.L., Chen, P.Y., and Tavassoli, F.A. Focal alterations of p27 expression and subjacent myoepithelial cell layer disruptions are correlated events in ER (-) ductal intraepithelial neoplasia. Proceedings of Department of Defense Breast Cancer Research Program Meeting., 1: P9,14, 2002
7. Man, Y.G., Vang, R.S., Saenger, J.S., Strauss, B., Bratthauer, G.L., Chen, P.Y., and Tavassoli, F.A. Co-expression of maspin and wilms' tumor 1 proteins in mammary myoepithelial cells---implication for tumor progression and invasion. Proceedings of Department of Defense Breast Cancer Research Program Meeting., 1: P9,16, 2002
8. Moinfar, F., Man, Y.G., Arnould, L., Bratthauer, G.L., Ratschek, M., and Tavassoli, F.A. Concurrent and independent genetic alterations in the stromal and eoithelial cells of mammary carcinoma: Implications for tumorigenesis. Cancer Res., 60: 2562-2566, 2000
9. Man, Y.G., Mannion, C., Albores-Saaverdra, J., Bratthauer, G.L., Kuhls, E., and

Tavassoli, F.A. Allelic losses at 3p and 11p are detected in both epithelial and stromal components of cervical small cell neuroendocrine carcinoma. Appl Immunohistochem Mol Morphology., 9: 340-345, 2001

10. Schmitt, F.C. Multistep progression from an oestrogen-dependent growth towards an autonomous growth in breast carcinogenesis. Eur J Cancer., 31A: 2049-2052, 1995
11. Clarke, R., Brunner, N., and Katzenellenbogen, B.S. Progression of human breast cancer cells from hormone-dependent to hormone-independent growth both in vitro and in vivo. Proc. Natl Acad Sci USA., 86: 3649-3653, 1989
12. Murphy, L.C. Mechanism of hormone independence in human breast cancer. In vivo., 2: 95-106, 1998
13. Sheikh, M.S., Garcia, M, Pujol. P., Fontana, J.A., and Rochefort, H. Why are estrogen receptor negative breast cancers more aggressive than the estrogen receptor positive breast cancers ? Invasion Metastasis., 14: 329-336, 1994-95
14. Man, Y.G., and Tavassoli, F.A. A simple epitope retrieval method without the use of microwave oven or enzyme digestion. Appl Immunohistochem., 4: 139-141, 1996
14. Man, Y.G., Ball, W. D., Culp, A.J., Hand, A.R., and Moreira, J.E. Persistence of a perinatal cellular phenotype in the ducts of adult glands. J Histochem Cytochem., 43: 1203-1215, 1995
16. Man, Y.G., Schammel, D.P., and Tavassoli, F.A. Detection of telomerase activity in microdissected breast lesions. Cell Vision., 5: 85-85, 1998
17. Man, Y.G., Moinfar, F., Bratthauer, G.L., Kuhls, E., and Tavassoli, F.A. An improved method for DNA extraction from paraffin sections. Pathology-Research & Practice., 197: 635-642, 2001
18. Man, Y.G., Moinfar, F., Bratthauer, G.L., and Tavassoli, F.A. Five useful approaches for generating more valid gel images for LOH and clonality analysis with an automated DNA sequencer. Diag Mol Pathol., 9: 84-90, 2000
19. Man, Y.G., Kuhls, E., Bratthauer, G.L, Moinf, F., and Tavassoli, F.A. Multiple use of slab gels in sequencing apparatus for separation of polymerase chain reaction products. Electrophoresis., 22: 1915-1919,2001
20. Robinson, G.W., McKnight, R.A., Smith, G.H., and Hennighausen, L. Mammary epithelial cells undergo secretory differentiation in cycling virgins but require

pregnancy for the establishment of terminal differentiation. Development (Camb)., 121: 2079-2090, 1995

21. Chodosh, L.A., Cruz, C.M.D., and Gardner, H.P. Mammary gland development, reproductive history, and breast cancer risk. Cancer Res., 59: 1765s-1772s, 1999
22. Russo, J., and Russo, I.H. Developmental pattern of human breast and susceptibility to carcinogenesis. Eur J Cancer Prev., 2(suppl.3): 85-100, 1993
23. Sternlight, M.D., and Barsky, S.H. The Myoepithelial defense: a host defense against cancer. Med Hypotheses., 48(1): 37-46, 1997
24. Sternlight, M.D., Safarians, S., Rivera, S.P., and Barsky, S.H. Characterization of the extracellular matrix and proteinase inhibitor content of human myoepithelial tumors. Lab Invest., 74: 781-796, 1996
25. Shao, ZM., Nguyen, M., Alpaugh, M.L., O'Connell, J.T., and Barsky, S.H. The human myoepithelial cells exerts antiproliferative effects on breast carcinoma cells characterized by p21WAF1/CIPI induction, G2M arrest, and apoptosis. Exp Cell Res., 241: 394-403, 1998
26. Tobacman, J.K., Hinkhouse, M., and Khalkhali-Ellis, Z. Steroid sulfatase activity and expression in mammary myoepithelial cells. J Steroid Biochem Mol Bio., 81: 65-68, 2002
27. Tobacman, J.K. Filament disassembly and loss of mammary myoepithelial cells after exposure to lambda-carrageenan. Cancer Res., 57: 2823-2826, 1997
28. Sapino, A., Macri, L., Tonda, L., and Bussolati, G. Oxytocin enhances myoepithelial cell differention and proliferation in the mouse mammary gland. Endocrinology., 133: 838-842, 1993
29. Zhang, R., Man, Y.G., Strauss, B.L., Vang, R.S., Saenger, J.S., Barner, R., Wheeler, D.T., Liang, C.Y. A subset of morphologically identifiable mammary myoepithelial cells lacks expression of corresponding phenotypic markers. Mod Pathol., In press (Abstract)
30. Goldfarb, R.H., and Liotta, L.A. Proteolytic enzymes in cancer invasion and metastasis. Semin Thromb Hemost., 12: 294-307, 1986
31. Lynch, C.C., and Matrisian, L.M. Matrix metalloproteinases in tumor-host communication. Differentiation., 70: 561-573, 2002

32. Bissell, M.J., Radisky, D.C., Rizki, A., Weaver, V.M., and Petersen, O.W. The organizing principle: microenvironmental influences in the normal and malignant breast. Differentiation., 70: 537-546, 2002

33. Coussens, L.M., Fingleton, B., and Matrisian, L.M. Matrix metalloproteinase inhibitors and cancer: trial and tribulations. Science., 295 (5564): 2387-2392, 2002

34. Muschler, J., Levy, D., Boudreau, R., Henry, M., Campbell, K., Bissell, M.J. A role for dystroglycan in epithelial polarization: loss of function in breast tumor cells. Cancer Res., 62: 7102-7109, 2002

35. Gudjonsson, T., Ronnov-Jessen, L., Villadsen, R., Rank, F., Bissell, M.J, Petersen, O,W. Normal and tumor-derived myoepithelial cells differ in their ability to interact with luminal breast epithelial cells for polarity and basement membrane deposition. J Cell Sci., 115: 39-50, 2002

36. Brinckerhoff, C.E., and Matrisian, L.M. Matrix metalloproteinases: a tail of a frog that became a prince. Nat Rev Mol Cell Biol., 3: 207-214, 2002

37. Man, Y.G. Contribution of intercalated duct cells to normal cellular replacement and regeneration: Assessed by immunocytochemical and autoradiographic methods (Ph.D dissertation). UML Press, 1998

38. Man, Y.G., Ball, W.D., Marchetti, L., and Hand, A.R. Contributions of intercalated duct cells to normal parenchyma of submandibular glands of adult rats. Anat Rec., 263:202-214, 2001

39. Russo, J., Ao, X., Grill, C., and Russo, I.H. Pattern of distribution of cells positive for estrogen receptor alpha and progesterone receptor in relation to proliferating cells in the mammary gland. Breast Cancer Res Treat., 53: 217-227, 1999

40. Marquis, S.T., Rajan, J.V., and Wynshaw-Boris, A. The developmental pattern of BRCA1 expression implies a role in differentiation of the breast and other tissues. Nat Genet., 11: 17-26, 1995

41. Peng, H., Feldman, I., and Rauscher, F.J 3rd. Hetero-oligomerization among the TIF family of RBCC/TRIM domain-containing nuclear cofactors: a potential mechanism for regulating the switch between coactivation and corepression. J Mol Biol., 320: 629-644, 2002

42. Singer, C.F., Rasmussen, A., Lippman, M.E., and Cullen, K.J. Coexpression of

stromelysin-3 and insulin-like growth factor II in tumors of ectodermal, mesodermal, and endodermal origin: indictor of a fetal cell phenotype. J Clin Endocrinol Metab., 82: 1917-1922, 1997

43. Man, Y.G., Martinez, A., Avis, I.M., Hong, S.H., Cuttitta, F., Venzon, D.J., and Mulshine, J.L. Phenotypically different respiratory epithelial cells with hnRNP A2/B1 over-expression display similar genetic alterations. Am J Respir Cell Mol Biol., 23: 636-645, 2000

Table 1. DNA markers used for comparison of genetic alterations in ER (-) and ER (+) cells

#	Name	Chromosomal location	Harbored gene	Size(base pair)
1	D3S1300	3p21.1 – p14.2	FHIT	217 - 241
2	D3S1481	3p14.2	FHIT	104
3	D3S1581	3p21.2 – p14.2	FHIT	78 - 102
4	D11S902	11p15 – p13	?	145 – 163
5	D11S904	11p14 – p13	Wilms' tumor 1	185 – 201
6	D11S907	11p13	Wilms' tumor 1	163 – 173
7	D11S914	11p13 – p12	Wilms' tumor 1	275 – 285
8	D13S119	13q14.3 – q22	?	124 – 140
9	D13S173	13q32 – q34	?	166 - 178
10	D13S219	13q12.3 – q13	?	117 - 127
11	D13S263	13q14.1 – q14.2	?	145 - 165
12	D16S518	16q23.1 – q24.2	CDH 1(adjacent to it)	272 - 290
13	D16S402	16q24.2	CDH 1 (adjacent to it)	161 - 187
14	D17S791	17q	BRCA 1	165 - 199
15	TP53	17p13	P53	104

Table 2. Frequency of ME cell layer disruptions and the status of ER expression

Total cross sections	Total disruptions	Focal loss of ER	ER positive	P
5,698	405 (7.1%)	350 (86.4%)	55 (13.6%)	< 0.01

Figure legend

Figure 1. Disruptions of ME cell layers are independent of the size, length, architecture, and overall ER negativity of the ducts, or histological grades of the lesions.

Paraffin-embedded breast tissue sections were double immunostained with antibodies to estrogen receptor (ER) and smooth muscle actin (SMA), and developed with DAB (black or brown) and AEC (red) chromogens, respectively. All sections in this and following figures were immunostained with the same protocol, unless indicated otherwise.

Distinct ME cell layers are seen in the following structures:

1a. a large duct with DCIS, 100X; 1b. a long normal duct, 40X;

1c. a duct with IDH, 100X; 1d. intermediate grade ER negative DCIS, 100X

Figure 2. ME cell layer disruptions and overlying small ER negative cell clusters (<15 cells) in ER positive DCIS

2a. H & E staining of a large duct with DCIS, 100X; 2b. the adjacent section of 2a, immunostained, 100X; 2c. a higher magnification of 2a; 2d. a higher magnification of 2b

The ME cell layer disruption and overlying ER negative cells are identified with a arrow

Figure 3. ME cell layer disruptions and overlying larger ER negative cell clusters (>15 cells) in ER positive neoplastic and hyperplastic ducts

3a. DCIS, 100X; 3b. a small duct with AIDH, 100X; 3c. a hyperplastic duct, 100X; 3d. two hyperplastic ducts, 200X

ME cell layer disruptions and ER negative cell clusters are identified with arrows

Figure 4. Multiple ME cell layer disruptions and overlying ER negative cell clusters in DCIS

4a. 200X; 4b.the adjacent section of 4a, 400X; 4c. 200X; 4d. the adjacent section of 4c, 400X.

ME cell layer disruptions and ER negative cell clusters are identified with arrows

Figure 5. ME cell layer disruptions and associated ER positive cells in hyperplastic ducts

5a – 5b. two ER positive hyperplastic ducts show attenuated and disrupted ME cell layers, 200X. The disruptions are identified with arrows

Figure 6. ME cell layer disruptions and overlying ER negative cell clusters in normal and hyperplastic appearing ducts

6a – 6c. normal appearing ducts, 400X; 6d – 6f. hyperplastic ducts, 400X

ME cell layer disruptions and ER negative cell clusters are identified with arrows

Figure 7. Comparison of the LOH pattern in ER negative cells and adjacent ER positive cells within the same duct

7a. H & E staining of a duct with AIDH, 200X; 7b. The adjacent section of 7a, immunostainined (Before microdissection), X200; 7c.microdissection of ER positive cells; 7d. microdissection of ER negative cells; 7e. LOH at 4 selected DNA markers. Asterisks indicate the ER (-) and ER (+) cells removed; arrows identify LOH.

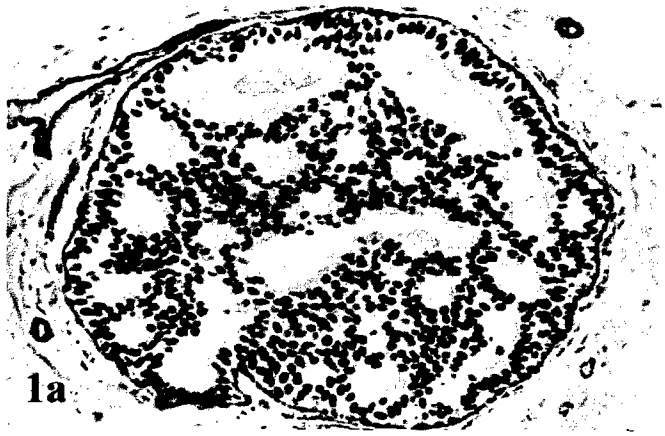
1a

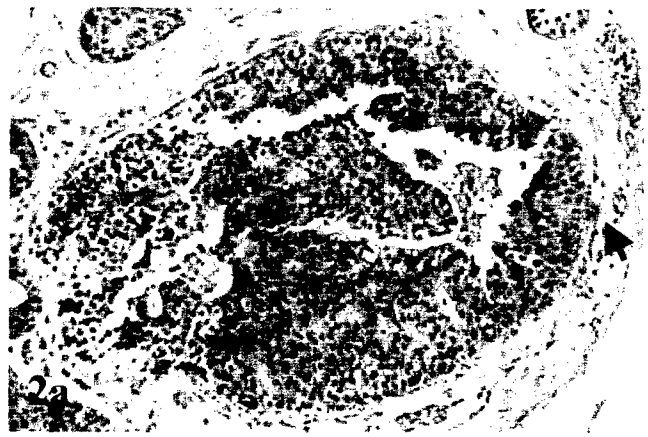
2a

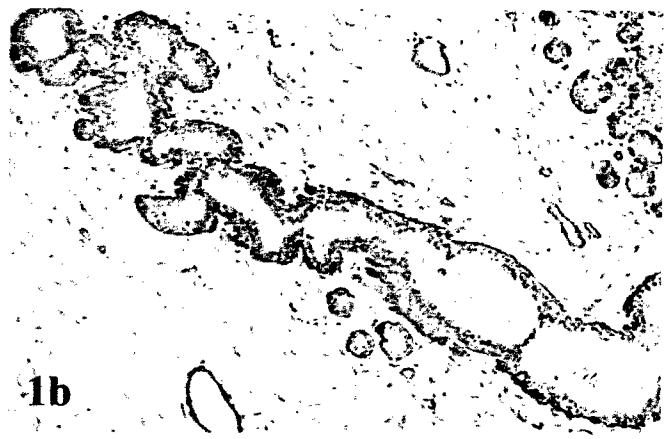
1b

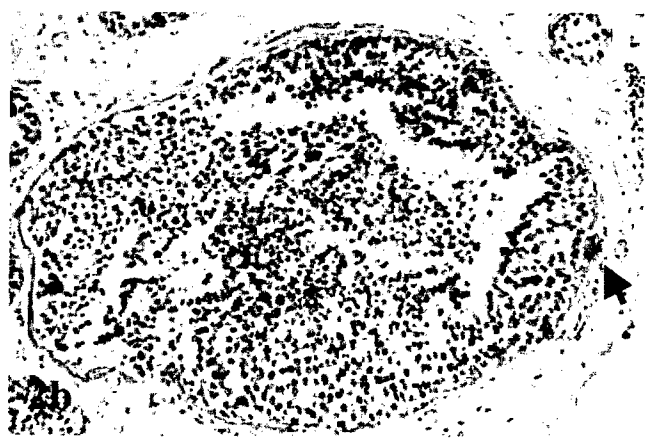
2b

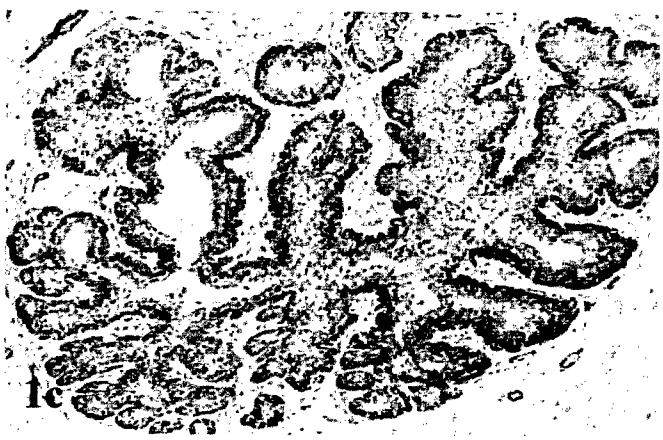
1c

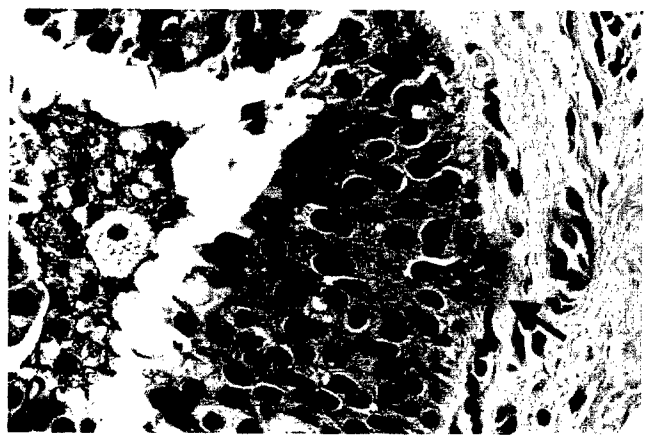
2c

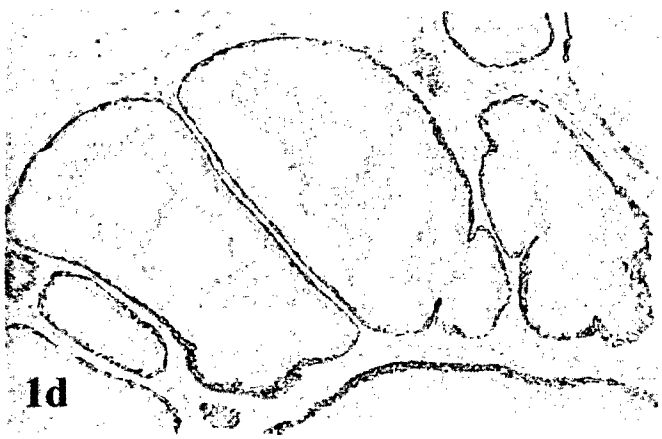
1d

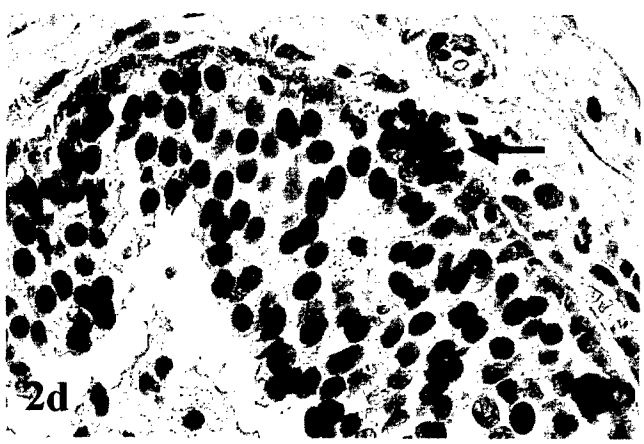
2d

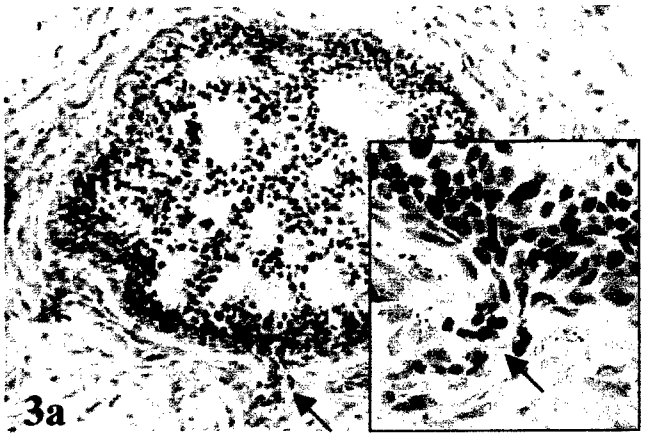
3a


4a

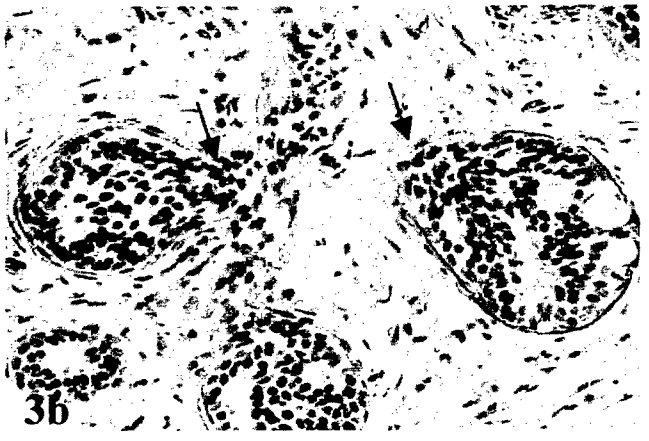
3b

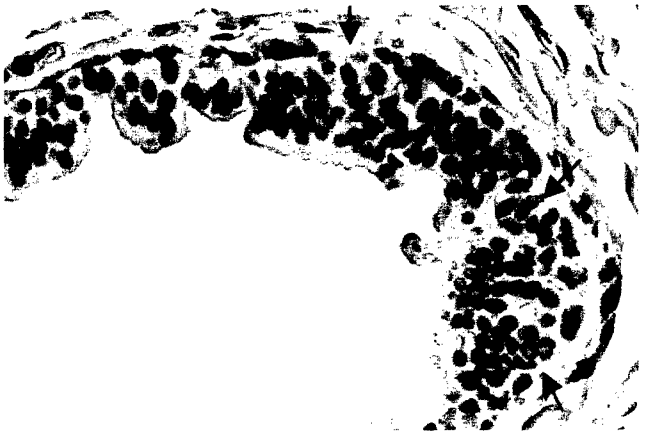


3c


4c


3d

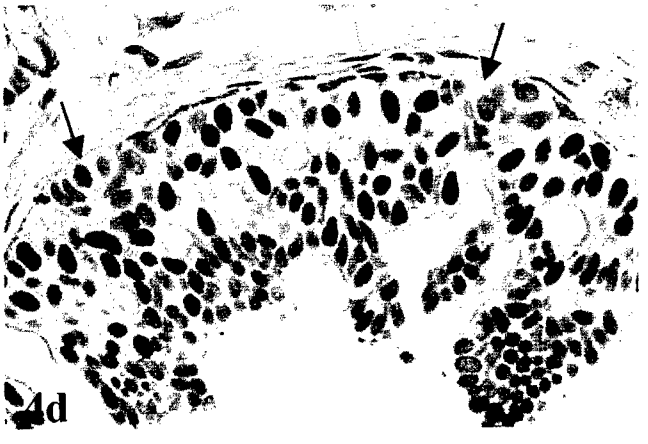
4d

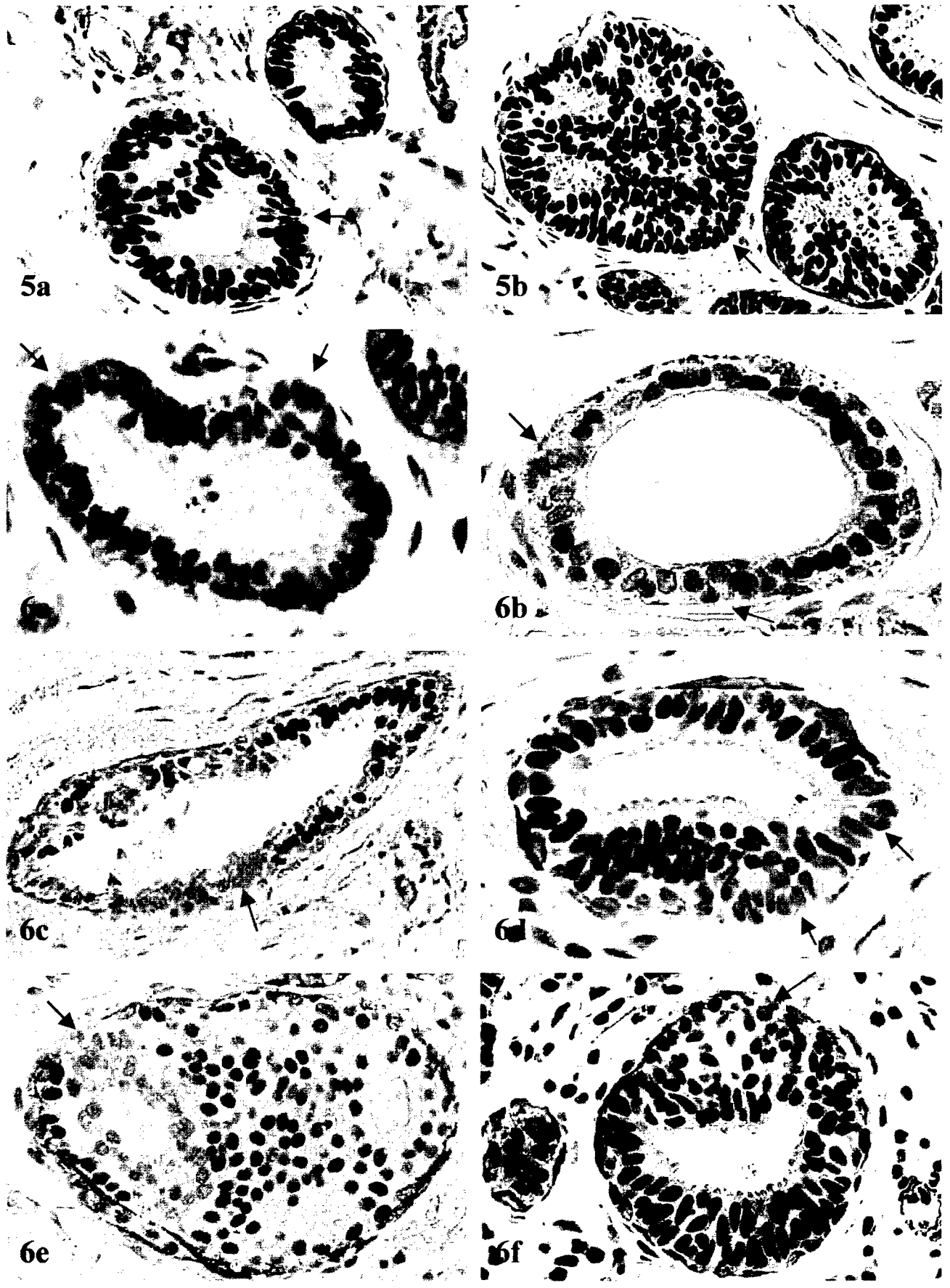
5a
5b
6a
6b
6c
6d
6e
6f

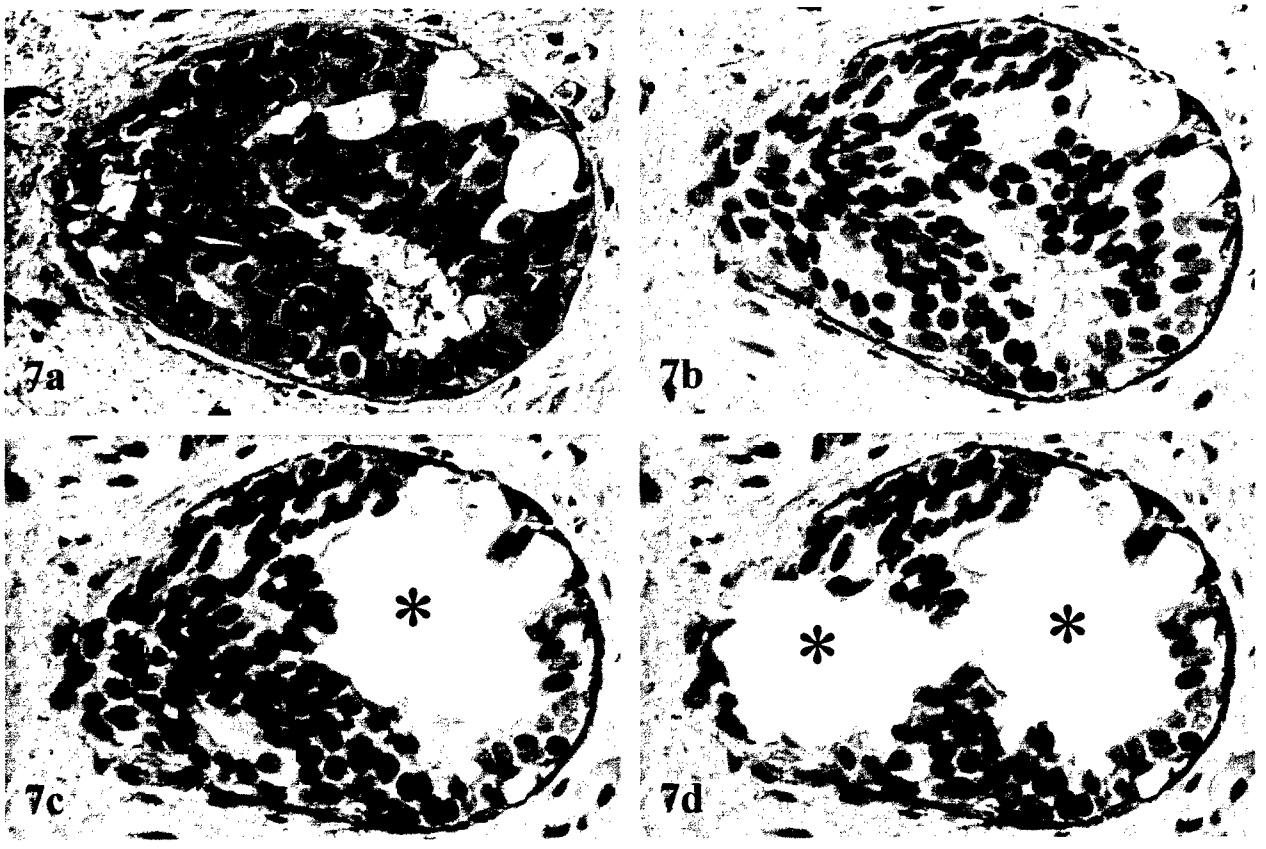

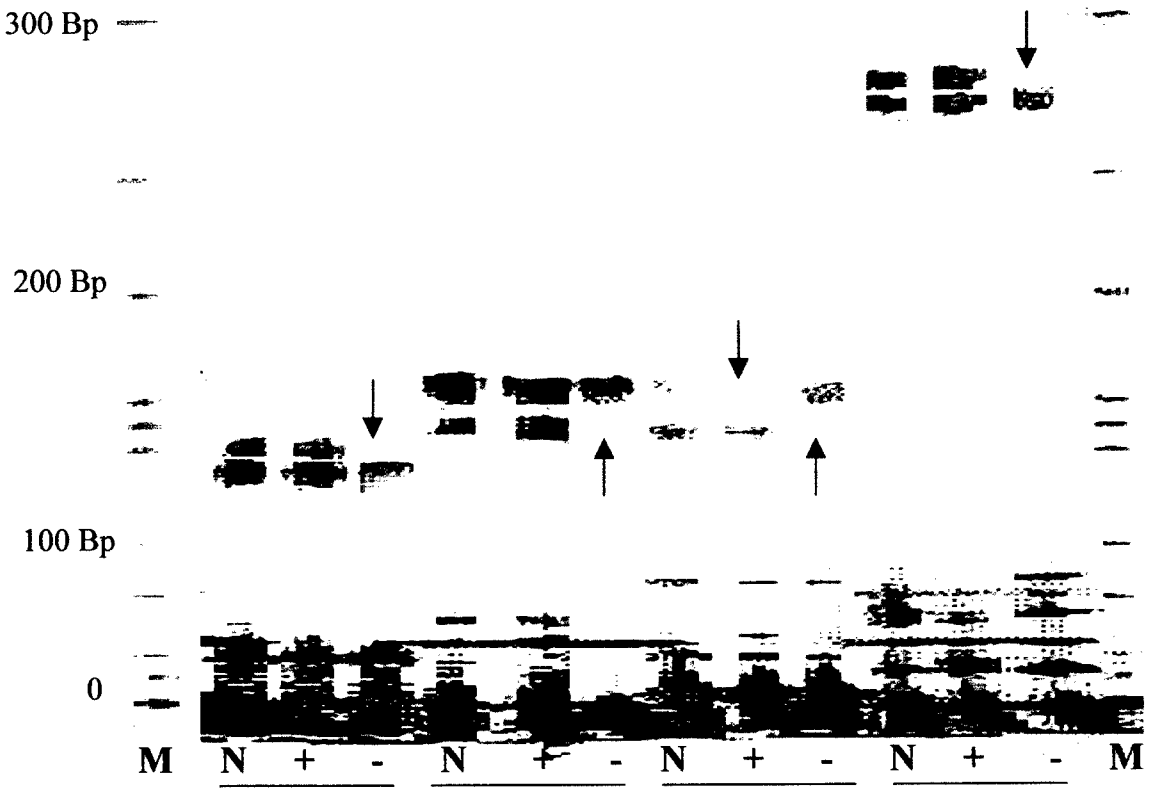

7e

M: DNA size marker; N: Normal; +: ER positive cells; -: ER negative cells; Bp: base pair

An antigen unmasking protocol that satisfies both immunohistochemical and subsequent molecular biological assessments

Yan-Gao Man, M.D., Ph.D. Ana Burgar, M.D.

Department of Gynecologic and Breast Pathology, Armed Forces Institute of Pathology (AFIP) and American Registry of Pathology (ARP), Washington, DC 20306-6000, USA

Running title: Antigen unmasking protocol for both immunohistochemical and genetic analyses

Key Words: Histotechniques; Antigen unmasking protocol; Immunohistochemical and molecular correlation; Polymerase chain reaction (PCR); Microdissection

Correspondence: Yan-gao Man, M.D. Ph.D.
Gynecologic and Breast Research Laboratory
Department of Gynecologic and Breast Pathology
Armed Forces Institute of Pathology and American Registry of Pathology,
6825 16th Street, NW, Washington, DC 20306-6000, USA

Phone: 202-782-0507 Fax: 202-782-3939 E-mail: man@afip.osd.mil

Summary

Immunohistochemical elucidation of many proteins in formalin-fixed, paraffin-embedded tissues requires a prior antigen unmasking treatment, which often damages both the morphology and genetic materials, making subsequent assessments difficult or impossible. This study attempted to develop a method that satisfies both immunohistochemical and genetic analyses. Consecutive sections were made from a variety of formalin-fixed, paraffin-embedded breast tissues, and a set of four adjacent sections from each case were treated with [1] routine H & E staining; [2] our unmasking protocol; [3] microwave oven irradiation; [4] pressure cooker incubation. After immunohistochemical staining, the tissue in each section was scraped off or the same cell clusters in four sections were separately microdissected for DNA extraction and PCR amplification. Compared to microwave and pressure cooker methods, our protocol showed the following advantages: [1] a better preservation of the morphology; [2] a substantial reduction of tissue detachments from slides; [3] effectiveness on all antibodies tested, including those require enzyme digestion or no prior unmasking; [4] higher PCR yields; [5] larger (higher molecular weight) amplified PCR products. Compared to the routine method on untreated tissues, our method consistently produced comparable quality and quantity of PCR products. Our protocol, however, takes a longer time to yield results.

Key Words: Histotechniques; Antigen unmasking protocol; Immunohistochemical and molecular correlation; Polymerase chain reaction (PCR); Microdissection

Introduction

Genetic alterations determine the scope and extent of, and also precede, the biochemical abnormalities, whereas the latter is the direct cause for a vast majority of the human diseases and pathological processes (1-2). Therefore, the assessment of the correlation between genetic and biochemical events holds significant promises in assisting clinical diagnosis and treatment. The introduction of several novel protocols has made it possible to correlate the immunohistochemical and molecular events in frozen and ethanol-fixed, paraffin-embedded tissues (3-5). The assessment in formalin-fixed, paraffin-embedded tissues, however, has been hampered by the lack of a reliable protocol that satisfies both immunohistochemical and subsequent molecular procedures. Because of the "cross-links" induced by the formalin fixation, the immunohistochemical elucidation of a wide variety of gene products, including p53 and most onco-proteins, growth factors and their receptor s, different hormone receptors, as well as most cell proliferation related molecules, requires a prior antigen unmasking treatment, using a proteolytic enzyme or high temperature (6-8). The application of these antigen unmasking methods, however, is often a difficult task, as an under treatment could yield false negative results, whereas an over treatment could damage the morphology and genetic materials, making further analyses difficult or impossible (9-11). In a recent study, DNA extracts from formalin-fixed, paraffin embedded tissue sections pre-treated with trypsin or heating in a pressure cooker or a microwave oven were subjected to PCR amplification for a 110-bp portion of the beta-globin gene (12). The PCR efficiency was evaluated by two parameters: [1] the cycle count in which the first visible band was obtained ($CYCLE_{min}$) and [2] the maximum amount of PCR products ($CONC_{max}$). The study found that "The trypsin treatment significantly prolonged the $CYCLE_{min}$ ($p < 0.01$), and the PCR amplification did not reached the "plateau" level with a maximum of 60 cycles. The PCR efficiency was worse in microwave or pressure cooker treatment, with neither $CYCLE_{min}$ nor $CONC_{max}$ being obtained" (12). The authors concluded that "A

successful PCR amplification may not be expected in sections that are pretreated in a microwave oven or pressure cooker" (12).

Attempting to reduce the destructive effects of antigen unmasking methods on tissues, we had previously developed an antigen unmasking protocol, which involves a 30-60 minute incubation of paraffin sections at 80 ^{0}C and an overnight incubation of deparaffinized sections in a regular oven at 70 to 80 ^{0}C in 10mM citrate buffer (13). With this protocol, a variety of cytoplasmic and nuclear antigens known to require microwave irradiation or enzymatic digestion for their optimal detection could be clearly demonstrated with better preservation of the morphology, less background, and more uniform immunoreactivities. Our subsequent study further revealed that this protocol not only facilitated immunohistochemical detection of estrogen receptor (ER) proteins, but also facilitated the detection of ER mRNA with in situ hybridization and in situ RT PCR techniques (14), suggesting that this protocol might be able to satisfy both immunohistochemical and subsequent molecular biological assessments. This study intended to confirm previous findings, by comparing the PCR efficiencies among immunostained tissues that were pre-treated with our protocol or under a high temperature using a microwave oven or a pressure cocker.

Materials and Methods

1. Reagents and instrument

Xylene, ethanol, and hematoxylin were obtained from Fisher Scientific (Pittsburgh, PA). Positively charged microscope slides were purchased from CMS (Houston, TX). A pressure cocker designated for the antigen unmasking procedure, along with the antigen retrieval solution were purchased from Biocare Medical (Walnut Creek, CA). A microwave was commercially purchased and inspected by a certified technician of our institute. Immunohistochemical staining reagents were from Vector Laboratories (Burlingame, CA). DNA extraction related reagents were obtained from Sigma (St. Louis, MO). An automated 377 DNA sequencer along with the software and the User's Manual, PCR amplification kits, and the DNA size standard, were from Perkin-Elmer (Foster City, CA). Fluorescent dye-labeled DNA markers were purchased from Research Genetics (Huntsville, AL). Electrophoresis reagents, including 40% polyacrylamide gel solution, ammonium persulfate, and TEMED, were from Bio-Rad (Forster City, CA).

2. Tissue samples

Formalin-fixed, paraffin-embedded breast and other tissues were retrieved from the files of Armed Forces Institute of Pathology. Consecutive sections of 4-5 μm thickness were cut and placed on positively charged microscope slides. To minimize contamination or carrying over that may interfere with a subsequent molecular analysis, a "clear" cutting method was used, which involves the use of distilled water, gloves, and a new blade for each case.

3. Antigen retrieval procedure

A set of four consecutive sections containing the same tissue structures were prepared from each of 45 cases, and the sections were treated as the following:

(1). Routine H & E stain

Sections were routinely deparaffinized with xylene, cleaned in ethanol and water, and processed for DNA extraction, as previously described (15).

(2). Our antigen unmasking protocol

Sections were first incubated in a regular oven at 80°C for 30 minutes, and were then deparaffinized with Xylene and cleaned in ethanol and water. Deparaffinized sections were incubated overnight with 1X antigen retrieval solution or home-made 10mM sodium citrate buffer (13) in a regular oven at 65-80 ^{0}C, and then, were processed for immunostaining.

(3). Microwave oven irradiation

Sections were routinely deparaffinized with xylene, and cleaned in ethanol and water. Antigen unmasking was carried according to a commonly practiced protocol (6), which involves a 10 minute (2 X 5 minutes) irradiation of deparaffinized sections in 10mM citrate buffer. After the microwave irradiation, sections were cooled at room temperature, and processed for immunostaining.

(4). Pressure cooker incubation

Sections were routinely deparaffinized with xylene, and cleaned in ethanol and water. Antigen unmasking was carried out according to the protocol provided by the manufacturer. Briefly, the deparaffinized sections were placed in warm 1X antigen retrieval solution and heated in the pressure cooker for 3 min. After heating, sections were transferred to fresh 1X antigen retrieval solution and heated under the same condition for 10 min. Then, sections were cooled at room temperature for 10 minutes, and processed for immunostaining.

4. Immunohistochemical staining

The antibodies tested and manufacturers' recommendations for the prior treatment are listed in Table 1. Immunohistochemical staining was carried out as previously described (13, 16).

5. DNA extraction

After immunohistochemical staining, the tissue in each of the sections was scraped off the slide, and placed in a separate PCR tube for DNA extraction. Since tissue detachments were often seen in sections treated with the microwave oven or pressure cooker method, microdissection were used to obtain a comparable number of cells from the same and well preserved areas in different sections of

the same case. Microdissected cells from each of the four sections in the same case were identically treated for DNA extraction, and subsequent PCR amplification and detection, to further ensure the comparison among the samples are carried out under the same condition (except the prior treatment).

6. PCR amplification, electrophoresis, and gel image analysis

A panel of 15 DNA markers at 6 different chromosomes was used for the comparison of the PCR efficiencies among different samples. The expected sizes of amplified PCR products among DNA markers varied from 95 to 290 base pairs (bp). The main features of the DNA markers are listed in Table 2. An equal amount of DNA extract (1.0-1.5 μl) from each sample was mixed with 10 μl of PCR solution containing a pair of fluorescence labeled primers. The mixture was covered with 40 μl of mineral oil. PCR amplification was carried out in a programmable thermal cycler (Perkin-Elmer, Forster City, CA) at the following settings: after a denaturation at 94°C for 10 min, samples were amplified for 35-40 cycles at 94°C, 55°C, and 72°C, each for 1 min with a final extension at 72°C for 10 min. After amplification, 2-3 μl of PCR solution was mixed with 6-8μl of gel loading buffer, and 1.0-1.5 μl of mixture was subjected to electrophoresis in 5-6 % polyacrylamide gels. The amplified PCR products were detected with a 377 DNA sequencer (Perkin-Elmer, Forster City, CA), and the gel images were produced in accordance with manufacture's specifications and our recently developed protocols (17-18). The specific PCR products were located, and the intensity of the DNA bands and the height of the peaks in different samples were compared (19).

Results and Discussion

According to the manufacturers, 29 of the 43 antibodies listed in Table 1 require microwave irradiation or pressure cooker incubation, 8 require enzymatic digestion, and 6 require no special treatment for the optimal demonstration of the corresponding antigens. Using our protocol, an overnight incubation at 65-80 ^{0}C, however, distinct immunostaining was readily appreciable for each of the 43 antibodies. Compared to other antigen unmasking treatments on the adjacent sections, our protocol also possesses the following advantages: [1] a better preservation of the morphological detail; [2] a substantial reduction of tissue detachments from slides; [3] a stronger immunoreactivity. Figures 1a to 1h show such comparisons in four adjacent sections pretreated with different methods.

DNA extracts from tissues scraped off or microdissected from sections pretreated with our protocol consistently generated higher PCR yields, and also produced PCR products with higher molecular weights, compared to DNA extracts from tissues sections pretreated with microwave oven irradiation or pressure cooker incubation. DNA extracts from tissues scraped off or microdissected from sections pretreated with our protocol consistently generated a similar quality and quantity of PCR products, compared to DNA extracts from routine H & E stained sections. Figures 2 to 5 show tissues microdissected from each of the 4 adjacent sections, and the comparisons of the resultant PCR products.

Our protocol is also effective for antigens that require enzyme digestion or no pretreatment for their optimal elucidation. Figures 6a and 6b show triple immunohistochemical staining in the same section pretreated with our protocol, for three different antigens, Ki-67, epithelial specific antigen, and smooth muscle actin, which require three different treatments for their optimal detection.

Antigen unmasking methods, using either microwave oven or pressure cooker under a high temperature, or proteolytic digestion with different enzymes, have been routinely used in clinical and research laboratories, for the optimal detection of a wide variety of antigens in formali-fixed, paraffin-embedded tissues (6-8). These methods, however, are not easy to use, since an over-

treatment could result in the destruction of the morphology and detachment of the tissues, while an under-treatment may yield false negative results (9-11). Unfortunately, there are no objective criteria available to monitor the unmasking process, or to assess the unmasking effects before the completion of the entire immunostaining process. Therefore, a series of pre-tests have to be conducted to identify the optimal condition. A number studies have shown that the optimal condition for different antigens varies substantially; also, the optimal condition for the same antigen changes with the type of the tissues, length of the fixation, and thickness of the sections (9-11). Consequently, the identification of the optimal condition for multiple antigens could be a time- and reagent-consuming process, or is impossible to achieve if there are only limited sections available. In contrast, our protocol is easy and safe to use, as it only involves an overnight incubation of the deparaffinized sections in a regular oven in antigen unmasking solution. The incubation time and temperature are very flexible, ranging from 65 ^{0}C to 80 ^{0}C and from less than 10 to over 30 hours, respectively. Also, a variety of solutions could be used to produce a similar or even better result. A recent study (20) has shown that an overnight incubation at 70-80 ^{0}C in Tris-HCL buffer (pH 9) could produce more distinct and stronger signal for estrogen receptor, compared to an overnight incubation at the same temperature in sodium citrate buffer (pH 6).

Our preference for an overnight incubation at $\cong$70 ^{0}C in sodium citrate buffer is based on three reasons or assumptions: [1] this temperature is higher than the melting point temperature all subtypes of paraffin such that it could dissolve and wash off any possible paraffin residue that repels water-based solutions, preventing the physical contact between tissues and reagents; [2] this temperature is lower than the denaturing temperature of DNA, RNA, and many proteins such that it may have less destructive effects on these molecules, preventing tissue loss or detachment from the slides; [3] the citrate buffer is acidic (pH 6), which might be able to gradually disrupt the masking proteins and "cross-links" induced by formalin fixation, increasing the accessibility of probes or antibodies to their targets. Consisting with our assumptions, our previous study has shown that our protocol not only

facilitates immunohistochemical detection of estrogen receptor (ER) proteins, but also facilitates the detection of ER mRNA with the in situ hybridization and in situ RT PCR techniques (14). In our current study, the quality and quantity of amplified PCR products are consistently better and higher in DNA extracts from tissues pre-treated with our unmasking method than those from tissues pre-treated with a microwave oven or pressure cooker, and are very comparable to those from the adjacent untreated control tissues, further supporting our assumptions. In addition, our assumptions were supported by the results of a most recent study (21), which compared the DNA yields and PCR efficiencies among 33 serial sections of formalin-fixed, paraffin-embedded tissues that were inserted into 33 microtubes and subject to antigen retrieval under three temperatures (80, 100, and 120 ^{0}C) and 11 variable pH values (2 to 12). The study revealed that the incubation of tissues at a higher temperature and a at pH 6-9 gave higher yields of DNA, and that the PCR products of these DNA extracts were comparable to those of the control sample subjected to the standard non-heating, enzymatic DNA extraction method (21).

Taken together, these results suggest our antigen unmasking protocol could satisfy both the immunohistochemical and subsequent molecular analyses in formalin-fixed, paraffin-embedded tissues. With our protocol, we have recently revealed a subset of morphologically comparable tumor cells within the same duct that display substantially different immunoreactivities to estrogen receptor, and also showed a different genetic profile (22-23). These findings suggest that our protocol may have both scientific and clinical values in assisting the assessment of the correlation between genetic and biochemical events in cells with antigens that could not be elucidated without a pre-antigen unmasking treatment. The drawback of our protocol, however, is that a significantly longer time is needed to complete the experimental procedure.

Acknowledgement

The authors are grateful to Doug Landry and Jomie Nola of AFIP exhibition section and Kenneth J. Vrtacnik of AFIP photography Lab, for their technical assistance in preparing some of the figures.

This study was supported in part by The Congressional Directed Medical Research Programs, grants DAMD 17-01-0129 and DAMD17-01-0130 to Yan-gao Man, M.D., Ph.D.

References

1. Lengauer C, Kinzler KW, Vogelstein B (1998) Genetic instabilities in human cancers. Nature 369: 643-649
2. Offringa R, van der Burg SH, Ossendorp F, Toes REM, Melief CJM (2000) Design and evaluation of antigen vaccination strategies against cancer. Curr Opin Immunol 12: 576-582
3. Heinmoller E, Liu Q, Sun Y, Schlake G, Hill KA, Weiss LM, Sommer SS (2002) Toward efficient analysis of mutations in single cells from ethanol-fixed, paraffin-embedded, and immunohistochemically stained tissues. Lab Invest 82: 443-453
4. Hirose Y, Aldape K, Takahashi M, Berger MS, Feuerstein BG (2001) Tissue microdissection and degenerate oligonucleotide primed-polymerase chain reaction (DOP-PCR) is an effective method to analyze genetic aberrations in invasive tumors. J Mor Diagn 3: 62-67
5. Ehrig T, Abdulkadir SA, Dintzis SM, Milbrandt J, Watson MA (2001) Quantitative amplification of genomic DNA from histological tissue sections after staining with nuclear dyes and laser capture microdissection. J Mol Diagn 3: 22-25
6. Shi SR, Key ME, Kalra KL (1991) Antigen retrieval in formalin-fixed, paraffin-embedded tissues: an enhancement method for immunohistochemical staining based on microwave oven heating of tissue sections. J Histochem Cytochem. 39: 741-748
7. Momose H, Mehta P, Battifora H (1993) Antigen retrieval by microwave irradiation in lead thiocynate: comparison with protease digestion retrieval. Appl Immunohistochem 1: 77-82
8. Magi-Galluzzi C, Montironi R, Prete E, Kwan PW, DeLellis RA (1996) Effect of microwave oven heating times on androgen receptor antigen retrieval from paraffin-embedded prostatic adenocarcinoma. Anticancer Res 16: 2931-29369
9. Munakata S, Hendricks JB (1993) Effect of fixation time and microwave oven heating time on retrieval of the Ki-67 antigen from paraffin-embedded tissue. J Histochem Cytochem 41: 1241-1246

10. Leong ASY, Milios J (1993) An assessment of the efficiency of the microwave antigen-retrieval procedure on a range of tissue antigens. Appl Immunohistochem 1: 267-274

11. Dookham DB, Kovatich AJ, Miettinen M (1993) Non-enzymatic antigen retrieval in immunohistochemistry: Comparison between different antigen retrieval modalities and proteolytic digestion. Appl Immunohistochem 149-155

12. Murase T, Inagaki H, Eimoto T (2000) Influence of histochemical and immunohistochemical stains on polymerase chain reaction. Mod Pathol 13: 147-151

13. Man YG, Tavassoli FA (1996) A simple epitope retrieval method without the use of microwave Oven or enzyme digestion. Appl Immunohistochem 4: 139-141.

14. Man YG, Zhaung ZP, Bratthauer GL, Bagasra O, Tavassoli FA (1996) Detailed RT-ISPCR protocol For preserving morphology and confining PCR products in routinely processed paraffin Sections. Cell Vision 3: 389-396

15. Man YG,Moinfar F,Bratthauer GL,Kuhls EA,Tavassoli FA (2001) An Improved Method for DNA extraction from Paraffin Sections. Pathol.Res.Pract 197: 635-642

16. Man YG, Ball WD, Culp DJ, Hand AR, Moreira JE (1995) Persistence of a perinatal cellular phenotype in submandibular glands of the adult rat. J Histochem Cytochem 43: 1203-1215

17. Man YG, Moinfar F, Bratthauer GL, Tavassoli FA (2000) Five useful approaches for generating more valid gel images of LOH and clonality analysis with an automated 377 DNA sequencer. Diagn Mol Patho 9: 84-90

18. Man YG, Kuhls EA, Bratthauer GL, Moinfar F, Tavassoli FA (2001) Multiple use of stab gels in sequencing apparatus for separation of polymerase chain reaction products. Electrophoresis 22: 1915-1919

19. Man YG, Martinez A, Avis IM, Hong SH, Cuttitta F, Venzon DJ, Mulshine JL (2000) Phenotypically different respiratory epithelial cells with hnRNP A2/B1 over-expression display similar genetic alterations. Am J Respir Cell Mol Biol 23: 636-645

20. Koopal SA, Coma MI, Tiebosh ATMG, Suurmeijer AJH (1998) Low temperature heating ivernight in Tris-HCL buffer (pH9) is a good alternative for antigen retrieval in formalin-fixed paraffin-embedded tissue. Appl Immunohistochem 6: 228-233

21. Shi SR, Cote RJ, Wu L, Liu C, Shi Y, Liu D, Lim H, Taylor CR (2002) DNA extraction from archival formalin-fixed, paraffin-embedded tissue sections based on the antigen retrieval principle: heating under the influence of pH. J Histochem Cytochem 50: 1005-1011

22. Man YG, Shekitka KM, Bratthauer GL, Tavassoli FA (2002) Immunohistochemical and genetic alterations in mammary epithelial cells overlying focally disrupted myoepithelial cell layers. Breast Cancer Res Treat, 76: S142, 569 (Abstract)

23. Man YG, Strauss BL, Saenger JS, Vang RS, Barner R, Wheeler D, Martinez A, Mulshine JL. (2003) Identification of invasive precursor cells in normal and hyperplastic appearing breast tissues. Cancer Res, In press (Abstract)

Table 1. Antibodies tested and manufacturer's recommendation for pretreatment

No	Antibody	Manufacturer	Manufacturers recommend pretreatment
1	AR	Vector	Microwave oven or pressure cooker
2	Bcl-2	Vector	Same as above
3	CD10	Vector	Same as above
4	CD31	Vector	Same as above
5	CD44	Vector	Same as above
6	CD117	Vector	Same as above
7	c-erbB 2	Vector	Same as above
8	CK5	Vector	Same as above
9	CK8	Vector	Same as above
10	CK 34βE12	Vector	Same as above
11	CK AE1/AE3	Vector	Same as above
12	Collagen 4	Dako	Same as above
13	Cyclin A	Vector	Same as above
14	Cyclin D3	Vector	Same as above
15	E-Cadherin	Vector	Same as above
16	EGFR	Vector	Same as above
17	ER	Vector	Same as above
18	Ets-1	Vector	Same as above
19	Ki-67	Dako	Same as above
20	Maspin	Vector	Same as above
21	P16	NeoMarkers	Same as above
22	P21	Dako	Same as above
23	P24	Vector	Same as above
24	P27	Vector	Same as above
25	P53	Dako	Same as above
26	PR	Vector	Same as above
27	Topoisomerase IIα	Vector	Same as above
28	WT-1	Cell Marque	Same as above
29	Vimentin	Vector	Same as above
30	Calponin	Vector	Trypsin digestion (TD)
31	CD34	Vector	TD
32	CK10	Vector	TD
33	CK19	Vector	TD
34	ESA	Vector	TD
35	Fibronectin	Vector	TD
36	Tenancy	Vector	TD
37	SMA	Vector	TD or None
38	PAP	Vector	None
39	PCNA	Vector	None
40	PS2	Vector	None
41	PSA	Vector	None
42	S100	Vector	None
43	EMA	Vector	None

Table 2. DNA markers used for comparison of PCR efficiencies among samples

#	Name	Chromosomal location	Size(base pairs)
1	D3S1067	3p21.1 – 14.3	95
2	D3S1300	3p21.1 – p14.2	217 - 241
3	D3S1311	3q27 - qter	134 - 152
4	D8S137	8p21.3 – p11.1	150 -162
5	D8S505	8p	203 -213
6	D11S29	11q23.3	143 - 163
7	D11S904	11p14 – p13	185 - 201
8	D11S914	11p13 – p12	275 - 285
9	D13S119	13q14.3 – q22	120 - 140
10	D13S263	13q14.1 – 14.2	145 - 165
11	D13S219	13q12.3 – q13	117 - 127
12	D16S518	16q23.1 – q24.2	272 - 290
13	D16S402	16q24.2	161 - 187
14	D17S785	17q11 – q23	181 - 207
15	D17S791	17q	165 - 199

Figure legends

Figures 1a-1h: Immunohistochemical staining for ER (brown) and ESA (red) in pretreated sections with different antigen unmasking methods

1a: Routine H & E staining; 1b: Our protocol; 1c: Microwave oven; 1d: pressure cooker; 1e, 1f, 1g, and 1h are the higher magnification of 1a, 1b, 1c, and 1d, respectively.

Arrows identify tissue detachment

Figures 2-5: Comparison of the PCR efficiencies among cells microdissected from pre-treated and immunostained sections

2: Routine H & E staining; 3: Our protocol; 4: Microwave oven; 5: Pressure cooker.

a: before microdissection; b: after microdissection; c: amplified PCR products.

Arrows identify tissue detachments or LOH; Asterisks indicate tissues removed for DNA extraction and PCR amplification.

Figures 6a-6b: Triple immunohistochemical staining in a section pretreated with our protocol

1. Ki-67 (black), recommended for a pre-treatment with microwave oven or pressure cooker; 2. ESA (brown), recommended for a pre-treatment with trypsin digestion; 3. SMA (red), pre-treatment is not needed.

1a

1e

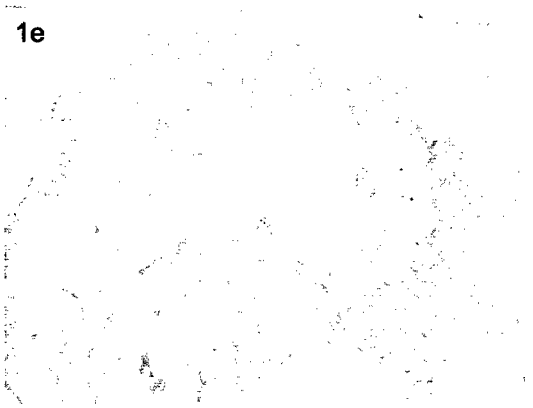

1b

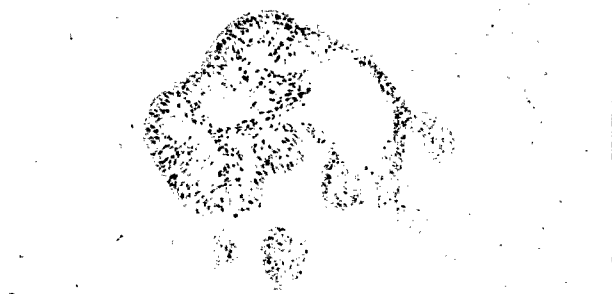

1f

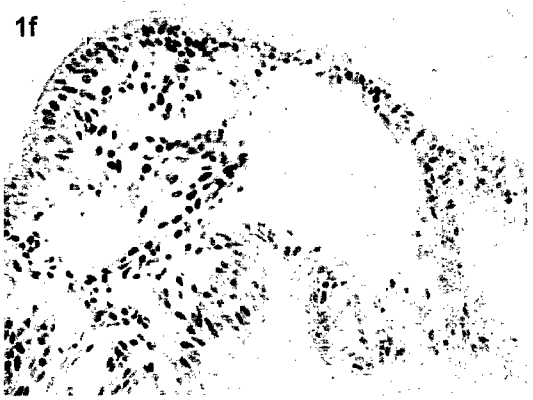

1c

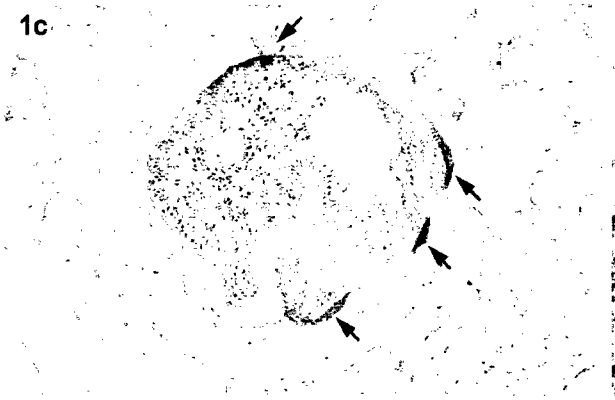

1g

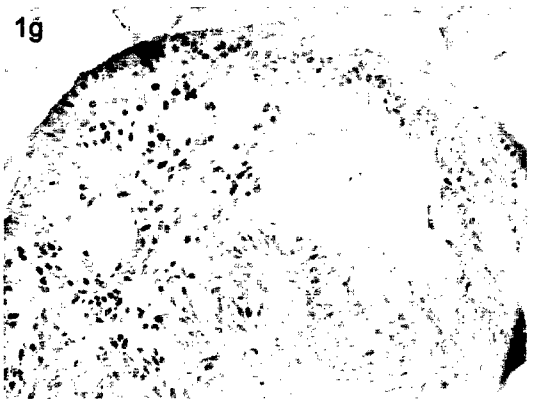

1d

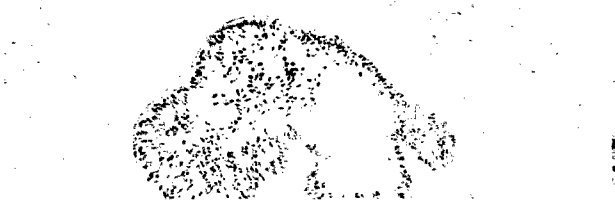

1h

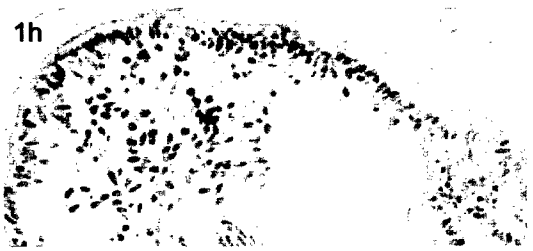

2a

3a

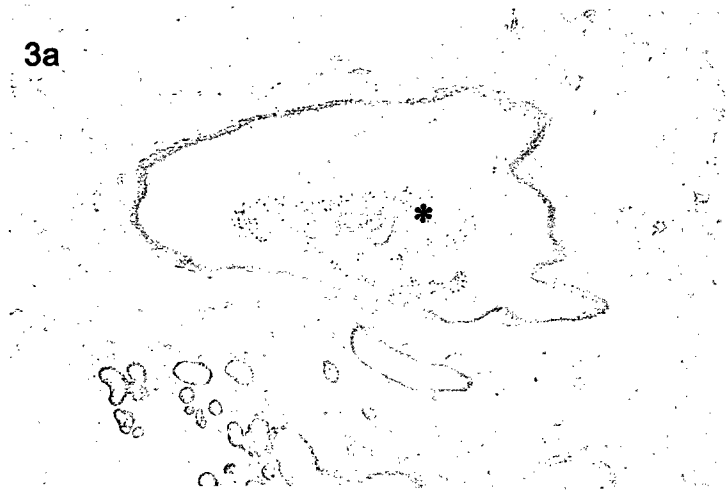

2b

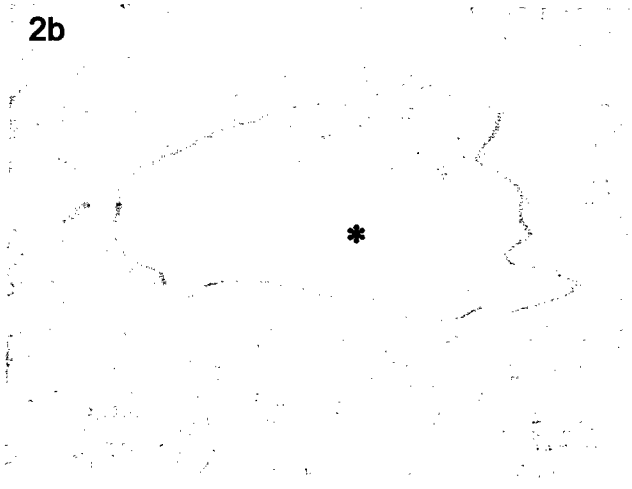

3b

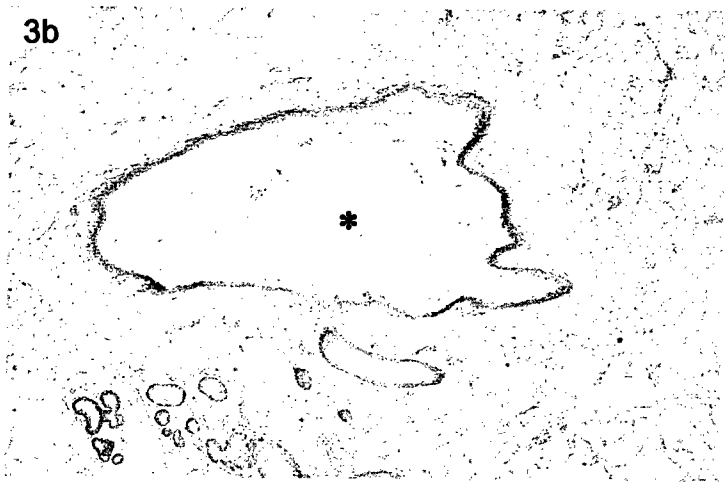

2c

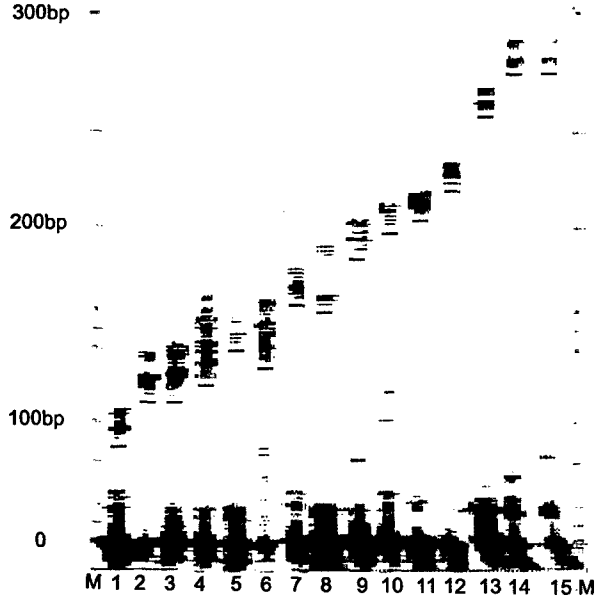

3c

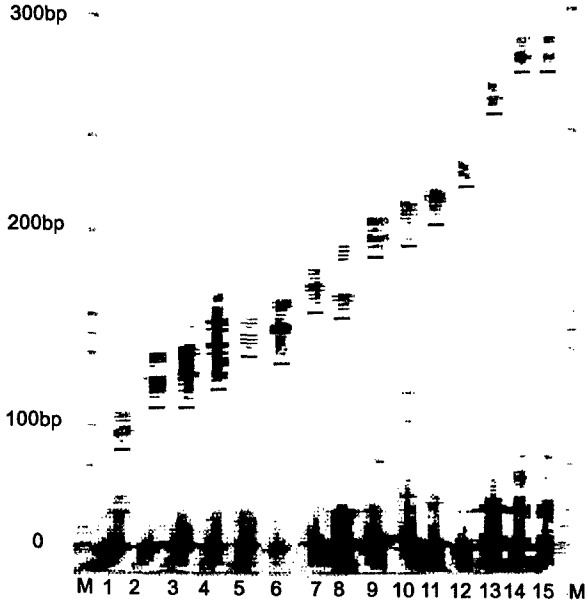

4a

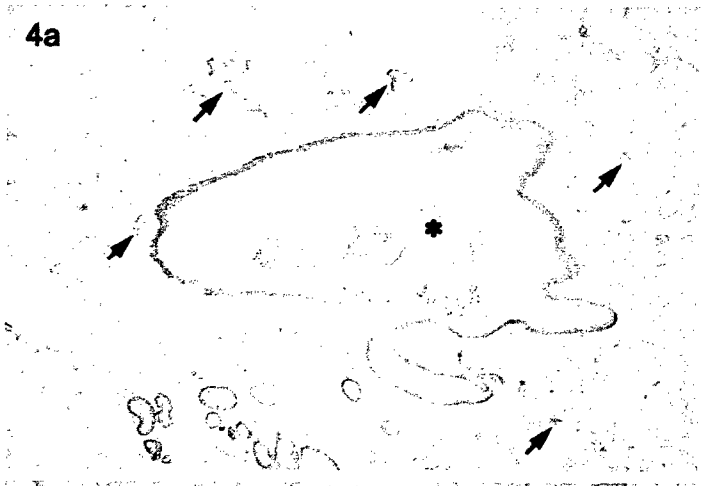

5a

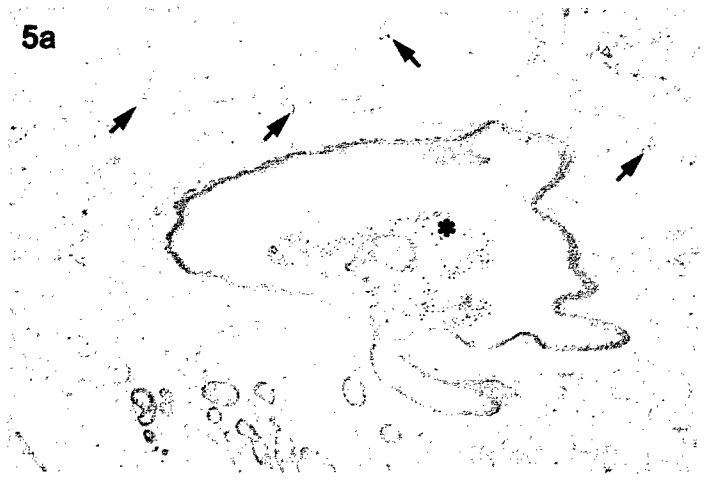

4b

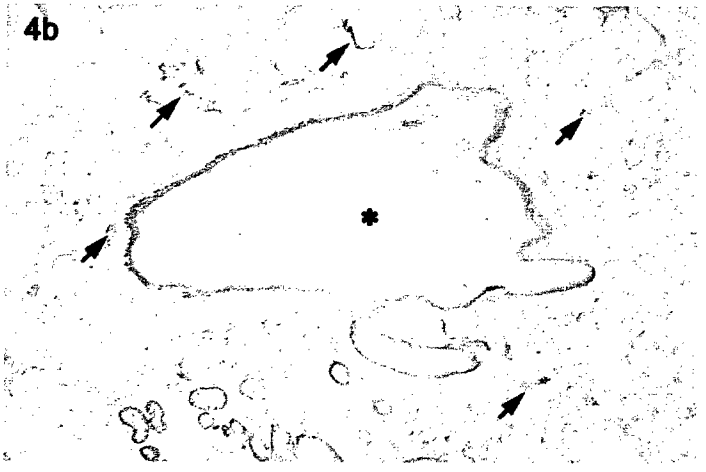

5b

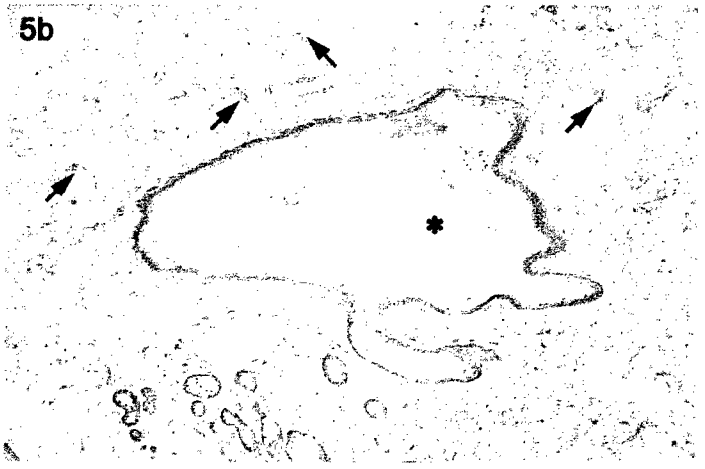

4c

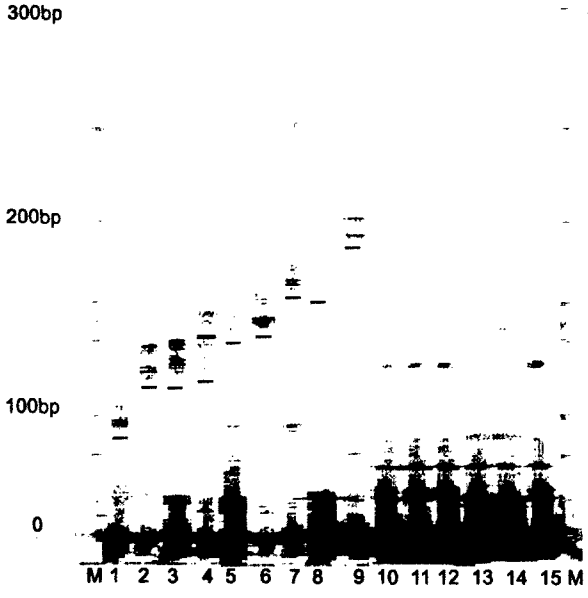

5c

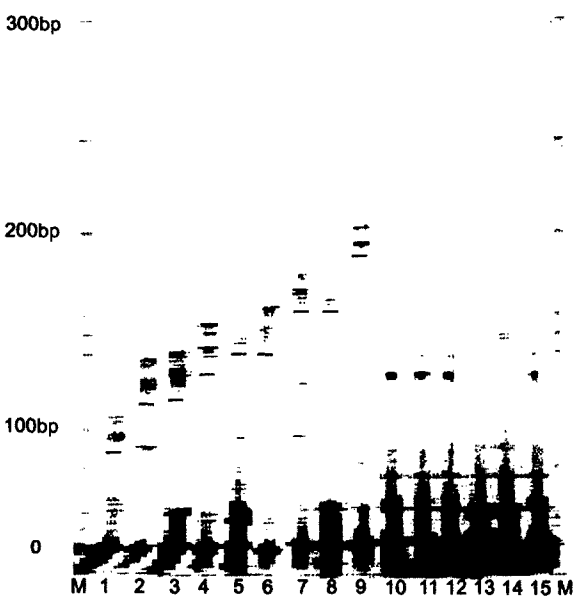

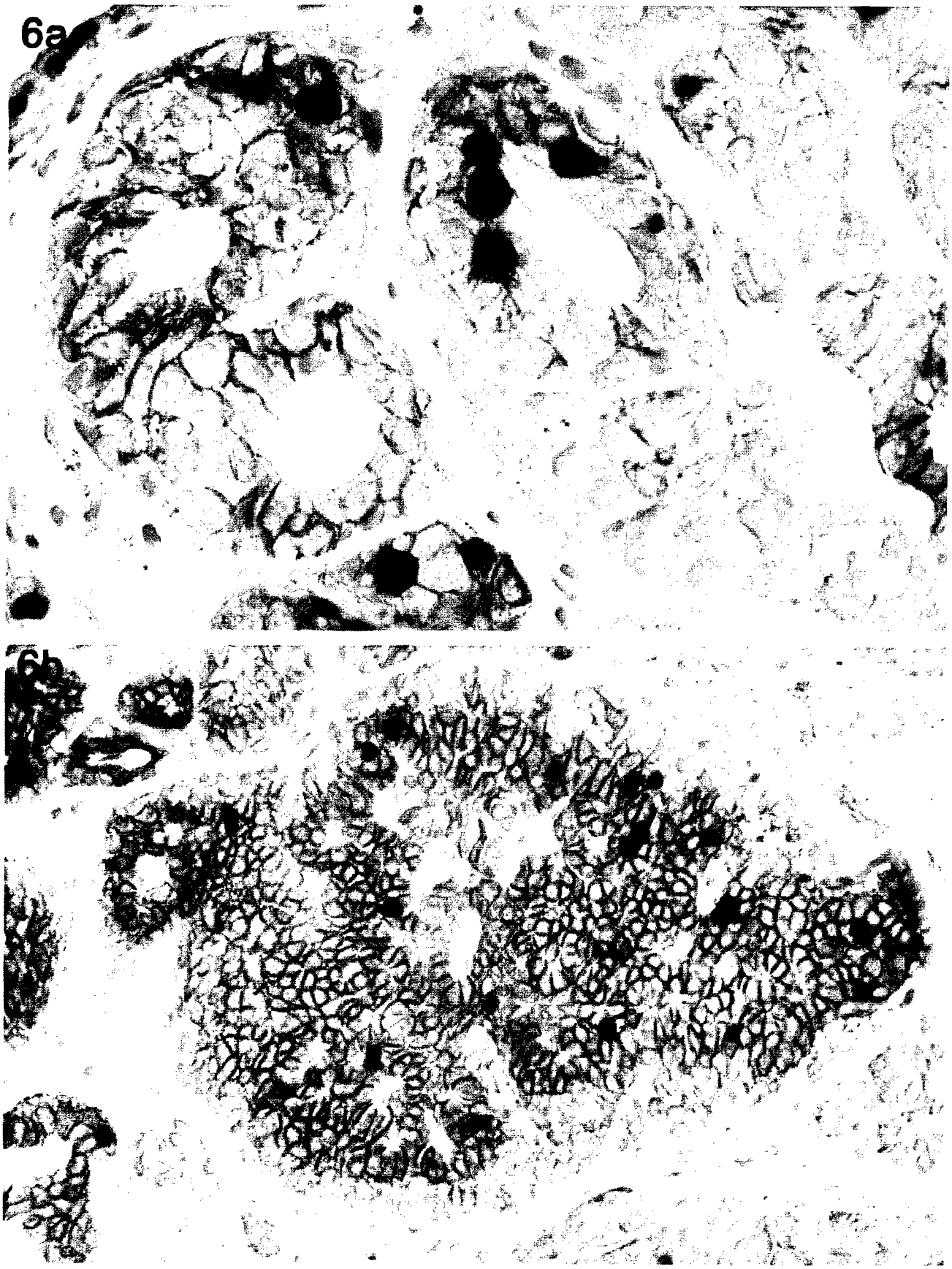
6a
6b

Morphologically Similar Epithelial Cells And Stromal Tissues In Primary Bilateral Breast Tumors Display Different Genetic Profiles: Implications for Treatment

Yan-gao Man, MD., Ph.D., Gregg G. Magrine*, Ph.D., Ruth A. Lininger, MD., Ting Shen., MD., Ph.D., Elizabeth Kuhls, MD., Gary L. Bratthauer, MS., MT, Frederic M Waldman*, MD., Ph.D

Department of Gynecologic and Breast Pathology, Armed Forces Institute of Pathology and American Registry of Pathology, Washington, DC 20306-6000
*Cancer Center and Department of laboratory Medicine, University of California, San Francisco, CA 94143-0808

Dr. Ruth A. Lininger's current address: Department of Pathology and Laboratory Medicine, University of North Carolina School of Medicine, Chapel Hill, NC 27599

Dr. Ting Shen's current address: Department of Pathology and Laboratory Medicine, Temple University Hospital, Philadelphia, PA 19140

Corresponding author: Yan-gao Man, MD., Ph.D.
Director of Gynecologic and Breast Research Laboratory
Department of Gynecologic & Breast Pathology
The Armed Forces Institute of Pathology and
American Registry of Pathology
6825 16th Street, NW
Washington, DC 20306-6000

Phone: 202-782-1612; Fax: 2020782-3939; E-mail: man@afip.osd.mil

Running title: LOH and CGH profiles of primary bilateral breast tumors

Key words: Primary bilateral breast tumor; Stromal-epithelial interaction; Loss of heterozygosity; Comparative genomic hybridization

The opinions and assertions contained herein are the private viewpoints of the authors and do not reflect the official views of the Department of Defense or Department of the Army

Abstract

Morphologically similar epithelial (EP) cells and stromal (ST) tissues in the right and left breast of 18 patients with bilateral primary breast tumors were microdissected and compared for the frequency and pattern of loss of heterozygosity (LOH) and microsatellite instability (MI), and profiles of comparative genomic hybridization (CGH). Of the 18 paired bilateral EP samples assessed with 10 DNA markers at 5 chromosomes, 78 loci displayed alterations; of which, 23 (29.5%) showed concurrent and 55 (70.5%) displayed independent LOH and/or MI. Of the 18 paired bilateral ST samples assessed with the same markers, 70 loci displayed alterations, of which, 9 (12.9%) showed concurrent and 61 (87.1%) displayed independent LOH and/or MI. Overall, all 10 markers and 30 (83.3%) of the 36 paired bilateral EP and ST samples showed more independent, whereas only 3 (8.3%) showed more concurrent LOH and/or MI. The frequency of independent LOH and/or MI was significantly higher ($p<0.01$) than that of concurrent LOH and/or MI in both EP cells and ST tissues. On the other hand, EP cells of a pulmonary small cell carcinoma simultaneously metastasized to both breasts displayed concurrent LOH at each of the 4 altered loci. Of the 7 cases selected for CGH, 6 (86%) displayed chromosomal changes (gain or loss of DNA copy numbers) in either the EP or ST component, while none showed an identical pattern and frequency of changes in both breasts. In one case, however, there was an identical change, loss of 13 q, in both the EP and ST components of one breast. These findings suggest that the genetic profiles and/or clinical behavior of cells in the left and right breast of bilateral tumors might differ substantially. Consequently, different intervention strategies might be needed for the optimal management of bilateral breast tumors.

Introduction

Bilateral breast carcinomas, reflecting either two independent primary lesions or one primary lesion with metastasis, account for 3-9% of all breast malignancies (1-3). Since patients with metastatic lesions generally have a substantially worse prognosis and require more aggressive clinical interventions than patients with independent primary lesions, their differentiation directly impacts the treatment options and clinical outcome (4-6). Unfortunately, it is often difficult or impossible to reliably make the etiologic distinction between two independent primaries versus a single primary tumor with metastasis by current histopathological and immunohistochemical methods, if the two tumors are morphologically similar (7-9).

Recently, the potential benefit of molecular biologic approaches to assist clinical differential diagnosis has been evaluated in several studies, revealing that the EP cells in two independent primaries and one primary with metastasis often display different frequencies and patterns of LOH and/or MI at several chromosomal loci, which may serve as useful markers for discrimination of these tumors (10-12). Our own studies have further demonstrated that the EP cells and surrounding ST tissues often display a high frequency of concurrent LOH and MI (13-14), suggesting the possible involvement of ST cells in carcinogenesis and the potential diagnostic values of assessing the genetic profiles of ST cells. Since metastatic EP cells are directly derived from the primary tumor with or without further acquisition of genetic alterations, cells in the primary and metastatic sites should share the same or a similar (partial overlap) genetic profile. In contrast, as the ST cells surrounding the metastatic cells are native to the site, having no direct physical association with the EP cells before their metastasis, they are not expected to share the same or similar genetic profile with their metastatic counterparts. Therefore, a simultaneous assessment and comparison of the genetic profiles in both EP and ST cells might provide a more effective approach for differentiation between primary and metastatic lesions. Based on these observations and assumptions, this study intended to expand the spectrum of previous molecular studies by simultaneously

assessing and comparing the genetic profiles in both EP and ST cells, using LOH assessment and comparative genomic hybridization (CGH) techniques.

LOH is a common event in sporadic breast tumors, signifying a potential loss of tumor suppressor genes or increased genetic instabilities during tumor evolution. LOH assessment has been widely used to detect small deletions and deletion borderlines, and has been a useful tool in localizing a number of breast cancer-related genes, including breast cancer susceptibility gene 1 (BRCA1). LOH assessment, however, may require hundreds or thousands of primer sets to elucidate the DNA sequence of a selected target, due to the small size (generally no more than 200 base pairs) of the PCR product generated by each primer set. In addition, if comparative studies are conducted to assess the similarity or difference between paired samples with an unknown genetic profile, multiple primer sets from several or all the chromosomes may have to be tested, in order to identify the desired targets. In contrast, the CGH technique has been widely used as a genome-wide screening tool to study gains or losses of genetic materials in a variety of solid tumors (15-18) and to determine the clonal relationship between the initial ductal carcinomas in situ (DCIS) and their recurrences (19). The most prominent advantage of the CGH technique is that it allows assessment of the entire chromosomal set and mapping of gains or losses in each chromosome in a single experiment. The most distinct drawbacks of this technique are the fuzziness of the deletion borderlines and the low sensitivity, incapable of detecting deletions smaller than 1-2 megabases (16-18). These drawbacks, however, could be largely eliminated by LOH assessment with the "chromosomal walking" technique, using selected primers to generate the entire sequence of potentially altered regions suggested by CGH (20). On the other hand, the CGH technique could rapidly identify or narrow down the potential targets for LOH assessment. The two procedures were, therefore, combined in the assessment of about one half (7/18) of our study cases.

Materials and Methods

Collection and classification of the tissue samples

Formalin-fixed, paraffin-embedded biopsy samples or unstained sections from 18 female patients with primary bilateral breast tumors were retrieved from the files of Armed Forces Institute of Pathology. Of the 18 patients, 16 were older than 40 years, and 2 were 17 and 27 years old. Of the 18 paired tumors, 16 occurred synchronously and 2 metachronously. In metachronous tumors, the interval between the first and second tumor was 36 months. Of the 18 paired EP lesions, 15 were non-invasive, 2 were invasive, and 1 was metastatic (pulmonary small cell carcinoma with simultaneous metastasis to both breasts). The morphologic classification of the lesions was based on published criteria (6-9), and the main lesions are listed in Table 1. In addition, paraffin embedded breast tissues from bilateral reduction mammoplasty (RM) from 10 women who had no clinical, radiological, or histopathological abnormalities in their breasts were included in the study as external normal controls.

Microdissection and DNA extraction

Serial sections were cut at 5-7 μm thickness and placed on microscopic slides, incubated at 80 ^{0}C for 30 minutes, deparaffinized with xylene, washed with descending concentrations of ethanol and tap water, and lightly stained with hematoxylin. Morphologically similar EP and ST cells in the left and right breast were separately microdissected, placed in different tubes, and subjected to DNA extraction as previously described (13-14, 21). The tumor cells microdissected from each case were listed in Table 1. Clear-cut normal EP and ST cells at least 1 cm away from the lesions, and from the tissues of 10 normal controls were also microdissected and used as the internal and external controls.

Assessment for Loss of heterozygosity (LOH) and microsatellite instability (MI)

Fluorescent dye labeled polymorphic DNA markers were purchased from Research Genetics (Huntsville, AL). A panel of 10 markers reported to show a high frequency of LOH and MI in a wide variety of mammary carcinomas (13, 22) was selected for the LOH and MI assessment; these markers are

listed in Table 2. Gene Amp PCR kits, Taq gold DNA polymerase, gel loading buffer, and the DNA size standard were bought from Perkin-Elmer (Foster City, CA). PCR amplification was carried out as previously described (13, 22). After amplification, 2-3 μL of PCR solution was mixed with 6-8 μL of gel loading buffer, and 1.0-1.5 μL of the mixture was subjected to electrophoresis in 6% polyacrylamide gels (Bio-Rad, Foster City, CA). The signal was detected with a 377 DNA sequencer (Perkin-Elmer, Foster City, CA), as previously described (13,22). All the tissue samples amplified with each of the 10 DNA markers were examined for LOH and MI. LOH was defined as "the complete absence or at least a 75% reduction of one allele", and MI was defined as "an addition or deletion of one or more repeat units that result in a shift of micro-satellite alleles" (13,22). A concurrent LOH was defined as "the loss of an identical allele in cells from both sides for a given marker". An independent LOH was defined as "the loss of an allele in cells from one side, or the loss in cells from two sides at different alleles for a given marker". All the samples that failed to produce distinct PCR products in three attempts of amplification or showed homozygosity were considered non-informative. The frequency of independent and concurrent LOH and/or MI in paired bilateral EP or ST samples that were informative at both breasts were statistically compared with the Student's t-Test. Seven cases with sufficient DNA extracts were selected for CGH analysis

Production of the gel images of LOH assessments

The production of gel images was carried out according to the User's Manual provided by the manufacturer and to our recently published protocols (23-24).

Comparative genetic hybridization (CGH)

CGH was carried out according to previously published protocols (15,19). PCR amplified DNA products from 7 selected cases and the normal reference DNA from normal females were labeled with biotin-14-deoxyadenosine triphosphate (14-dATP) and fluorescein -12-deoxyuridine triphosphate (dUTP) (Du Pont NEN, Boston, MA), respectively, using a Bionick kit (Gibco BRL, Gaithersburg, MD). DNA

mixtures containing 500-1000 ngs of each labeled DNA and 50 μg of Cot 1 DNA (Gibco BRL, Gaithersburg, MD) at a total volume of 6-8 μL were hybridized to normal human-male metaphase lymphocyte spreads for 48 – 72 hours at 37 ^{0}C. After hybridization, slides were washed and processed for image analysis as previously described (15,19). The CGH profile was analyzed and changes at sub-regions of each chromosome were identified, as previously described (15,19).

Results

The left and right breast in each of the 18 cases contained morphologically similar ST tissues and EP lesions, which were generally distributed as distinct cell clusters, facilitating the acquisition of a relatively uniform cell population by microdissection (Figures 1a to 1c).

The frequency and pattern of LOH and/or MI detected among different DNA markers are listed in Table 3. Distinct LOH and/or MI were seen among the 36 paired bilateral EP and ST cells with each of the 10 DNA markers, though the frequencies varied substantially among the markers, ranging form 17.9% (D11S914) to 40.3%% (D13S219) in informative loci (Table 3).

Of the 36 paired bilateral EP and ST samples assessed with 10 DNA markers at 5 chromosomes, a total of 148 chromosomal loci showed alterations in one or both breast with a total of 180 LOH and/or MI (Table 3). Of the 10 DNA markers, all displayed more independent than concurrent LOH and /or MI (Table 3). Of the 36 paired samples, 30 (83.3%) displayed more independent, 3 (8.3%) showed more concurrent, and 3 (8.3%) showed an equal rate of independent and concurrent LOH and/or MI (Table 3). The 18 paired bilateral EP samples contained 78 altered chromosomal loci; of which, 23 (29.5%) showed concurrent and 55 (70.5%) displayed independent LOH and/or MI (Table 3). The 18 paired bilateral ST samples contained 70 altered loci; of which, 9 (12.9%) displayed concurrent and 61 (87.1%) displayed independent LOH and/or MI (Table 3). The rate of independent LOH and and/or MI is significantly higher ($p<0.01$) than that of concurrent LOH and MI in both EP and ST cells (Table 4). The case of pulmonary small cell carcinoma (case 10) with simultaneous metastasis to both breasts, however, showed concurrent LOH at each of the 4 DNA markers (Table 3). Figure 2 shows examples of LOH and MI in these paired bilateral EP and ST samples. No distinct LOH or MI was seen in either the EP or ST cells of the 10 bilateral reduction mammoplasty specimen from women having no clinical, histopathological, or radiological abnormalities in their breasts.

Results of the CGH assessment are summarized in Table 5. Of the 7 selected cases, chromosomal changes (gain or loss of DNA copy numbers) were found in the EP component in one side of 3 cases, in both sides of 3 cases, and also in the ST component in one side of 2 cases. The total CGH changes were distributed in 5 left and 4 right breasts. The most common change was loss of 16q, which was seen in 5 EP components of 4 cases, followed by loss of 11q, which was seen in 2 EP and 2 ST components of 4 cases. None of the cases that displayed CGH changes, however, showed an identical frequency and pattern of changes in the EP component of both breasts (Table 5). On the other hand, an identical CGH change, loss of 13q, was detected in both EP and ST components of the right breast of one case. Figure3 shows the CGH change in each case.

Discussion

The reported incidence of clinically detected female bilateral primary breast cancers accounts for 3-9% of the total breast malignancies (1-3). Occult or asymptomatic bilateral cancers, however, have been encountered in 34 -50% of contralateral mastectomy specimen prophylactically removed from patients with a primary breast cancer (25-27), in 21-68% of autopsy specimen of patients with a history of breast cancer, and in about 10% of mastectomy specimen removed for benign diseases (28-31). The substantially higher incidence of bilateral breast cancers in some of the autopsy and mastecomy specimen than in clinical reports raises a number of questions, including: [1] Why such a high percentage of contralateral cancers is occult or asymptomatic, enabling to escape from clinical detection? [2] Will asymptomatic or occult cancers manifest as clinically evident cancers if the patient's life-span increases? [3] How could we accurately identify the specific individual with asymptomatic or occult cancer, or at an increased risk for developing bilateral cancers? More importantly, the higher incidence of bilateral breast cancer in autopsies and mastecomies in patients with breast cancer history suggests that some of the bilateral carcinomas in one side might either regress or become latent during the patient's lifetime. This further suggests that the clinic behavior and molecular mechanism of tumor development and progression in left and right breast may be substantially different. Consequently, comparisons of the genetic profiles of cells in bilateral breast cancers, especially those with progressive cancer in one side and with latent or regressive lesion in the other, may lead to the identification of specific factors that promote development and progression or promote regression and latency. The utilization of the factors that promote tumor regression and latency may provide a novel approach for the management and treatment of patients with breast cancers.

It is interesting to note our findings of LOH and MI assessments are very similar to those of a recent study (10). In that study, tissue sections from 31 young (age < 50) patients with bilateral primary breast cancers were subjected to mutation analyses for breast cancer susceptibility genes 1 and 2, and to

LOH assessment with 6 DNA markers. Of the 31 paired (left and right) samples, 3 showed no LOH on all 6 DNA markers. The rest 28 paired samples contained a total of 77 LOH at 58 paired chromosomal loci assessed with the 6 DNA markers. Of the 28 paired samples, 17 (61%) displayed more independent and 6 (21%) showed more concurrent LOH. Of the 77 LOH, 43 (56%) were distributed in the left and 34 (44%) in the right lesions. Of the 58 paired loci, 39 (67%) showed unilateral and 19 (33%) displayed bilateral LOH. Also, 5 of 6 DNA markers displayed more independent LOH. In our current study, of the 18 paired bilateral EP samples assessed with 10 DNA markers at 5 chromosomes, 78 loci displayed alterations; of which, 23 (29.5%) showed concurrent and 55 (70.5%) displayed independent LOH and/or MI. Of the 18 paired bilateral ST samples assessed with the same markers, 70 loci displayed alterations, of which, 9 (12.9%) showed concurrent and 61 (87.1%) displayed independent LOH and/or MI. Overall, all 10 markers and 30 (83.3%) of the 36 paired bilateral EP and ST samples showed more independent, whereas only 3 (8.3%) showed more concurrent LOH and/or MI. The results of our study and the previous report (10) are statistically similar. The slightly higher frequency of independent LOH seen in our study may result from the wider age range, and the use of microdissected cells and more markers.

By CGH, gains and/or losses of DNA copy numbers were found in one breast in three cases and in both breasts, also in three cases. The most common change was the loss of 16q, which was seen in 5 EP components of 5 breasts from 4 women; 3 of the four were LIN lesions. Loss of 11q was detected in 2 EP and 2 ST components of 4 breasts. None of the cases showed an identical pattern of chromosomal alterations in the EP components of both breasts, though 16q loss was present bilaterally in one woman with bilateral LIN. An identical CGH change, loss of 13q, however, was found in both the EP and ST components of the right breast in one case. To our knowledge, this is the first study that reveals the loss of DNA copy numbers in ST cells with the CGH technique. This finding is in an agreement with LOH assessments of our previous studies on both breast and cervical carcinomas, which have revealed that the EP and the surrounding ST cells share the same genetic profile at a majority of the DNA markers assessed

(13-14). Taken together, these findings suggest that ST cells may be concurrently involved, or even play initiative roles in development and progression of breast tumors.

The consistent detection of LOH in ST cells is hard to reconcile with the traditional belief that the ST component consists of multiple cellular phenotypes that are genetically and biofunctionally different (31-33), which could mask certain genetic alterations, including LOH, in a given ST cell type. There are two possible mechanisms, however, that could result in the occurrence or detection of LOH in ST tissues. First, a single genetically altered ST cell type could acquire growth advantages during the evolution and undergo a localized clonal expansion, forming genetically similar cell clusters. Consistent with this is that the ST component of some breast carcinosarcomas shares the same clonality with the EP component (34). Second, a genetically mutated multi-potential stem cell could give rise to different ST cells that contain the same genetic profile. Previous studies have well demonstrated that maturation arrest of stem cells is a common pathway for the cellular origin of both teratocarcinomas and malignant EP tumors, and that an entire functional mammary gland may be regenerated from a single cell (35-37).

The high frequency of LOH in ST cells is also hard to reconcile with the reported low incidence of malignancies in ST cells (38). There are several possible explanations. First, genetically altered ST cells might have more disadvantages for progression, due to the following reasons: [1] they are subjected to more immunological and biological surveillance because of their direct association with white blood cells and lymphocyte aggregates, which are generally absent in the normal EP component; [2] they are subjected to less influences of growth factors, suggested by the fact that although many growth factors have been identified, very few have been found to specifically target ST cells; [3] A constant remodeling and replacement of the extracellular matrix and ST tissues may disfavor the accumulation of genetic abnormalities in ST cells (39-41). Second, the development or progression of ST tumors may require more internal assaults or additional steps, because of the persistence of multiple cellular phenotypes in the ST component, and possible interactions among different ST cell types. Third, genetic or biochemical alterations in the ST component might have more impacts on the EP component than on itself, because of

two main reasons: [1] the normal EP component lacks blood and lymph vessels, and totally relies on the ST component for its normal functions, [2] a number of biomolecules produced by ST cells, including growth factors, proteinases, and matrix metalloproteinases, are key factors for normal EP morphogenesis, differentiation, wound healing, and also for tumor invasion and metastasis (39-43).

The substantial differences in LOH and MI frequencies and CGH profiles in both EP and ST components are in favor of two independent molecular mechanisms for the development and/or progression of bilateral breast tumors, and further suggest that the biological presentation and clinical behavior of the tumors in the left and right breast may be substantially different. Consequently, different treatment regimens might be needed for the optimal management of patients with bilateral breast tumors. No definitive conclusions, however, could be drawn at present because of several reasons. First, the high degree of heterogeneity of LOH and CGH profiles among cases, along with high frequencies of genetic abnormalities at multiple chromosomal loci suggest that the genetic alteration in each individual might be a unique event, or multiple molecular mechanisms might be involved. Second, the presence of a high degree of heterogenity of LOH and CGH profiles among cases may simply result from different cell clones, or the same clone at different differentiated states. Our previous study, which conducted a longitudinal molecular comparison of four women with reappearance of DCIS 2 to 15 years after an initial conservative resection, has shown that in three cases with ipsilateral recurrence disease, all the LOH seen in the initial tumors were also seen in the recurrent lesions, while all the three recurrent tumors show at least one additional LOH, suggesting that different cellular clones from the same progenitor might present different genetic profiles during evolution of breast tumors. Third, the small sample size may not be representative of the general population. Fourth, this study is more directed toward to elucidate the overall tendency rather than to draw specific conclusions. More comprehensive analyses are in progress to identify the unique features and the potential molecular mechanism between the left and right lesions of clinically detected and occult bilateral breast cancers.

Acknowledgement

The authors are very grateful to Dr. Fattaneh A. Tavassoli, the former chairperson of our department, for her support in initiation of this study, her assistance in the selection and morphologic classification of breast tissues used in this study, and her constructive suggestions on the manuscript. The authors greatly appreciate the technical assistance from Bob Flemone and Susan Cender of The Cancer Center and Department of Laboratory Medicine, University of California, San Francisco, CA. The authors are also indebted to Mr. Doug Landry of the AFIP exhibition section and Mr. Kenneth J. Vrtacnik of the AFIP Photography Lab for their assistance in preparation of the figures.

This study was supported in part by a grant from American Registry of Pathology (1006-7011) to Dr. Ruth A Lininger, and ~~Career Development Award and Idea Award~~ from Congressionally Directed Medical Research Programs (DAMD17-01-1-0129 and DAMD17-01-1-0130) Dr. Yan-gao Man,

References

1. Fisher ER, Fisher B, Sass R, Wickerham L, and collaborating NSABP investigators. Pathologic findings from the National Surgical Adjuvant Breast Project (Protocol No.4.).XI. Bilateral breast cancer. Cancer 1984; 54:3002-3011
2. Kollias J, Ellis IO, Elston CW, Blamey RW. Prognostic significance of synchronous and metachronous bilateral breast cancer. World J Surg 2001; 25:1117-1124
3. Donovan AJ. Bilateral breast cancer. Surg Clin North Am 1990; 70:1141-1149
4. Fracchia AA, Robinson D, Legaspi A, Greenall MJ, Kinne DW, Groshen S. Survival in bilateral breast cancer. Cancer 1985; 55:1414-1421
5 Staren ED, Robinson DA, Wir TR,, Economou SG. Synchronous, bilateral mastectomy. J Surg Oncol, 1995; 59:75-79
6. Healey EA, Cook EF, Orav EJ, Schnitt SJ, Connolly JI, Harris JR.. Contralateral breast cancer: clinical characteristics and impact on prognosis. J Clin Oncol 1993; 11:1545-1552
7. Sterns EE, Fletcher WA. Bilateral cancer of the breast: a review of clinical, histologic and immunohistologic characteristics. Surgery 1991; 110:617-622
8. Hungness ES, Safa M, Shaughness EA, Aron BS, Gazder PA, Hawkins HH, et al. Bilateral synchronous breast cancer: mode of detection and comparison of histologic features between the 2 breasts. Surgery 2000; 128:702-707
9. Dawson LA, Chow E, Goss PE. Evolving perspectives in contralateral breast cancer. Eur J Cancer 1998; 34:2000-2009
10. Kollias J, Man S, Marafie M, Carpenter K, Pinder S, Ellis IO, Blamey RW, Cross G, Brook JD. Loss of heterozygosity in bilateral breast cancer. Breast Cancer Res Treat 2000; 64:241-251
11. Shenson DL, Gallion HH, Powell DE, Pieretti M. Loss of heterozygosity and genomic instability in synchronous endometrioid tumors of the ovary and endometrium. Cancer 1995; 76(4):650-657
12. Emmert-Buck MR, Chuaqui R, Zhuang ZP, Nogales F, Liotta LA, Merino MJ. Molecular analysis of synchronous uterine and ovarian endometrioid tumors. Inter J Gynecol Pathol 1997; 16: 143-148
13. Moinfar F, Man YG, Arnould A, Bratthauer GL, Ratschek M, Tavassoli FA. Concurrent and independent genetic alterations in the stromal and epithelial cells of mammary carcinoma: Implications for tumorigenesis. Cancer Res 2000; 60:2562-2566
14. Man YG, Mannion C, Kuhls E, Moinfar F, Bratthauer GL, Albores-Saavedra J, Tavassoli

FA. Allelic losses at 3p and 11p are detected in both epithelial and stromal components of cervical small-cell neuroendocrine carcinoma. Appl Immunohistochem Mol Morphol 2001; 9:340-345

15. Kallionniemi A, Kallioniemi OP, Sudar D, Rutoviitz D, Gray JW, Waldman F, Pinkel D. Comparative genomic hybridization for molecular cytogenetic analysis of solid tumors. Science (Washington DC) 1992; 258:818-821
16. Kukasjarvi T, Tanner M, Pennanen S, Karhu R, Kallioniemi, Isola J. Genetic changes in intraductal breast cancer detected by comparative genomic hybridization. Am J Pathol 1997; 150:1465-1471
17. Ried T, Just KE, Holtgreve-Grez H, du Manoir A, Speicher MR, et al. Comparative genomic hybridization of formalin-fixed, paraffin-embedded breast tumors reveals different patterns of chromosomal gains and losses in fibroadenomas and diploid and aneuploid carcinomas. Cancer Res 1995; 55:5415-5423
18. James LA, Mitchell EL, Manasce L, Varley JM. Comparative genomic hybridization as a tool in tumor cytogenetics. J Pathol 1999; 187:385-395
19. Waldman FM, DeVries S, Chew KL, Moore II DH, Kerlikowske K, and Ljung BM. Chromosomal alterations in ductal carcinomas in situ and their in situ recurrences. J Natl Cancer Inst 2000; 92:313-320
20. Alimov A, Kost-Alimova M, Liu J, Li C, Bergerheim U, et al. Combined LOH/CGH analysis proves the existence interstitial 3p deletion in renal cell carcinoma. Oncogene 2000; 19:1392-1399
21. Man YG, Moinfar F, Bratthauer GL, Kuhls EA, Tavassoli FA. An improve method for DNA extraction from paraffin sections. Pathology-Research and Practice 2001; 197: 635-642
22. Moinfar F, Man YG, Bratthauer GL, Ratschek M, Tavassoli FA. Genetic abnormalities in mammary ductal intraepithelial neoplasis-flat type(clinging ductal carcinoma in situ). Cancer 2000; 88:2072-2081
23. Man YG, Moinfar F, Bratthauer GL, Kuhls E, Tavassoli FA. Five useful hits for making more valid gel images of LOH and clonality analusis with a 377 DNA sequencer, Diagn Mol Pathol 2000; 9:84-90
24. Man YG, Kuhls EA, Bratthauer GL, Moinfar F, Tavassoli FA. Multiple use of slab gels in sequencing apparatus for separation of PCR products. Electrophoresis 2001; 22:1915-1919
25. Hoffman E. The contralateral breast biopsy in ipsilateral carcinoma. Southern Med J 1990; 83:1009-1015
26. Ringberg A, Palmer B, Linell F, Rychterova V, Ljungberg O. Bilateral and multifocal breast

carcinoma. Eur J Surg Oncl 1991; 17: 20-29

27. Nielsen M, Christensen L, Andersen J. Contralateral cancerous breast lesions in women with clinical invasive breast carcinoma. Cancer 1986; 57:897-903
28. Lawson R. Mammary cancer: the other breast. Can Med Assoc J 1955; 73:676-677
29. Masood S. Occult breast lesions and aspiration biopsy: a new challenge. Diagn Cytopathol. 1993; 9: 613-614
30. Barton FE Jr. Breast cancer, subcutaneous mastectomy, breast reconstruction. Selected Readings in Plastic Surgery 1986; 3: 1-23
31. Ronnov-Jessen L, Petersen OW, Bissell MJ. Cellular changes involved in conversion of normal to malignant breast: Importance of the stromal reaction. Physiol Rev 1996; 76:69-125
32. Simian M, Hirai Y, Navre M, Werb Z, Lochter A, Bissell MJ. The interplay of matrix metalloproteinases, morphogens and growth factors is necessary for branching of mammary epithelial cells. Development 2001; 128::3117-3131
33. Bissell MJ, Radisky DC, Rizki A, Weaver VM, Petersen OW. The organizing principle: Microenvironmental influences in the normal and malignant breast. Differentiation 2002; 70: 537-546
34. Zhaung Z, Lininger RA, Man YG, Albuquerque A, Merino MJ, Tavassoli FA. Identical clonality of both components of mammary carcinosarcoma with differential loss of heterozygosity. Mod Pathol 1997; 10:354-362
35. Sell S, Piece GB. Maturation arrest of stem cells is a common pathway for the cellular origin of teratocarcinomas and epithelial cancers. Lab Invest 1994; 70:6-22
36. Kordon EC, Smith GH. An entire functional mammary gland may comprise the progeny from a single cell. Development 1998; 125:1921-1930
37. Drummond R. The malignant stem cells. Med Hypotheses 1994; 43:157-159
38. Wingo PA, Ries LA, Rosenberg HM, Miller DS, Edwards BK. Cancer incidence and mortality, 1973-1995:a report card for the U.S. Cancer 1998; 82:1197-1207
39. Schedin P, Strange R, Mitrenga T. Fibronectin fragments induce MM activity in mouse mammary epithelial cells: Evidence for a role in mammary tissue remodeling. J Cell Sci 1995; 113:795-806
40. Werb Z, Ashkenas J, MacAuley A, Wiesen JF. Extracellular matrix remodeling as a regulator of stromal-epithelial interactions during mammary gland development, involution and carcinogenesis. Braz J Med Biol Res 1996; 29:1087-1097
41. McCawley LJ, Matrisian LM. Matrix metalloproteinases:multifunctional contributors to tumor progression. Mol Med Today 2000; 6:149-156

42. Hansen RK, Bissell MJ. Tissue architecture and breast cancer: the role of extracellular matrix and steroid hirmones. Endocr Relat Cancer 2000; 7:95-113

43. Nelson AR, Fingleton B, Rothenberg ML, Matrisian LM. Matrix metalloproteinases: Biologic activity and clinical implications. J Clin Onco 2000; 18:1135-1149

44. Lininger RA, Fujii H, Man YG, Gabrielson E, Tavassoli FA. Comparison of loss heterozygosity in primary and recurrent ductal carcinoma in situ of the breast. Mod Pathol 1998; 11:1151-1159

Table 1. The age of patients and principal types of lesions

Case #	Age	Left (Year)	Right (Year)
1	73	Inf W/lob; **DCIS (G2);** LN 3(98)	Inf W/lob; **DCIS (G2);** LN 3(98)
2	54	**DCIS** (89)	**DCIS** (89)
3	63	**IDC** (G3) (94)	**IDC** (G3) (94)
4	58	**DCIS (G1)** (98)	Inv tubular; **DCIS (G1)** (98)
5	45	IDC; **DCIS (G2)** (99)	IDC (G2); **DCIS (G2)** (99)
6	55	DCIS (G1); **LN 2** (99)	**LN 2;** DIN 1a (99)
7	41	**IDC** (89)	**IDC** (89)
8	17	**AIDH** (97)	**AIDH** (97)
9	69	IDC; **DCIS** (97)	IDC; **DCIS** (97)
10	42	**Inf small cell Ca (metastasis)** (89)	**Inf small cell Ca (metastasis)** (89)
11	44	AIDH; **DCIS (G3);** LN 3 (98)	**DCIS (G3),** DIN 2 (98)
12	58	Inv lob; **LN 2** (99)	IDC (G3); **LN 2** (99)
13	63	**DCIS (G1)** (99)	IDC; **DCIS (G1)** (99)
14	62	Inf lob; **LN 2**; DCIS (00)	Inf lob & duct; **LN 2** (00)
15	86	**DCIS**; DIN 1c (97)	**DCIS**; DIN 2 (97)
16	54	**DCIS**; LN 1 (96)	IDC; **DCIS** (96)
17	44	IDC; DCIS (G2), **DIN 2** (95)	LN 2; **DIN 2** (98)
18	27	**DIN 1b** (00)	IDC; **DIN 3** (97)

The microdissected samples from each paired lesions are highlighted

Table 2. DNA markers used for comparison of genetic alterations in paired bilateral breast lesions

#	Name	Chromosomal location	Harbored gene	Size(base pair)
1	D3S1300	3p21.1 – p14.2	FHIT	217 - 241
2	D3S1481	3p14.2	FHIT	104
3	D11S904	11p14 – p13	Wilms' tumor 1	185 - 201
4	D11S914	11p13 – p12	Wilms' tumor 1	275 - 285
5	D13S219	13q12.3 – q13	?	117 - 127
6	D13S765	13	?	193
7	D16S518	16q23.1 – q24.2	CDH 1(adjacent to it)	272 - 290
8	D16S402	16q24.2	CDH 1 (adjacent to it)	161 - 187
9	D17S791	17q	BRCA 1	165 - 199
10	TP53	17p13	p53	104

Table 3. Comparison of the frequency and pattern of LOH and MI in paired EP and ST cells of bilateral breast tumors

#	Cell Type	D3S1300		D3S1481		D11S904		D11S914		D13S219		D13S765		D16S402		D16S518		TP53		D17S791		Con Pair	Ind pair
		L	R	L	R	L	R	L	R	L	R	L	R	L	R	L	R	L	R	L	R		
1	EP	Ø	Ø			Ø	Ø	—	—		—			▬	▬			Ø	Ø	—		*1*	*3*
	ST	Ø	Ø			Ø	Ø		—	▬	▬											*1*	*1*
2	EP		—	—								Ø	Ø			Ø	Ø					*0*	*2*
	ST	—										Ø	Ø			Ø	Ø				—	*0*	*2*
3	EP	—		—				Ø	Ø			—		▬	▬	—		▬	▬	—		*2*	*5*
	ST	—		—		—			—	—				—			—	—		—		*0*	*9*
4	EP	—				Ø	Ø			Ø	Ø			▬	▬	▬	▬	▬	▬		—	*3*	*2*
	ST					Ø	Ø			Ø	Ø					—	—	—			—	*0*	*3*
5	EP	—		▬	▬			Ø	Ø	▬	▬	▬	▬	Ø	Ø				—	▬	▬	*4*	*2*
	ST				—			Ø	Ø	—			—						—	—		*0*	*5*
6	EP			—		Ø	Ø			Ø	Ø			Ø	Ø	—						*0*	*2*
	ST					Ø	Ø			Ø	Ø	—				—		▬	▬		—	*1*	*3*
7	EP		—	—	—							▬	▬			—				—		*1*	*4*
	ST		—							—		—				▬	▬					*1*	*3*
8	EP	—		—	—	Ø	Ø					▬	▬							▬	▬	*2*	*2*
	ST	—										—						—		—		*0*	*4*
9	EP		—		—		—		—		—	—								Ø	Ø	*0*	*6*
	ST	▬	▬			—		▬	▬		—									Ø	Ø	*2*	*2*
10	EP	▬	▬	▬	▬	Ø	Ø			Ø	Ø	▬	▬			▬	▬			Ø	Ø	*4*	*0*
	ST		—			Ø	Ø			▬	▬	—				—						*1*	*3*
11	EP		—		—						—							Ø	Ø			*0*	*3*
	ST			▬	▬	—					—									—		*1*	*3*
12	EP			▬	▬		—							—			—	Ø	Ø	▬	▬	*2*	*3*
	ST						—	Ø	Ø	—	—	Ø	Ø	—				Ø	Ø	—		*0*	*4*
13	EP	Ø	Ø			—					—	Ø	Ø	—		—						*0*	*4*
	ST	Ø	Ø			—				—		Ø	Ø	—		—						*0*	*4*
14	EP			—				▬	▬		—	Ø	Ø					—		—		*1*	*4*
	ST		—		—	—						Ø	Ø	▬	▬			—		Ø	Ø	*1*	*4*
15	EP			—								—		Ø	Ø	▬	▬	—				*1*	*3*
	ST															—				—		*0*	*2*
16	EP			—		Ø	Ø	Ø	Ø		—			—		▬	▬	Ø	Ø			*1*	*3*
	ST					Ø	Ø	Ø	Ø	▬	▬			—			—	Ø	Ø			*1*	*2*
17	EP	Ø	Ø	Ø	Ø		—	—			—	—						Ø	Ø	▬	▬	*1*	*4*
	ST	Ø	Ø	Ø	Ø		—	—			—	Ø	Ø				—	Ø	Ø	Ø	Ø	*0*	*4*
18	EP			Ø	Ø		—	Ø	Ø		—	—		Ø	Ø	Ø	Ø			Ø	Ø	*0*	*3*
	ST			Ø	Ø		—	Ø	Ø		—		—	Ø	Ø	Ø	Ø			Ø	Ø	*0*	*3*
Con pair		2		4		0		2		4		4		4		5		3		4		*32*	
Ind pair		14		13		13		6		17		11		7		13		8		14			*116*

Morphologically comparable epithelial (EP) and surrounding stromal (ST) cells in two sides of primary bilateral breast tumor lesions were microdissected and subjected to assessments for LOH and microsatellite instability (MI). LOH was defined as the complete absence or at least 75% reduction of one allele, and MI was defined as an addition or deletion of one or more repeat units resulting in a shift of microsatellite alleles. A concurrent LOH was defined as "loss of an allele for a given marker in cells from both breasts". An independent LOH was defined as "loss of an allele only in cells from one breast, or cells in two breasts show LOH at different allele". –: Independent LOH or MI; —: Concurrent LOH or MI; Ø: Not informative; □: No loss; Con: Concurrent alteration; Ind: Independent alteration

Table 4. Comparison of frequencies of concurrent and independent LOH and MI in paired bilateral EP and ST samples

Cell type	Sample #	Informative foci	Altered foci	Conc-altered foci	Ind-altered foci	P
EP	18	147	78	23(29.5%)	55(70.5%)	< 0.05
ST	18	149	70	9(12.9%)	61(87.1%)	< 0.05
Total	36	296	148	32(21.6%)	116(78.4%)	< 0.05

Morphologically comparable epithelial (EP) and surrounding stromal (ST) cells in two sides of primary bilateral breast tumor lesions were microdissected and subjected to assessments for LOH and MI with 10 DNA markers in a 377 DNA sequencer. The rates of independent and concurrent LOH and MI were obtained by dividing the number of foci that showed independent and concurrent LOH and MI by the total number of altered foci, and the rates between these two categories were statistically compared with the Student's t-Test.
Con = Concurrent; Ind = Independent

Table 5. CGH profiles of 7 selected bilateral breast lesions

Case #	EP lesions in Both breasts	Cell type	Chromosomal changes	
			L	R
4	DCIS (G1)	EP	Loss: 16q	Losses: 6q; 11q; 16q
		ST	No change	No change
6	LN 2	EP	No change	No change
		ST	No change	No change
8	AIDH	EP	Gain: 1q Losses: 9p; 11q; 16q	No change
		ST	No change	No change
11	DCIS (G3)	EP	Gain: 1q	Loss: 13q
		ST	Loss: 11q	Loss: 13q
13	DCIS (G1)	EP	No change	Loss: 4p
		ST	No change	Not informative
14	LN 2	EP	Gains: 1q;8q; 16p Losses: 16q; 17p	Gains: 3p; 5q Losses: 4p; 5p
		ST	Losses: 11q; 11p (very small)	Losses: 3p; 8p (very small)
15	DCIS	EP	Gains: 6p; 12p; 14q Losses: 16p; 16q	No change
		ST	No change	No change

Morphologically comparable tumor epithelial (EP) and surrounding normal appearing stromal (ST) tissues in two sides of primary bilateral breast tumor lesions were microdissected and subjected to analysis with the comparative genetic hybridization (CGH) technique, using our previously published protocol (19).

Figure Legend

Figure 1. Microdissection of morphologically similar epithelial cells and stromal tissues of the left and right breast lesions

1a1-1ab: Solid tumors with dense stromal tissues. 1a1-1a3: Left lesion; 1a4-1a6: Right lesion, X 100

1b1-1b6: DCIS without necrosis. 1b1-1b3: Left lesion; 1b4-1b6: Right lesion, X 100

1c1-1c6: DCIS with necrosis. 1c1-1c3: Left lesion; 1c4-1c6: Right lesion, X 100

Figure 2. Examples of LOH in selected cases

Arrows identify LOH; M = DNA size marker; RE = Right epithelial cells; RS = Right stromal tissues; LE = Left epithelial cells; LS = Left stromal tissues

Figure 3. The CGH profile of each case ; Case 4 CGH profile (not shown) showed no changes

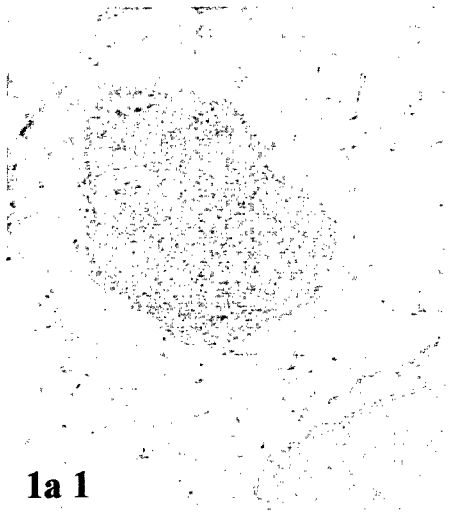

1a 1

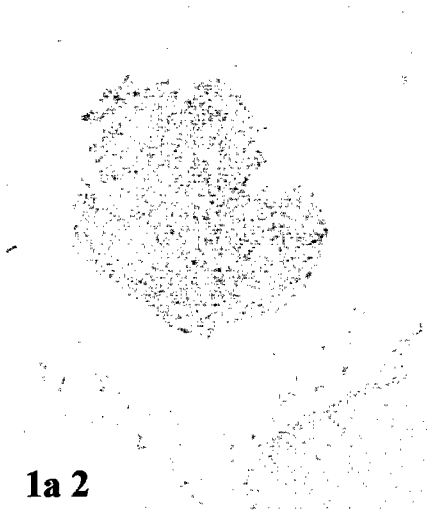

1a 2

1a 3

1a 4

1a 5

1a 6

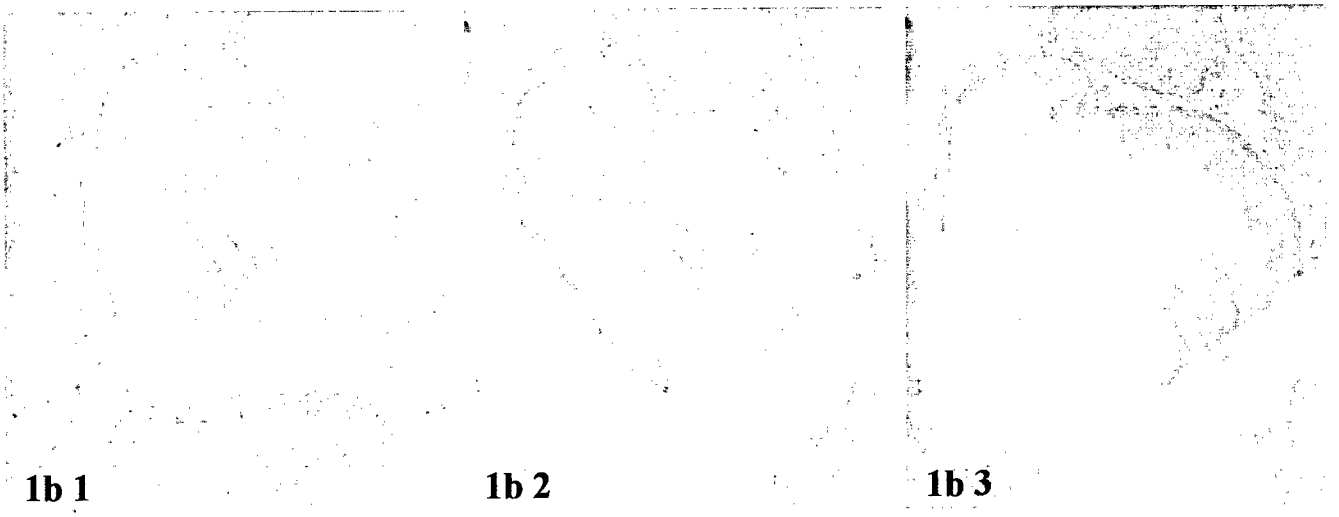

1b 1 1b 2 1b 3

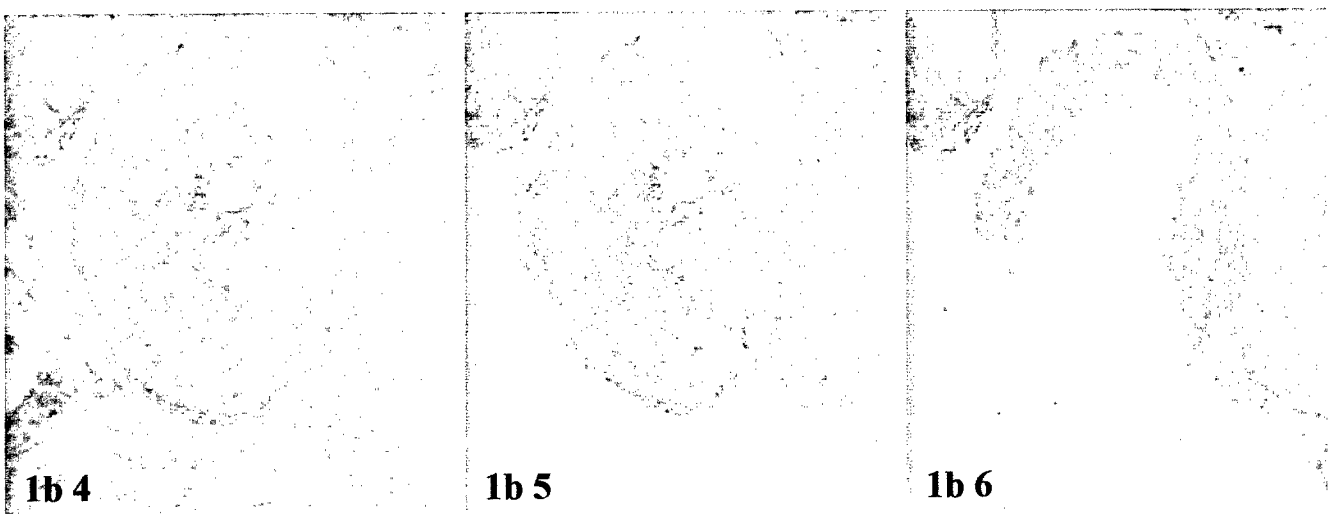

1b 4 1b 5 1b 6

1c 1

1c 2

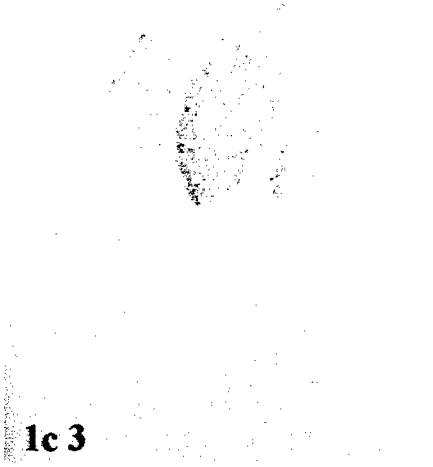

1c 3

1c 4

1c 5

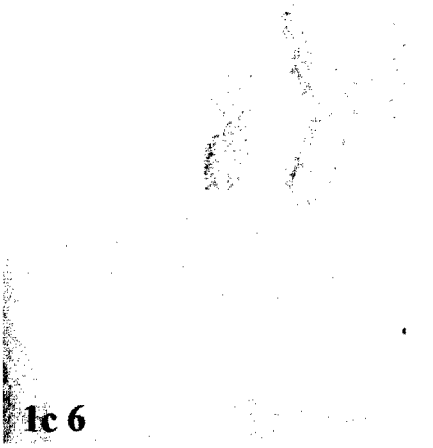

1c 6

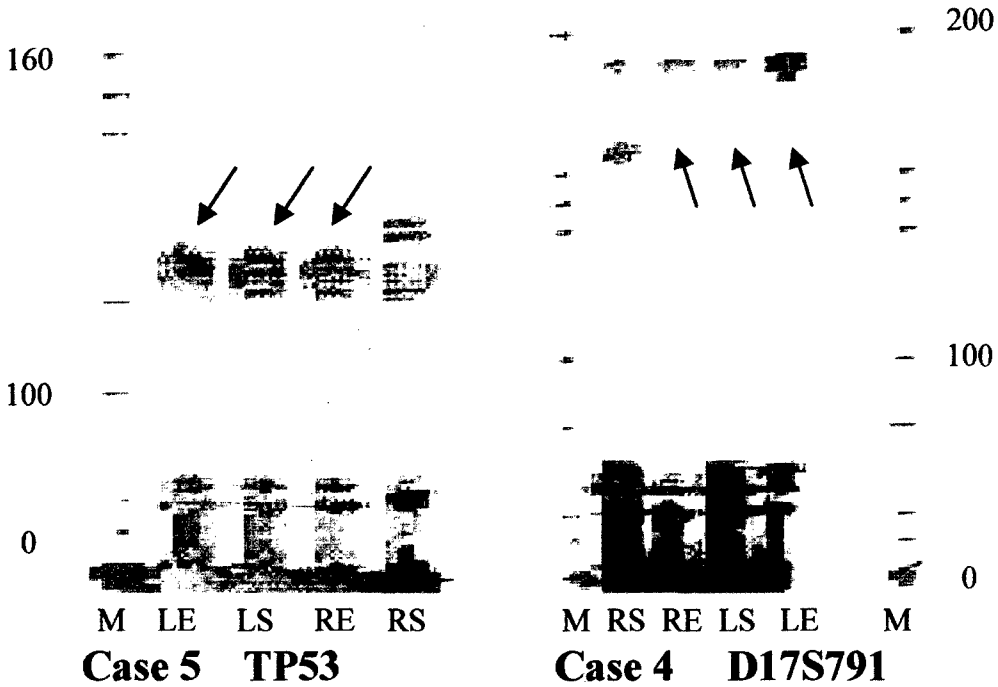

Case 5 TP53 **Case 4 D17S791**

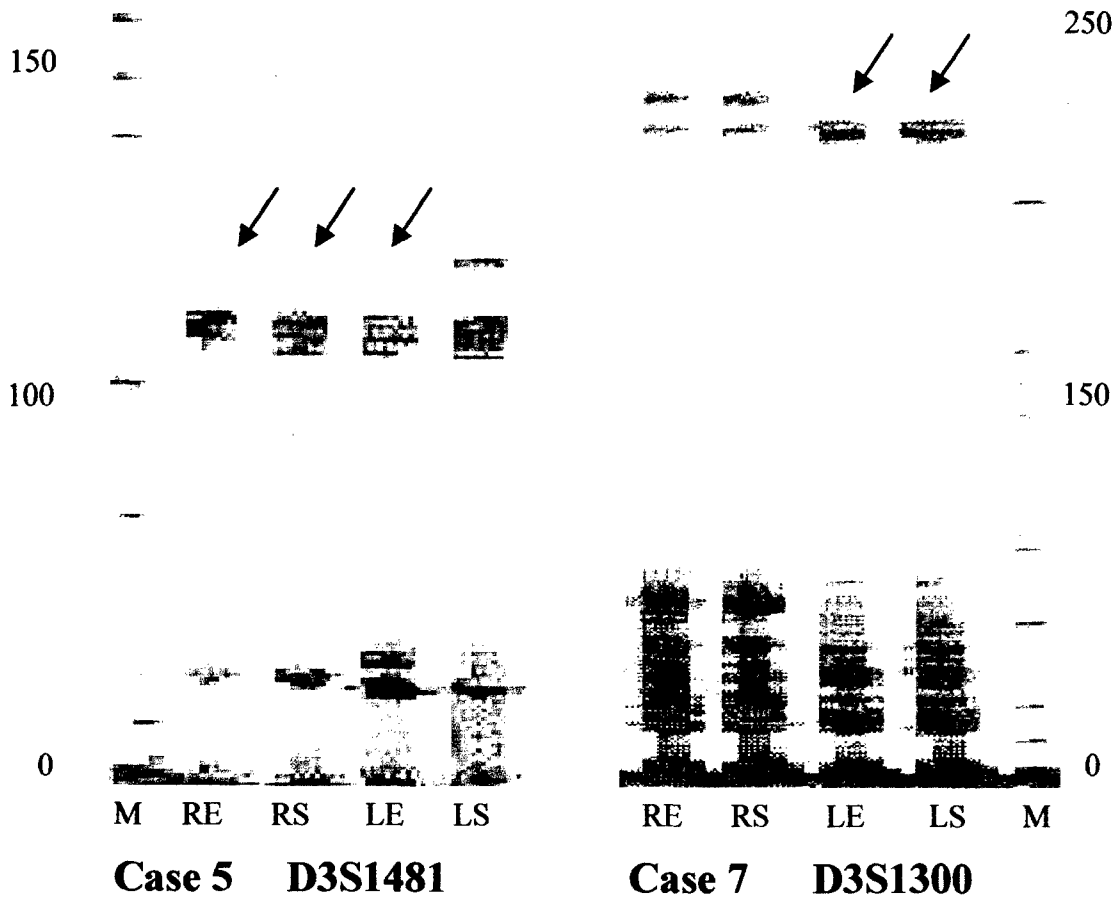
150
100
0
M
RE
RS
LE
LS
Case 5
D3S1481
250
150
0
RE
RS
LE
LS
M
Case 7
D3S1300

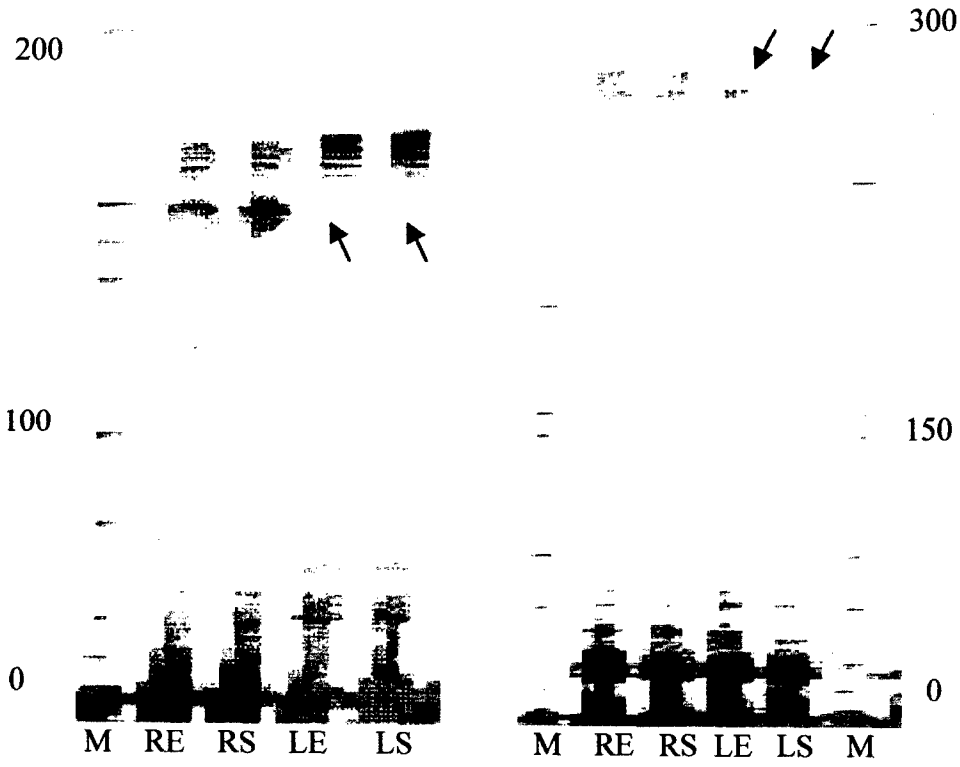

Case 12 D16S402 **Case 6 D16S518**

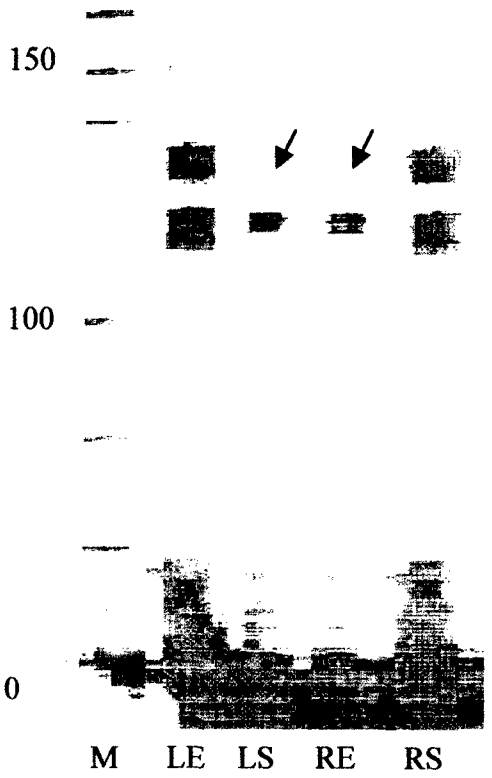

Case 13 D13S219

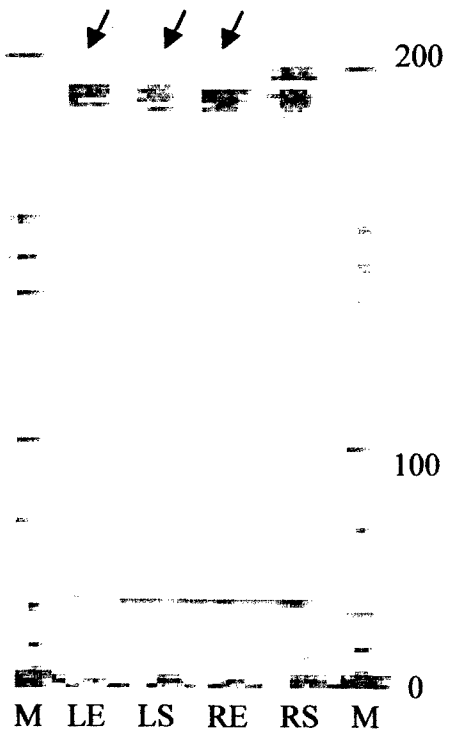

Case 7 D13S765

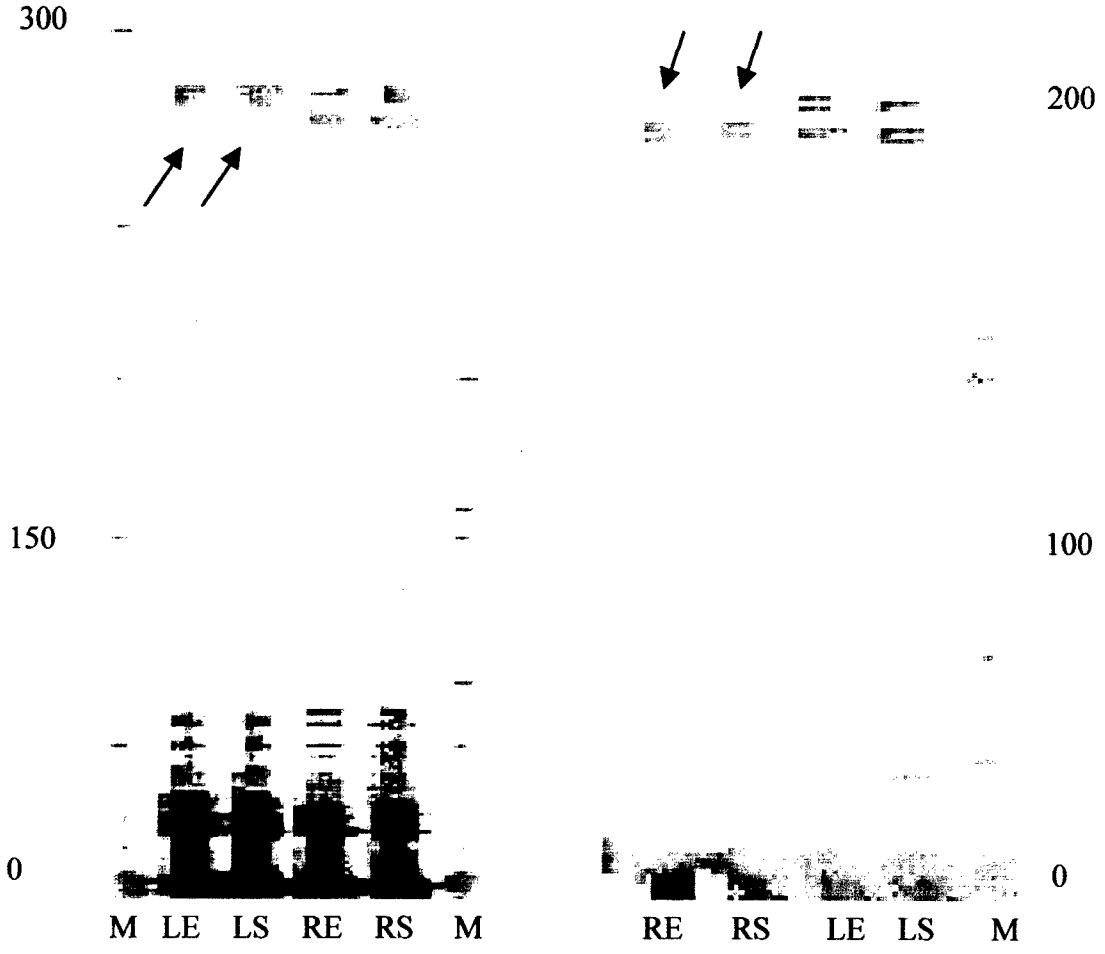

Case 17 D11S914 **Case 12 D11S904**

Case 1

	Left	Right
EP	16 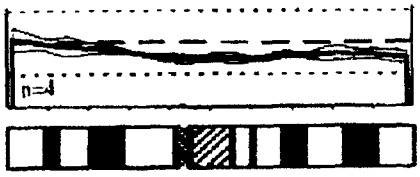	6 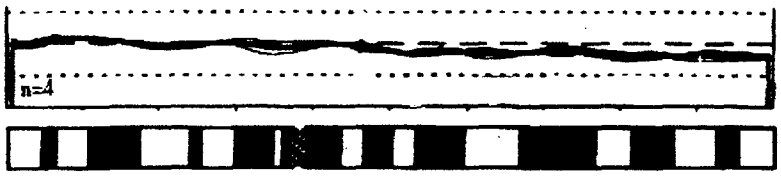 11 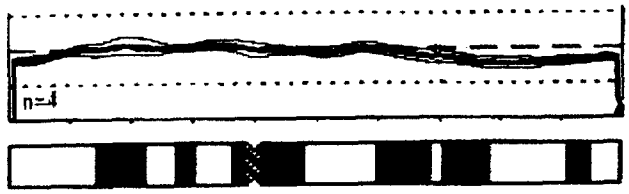 16 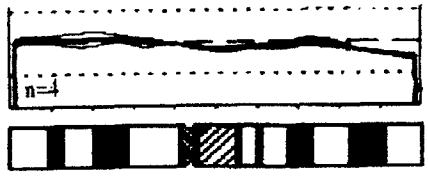
ST	**No changes**	**No changes**

Case 2

	Left	Right
EP	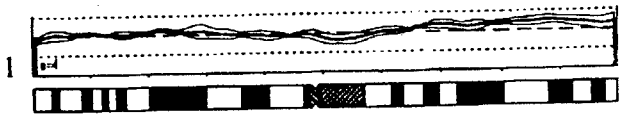	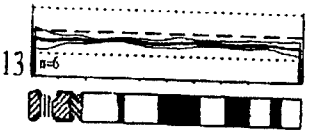
ST	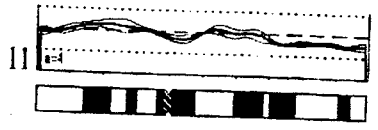	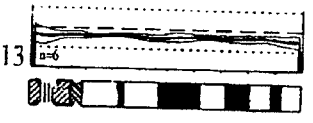

Case 3

	Left	Right
EP	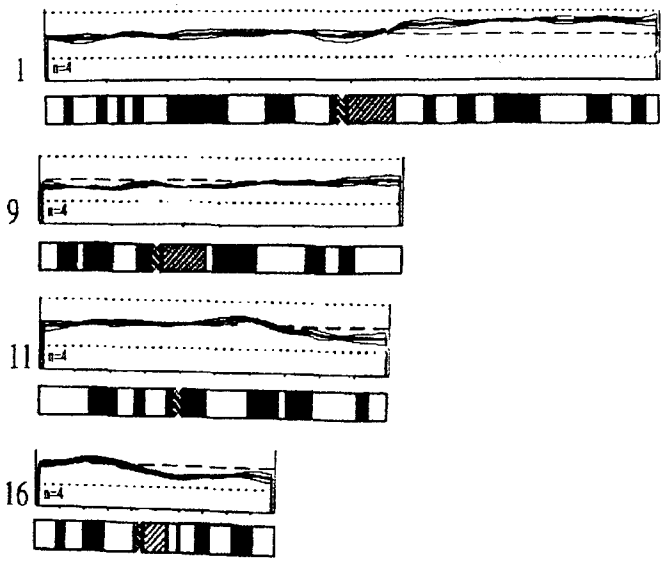	**No changes**
ST	**No changes**	**No changes**

CASE 4 – NOT SHOWN SHOWED NO CHANGES

Case 5

	Left	Right
EP	**No changes**	4 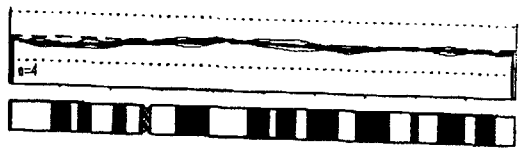
ST	**No changes**	**No changes**

Case 6

	Left	Right
EP	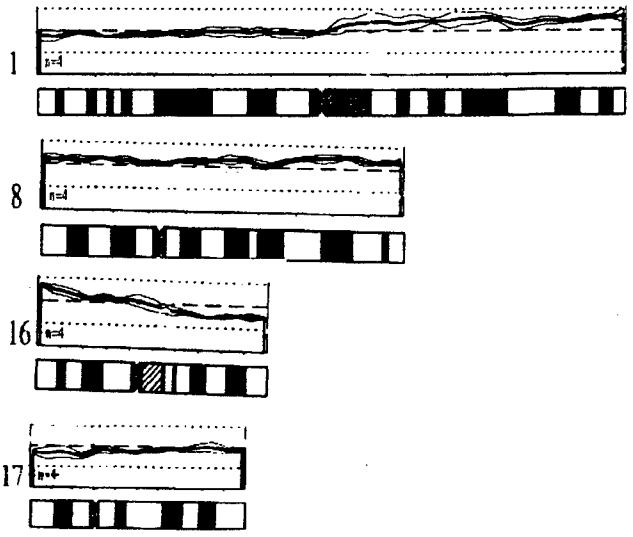	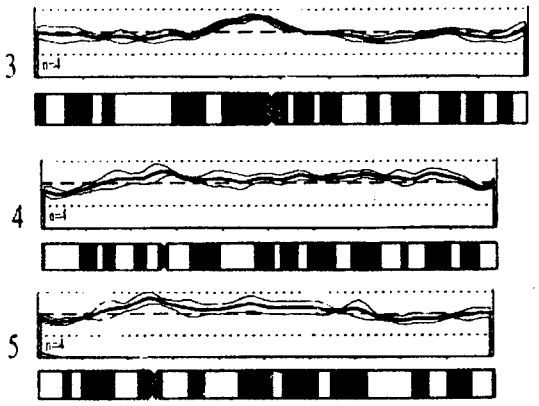
ST	**No changes**	

Case 7

	Left	Right
EP	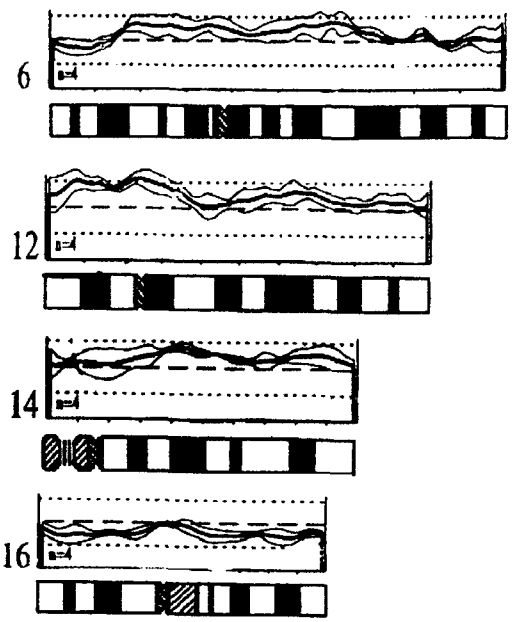	**No changes**
ST		**No changes**